

# **Xanthone and Flavone Derivatives as Potential Dual Agents for Alzheimer's Disease**

**Maria Inês Alves de Sousa Cruz**

Dissertation presented to the Faculdade de Farmácia da Universidade do Porto, to obtain the degree of Master in Pharmaceutical Chemistry

Work developed under the scientific supervision of Professor Madalena Maria de Magalhães Pinto and Professor Honorina Maria de Matos Cidade



July 2015

IN ACCORDANCE WITH THE APPLICABLE LAW, IS NOT ALLOWED TO REPRODUCE  
ANY PART OF THIS THESIS.

This work was developed in the “Centro de Química Medicinal-Universidade do Porto” (CEQUIMED-UP), Laboratório de Química Orgânica e Farmacêutica, Departamento de Química, Faculdade de Farmácia, Universidade do Porto.

This research was partially supported by the Strategic Funding UID/Multi/04423/2013 through national funds provided by FCT – Foundation for Science and Technology and European Regional Development Fund (ERDF), in the framework of the programme PT2020 and by the Project PEst-OE/SAU/UI4040/2014(FCT).



## **Poster Communications - Original research**

Some results presented in this dissertation are part of the following abstracts and poster communications:

**Maria Inês S. Cruz\***, Sara M. Cravo, Honorina Cidade, Madalena Pinto, "Xanthone derivatives with potential dual mode of action for Alzheimer's Disease", XX Encontro Luso-Galego de Química, Porto, Portugal, 26-28 November, 2014, P-29, p. 361.

**Maria Inês S. Cruz\***, Sara M. Cravo, Honorina Cidade, Madalena Pinto, "Xanthone Mannich base derivatives with potential dual mode of action for Alzheimer's Disease", III ENEQUI - 3º Encontro Nacional de Estudantes de Química, Aveiro, Portugal, 27-29 March, 2015.

**Maria Inês S. Cruz\***, Sara M. Cravo, Honorina Cidade, Madalena Pinto, "Synthesis of xanthone derivatives with potential dual mode of action for Alzheimer's Disease", IJUP15 - 5th Meeting of Young Researchs of U. Porto, Porto, Portugal, 13-15 May, 2015, P-42, p. 425.

\* Presenting author

## Acknowledgments

This dissertation was only possible due to scientific support and friendship of many people. Although it has not been easy, it was worth every moment and I would not change it for nothing. My words are not enough to acknowledge my two supervisors which have been with me during this year. They helped me tirelessly during the laboratorial work and writing the manuscript.

I would like to express my gratitude to my supervisor Professor Madalena Pinto for the guidance, constructive comments, critical thinking, contagious dynamism and for all her support throughout this work. During this year, Professor Madalena encouraged me in the most difficult moments of this research work, provided me good ideas and advices and supported me not only scientifically but also personally.

I wish to express my sincere thanks to my co-supervisor, Professor Honorina Cidade for helping me getting started in the synthesis procedures and for all patience that she showed during this year. I would like to acknowledge her guidance; continued support and her availability. In the most difficult moments, when I felt lost and despondent, Professor Honorina Cidade was always present, encouraged me, supported me and provided me valuable teachings.

To Professor Andreia Palmeira my gratitude for the collaboration and teaching in the area of docking studies which undoubtedly enriched this work.

I would also like to thank Dr. Sara Cravo for all technic and scientific support, for being present and assiduously accompanied me throughout the experimental work. I would also like to thank her for friendship and for enriching conversations.

I would like to thank all the Professors at the Laboratory of Organic and Pharmaceutical Chemistry of the Faculty of Pharmacy for their support and friendship.

I am also grateful to Gisela Adriano for technical support.

My sincere thanks to my lab colleague Pedro Brandão and to my colleagues of the Master in Pharmaceutical Chemistry, namely Joana Moreira and Ana Rita Neves, for their friendship, encouragement and for sharing skills.

Finally and most importantly, I would like to thank my wonderful parents and my brother, for all their emotional support, understanding, love and affection. Without them, nothing would be possible!

## Abstract

Alzheimer's Disease (AD) is a neurodegenerative disorder that is associated with elderly, being designated as multifactorial disease. The current therapy that is used to treat AD is based mainly on the administration of acetylcholinesterase (AChE) inhibitors. However, it is noted that this is not so effective. Thus, a promising therapy for treating this neurodegenerative disease may consist in administration of drugs that act on more than a target on biochemical scenery of AD. Therefore, in this work, the design, synthesis and evaluation of xanthenes and flavones as antioxidants with concomitant AChE inhibitory activity were accomplished.

Firstly, in this work, the hydroxylated xanthone (**ICX1**) was synthesized as well as its methylated derivative **ICX2**. Subsequently, amino derivatives of **ICX2** and baicalein (**B**) were also obtained by Mannich reaction. The structures of the synthesized compounds (**ICX1**; **ICX2**; **ICX2a** and **ICB1**) were established by IR and NMR.

Antioxidant activity of the obtained compounds and of a small library of other structure related aminoxanthone derivatives (**PPX1**; **PPX2**; **PPX3**; **PPX4**; **PEX1** and **PEX3**) previously synthesized in our research group was assessed by different methods. Xanthenes **ICX1** and **ICX2a** showed antioxidant activity by chelation iron and copper ions, while xanthenes **PEX1** and **PEX3** only had moderate antioxidant activity by scavenging free radicals. As the precursor baicalein (**B**), the amino derivative **ICB1** exhibited antioxidant effect through scavenging free radicals and by chelation metal ions.

AChE inhibitory activity of xanthone and flavone derivatives was also evaluated. Among all tested compounds, Mannich base derivatives **ICX2a** and **ICB1** showed moderate effect against AChE, being **ICB1** the most active compound. From this study, **ICX2a** and **ICB1** emerged as potential dual agents.

In the current work, docking studies of **ICB1** with AChE were performed in order to study its binding mechanism.

In conclusion, aminated xanthenes and flavones provide an adequate scaffold for the design of dual agents with antioxidant and AChE inhibitory activities. Therefore, the compounds obtained in this work may be served as model for the design of new xanthonic and flavonic derivatives with potential dual activity for treating AD.

**Keywords:** Alzheimer; Xanthenes; Flavones; Antioxidant; Acetylcholinesterase.

## Resumo

A doença de Alzheimer é uma doença neurodegenerativa associada com o avanço da idade, sendo designada como uma doença multifatorial. A terapêutica que atualmente é utilizada para tratar esta doença baseia-se principalmente na administração de inibidores da enzima acetilcolinesterase. No entanto, constata-se que esta não é totalmente eficaz. Assim, a administração de fármacos que atuem em mais do que um alvo no cenário bioquímico da doença de Alzheimer poderá ser considerada uma alternativa terapêutica promissora. Pelo exposto, nesta tese foram efetuados o planeamento, síntese e avaliação de xantonas e flavonas como antioxidantes com concomitante atividade inibidora da acetilcolinesterase.

Neste estudo foi sintetizada a xantona hidroxilada (**ICX1**), bem como o seu derivado metilado **ICX2**. Derivados aminados de **ICX2** e da baicaleína (**B**) foram também obtidos através da reação de Mannich. A estrutura dos compostos sintetizados foi estabelecida através da aplicação conjunta de diversas técnicas espectroscópicas, nomeadamente IV e RMN.

A atividade antioxidante dos compostos obtidos e de uma pequena biblioteca de outros derivados aminoxantónicos sintetizados anteriormente no nosso grupo de investigação (**PPX1**; **PPX2**; **PPX3**; **PPX4**; **PEX1** and **PEX3**), foi avaliada por diferentes métodos. As xantonas **ICX1** e **ICX2a** apresentaram atividade antioxidante como agentes quelantes de iões metálicos, enquanto **PEX1** e **PEX3** tiveram atividade antioxidante moderada através da captação de radicais livres. Tal como a baicaleína (**B**), o seu derivado **ICB1** exibiu um efeito antioxidante através da captação de radicais livres e por quelação de iões metálicos.

A atividade inibidora da acetilcolinesterase dos derivados xantónicos e flavónicos foi também avaliada. De entre os compostos testados, as bases de Mannich **ICX2a** e **ICB1** apresentaram um efeito moderado, sendo o composto **ICB1** o mais ativo. Deste estudo, os compostos **ICX2a** e **ICB1** surgiram como potenciais agentes *dual*.

No presente trabalho, foram também realizados estudos de *docking* do composto mais ativo (**ICB1**) com a acetilcolinesterase com o objetivo de estudar o seu mecanismo de ligação.

Em conclusão, as xantonas e flavonas aminadas mostraram possuir um esqueleto apropriado para o *design* de agentes *dual* com atividades antioxidante e inibidora da acetilcolinesterase. Os compostos obtidos neste estudo podem servir como modelos para o planeamento de novos derivados xantónicos e flavónicos com potencial atividade *dual* para o tratamento da doença de Alzheimer.

**Palavras-chave:** Alzheimer; Xantonas; Flavonas; Antioxidante; Acetilcolinesterase.

## Table of Contents

Acknowledgments .....	v
Abstract.....	vi
Resumo.....	vii
Table of Contents.....	viii
List of Figures.....	xi
List of Tables.....	xiv
List of Abbreviations and Symbols.....	xv
Outline of the Dissertation .....	xviii
<b>Chapter I. General Introduction .....</b>	<b>1</b>
1. Alzheimer´s disease (AD) .....	2
1.1. Alzheimer´s disease therapy .....	6
2. Xanthone derivatives .....	9
2.1. Chemistry of xanthenes.....	9
3. Flavone derivatives .....	10
3.1. Chemistry of flavones.....	10
4. Xanthone and flavone derivatives related with Alzheimer´s disease .....	13
4.1. Xanthone and flavone derivatives with anticholinesterase activity .....	13
4.2. Xanthone and flavone derivatives with antioxidant activity .....	26
4.3. Xanthone and flavone derivatives with dual activity .....	32
<b>Chapter II. Aims and Overview .....</b>	<b>41</b>
<b>Chapter III. Synthesis .....</b>	<b>44</b>
1. Xanthonic derivatives.....	45
1.1. Introduction .....	45
1.1.1. Synthesis of xanthenes: general methodologies .....	45
1.2. Results and discussion.....	54
1.2.1. Synthesis .....	54
1.2.1.1. 1,3,8- Trihydroxyxanthone ( <b>ICX1</b> ) .....	54
1.2.1.2. Amino derivatives of 1,3,8-trihydroxyxanthone .....	57
1.2.1.3. Methylated derivative of 1,3,8-trihydroxyxanthone ( <b>ICX2</b> ) .....	60

1.2.1.4. Amino derivative of 1,8-dihydroxy-3-methoxyxanthone ( <b>ICX2a</b> )	60
1.2.2. Evaluation of xanthenes purity	62
1.2.3. Structure elucidation	62
2. Flavone derivatives	66
2.1. Introduction	66
2.1.1. General methodologies for the synthesis of flavones	66
2.2. Results and discussion	70
2.2.1. Synthesis	70
2.2.1.1. Amino derivative of baicalein ( <b>ICB1</b> )	70
2.2.2. Evaluation of the flavone purity	71
2.2.3. Structure elucidation	71
3. Experimental	74
3.1. General Methods	74
3.2. Synthesis of xanthone derivatives	75
3.2.1. Synthesis of 1,3,8-trihydroxyxanthone ( <b>ICX1</b> )	75
3.2.2. Synthesis of 1,8-dihydroxy-3-methoxyxanthone ( <b>ICX2</b> )	76
3.2.3. Synthesis of 2- (dimethylamino)methyl)-1,8-dihydroxy-3-methoxyxanthone ( <b>ICX2a</b> )	76
3.2.4. Synthesis of baicalein amino derivative ( <b>ICB1</b> )	77
3.3. Evaluation of the purity	77
4. Conclusions	79
<b>Chapter IV. Biological Activity</b>	<b>80</b>
1. Antioxidant activity	81
1.1. Introduction	81
1.2. Results and discussion	82
1.2.1. DPPH radical scavenging activity	82
1.2.2. Iron chelating activity	84
1.2.3. Copper chelating activity	85
2. Acetylcholinesterase inhibitory activity	92
2.1. Introduction	92
2.2. Results and discussion	96
3. Xanthenes and flavones as dual agents: antioxidants and AChE inhibitors	98
4. Experimental	100
4.1. DPPH radical scavenging activity	100
4.2. Iron chelating activity	101

4.3. Copper chelating activity .....	101
4.4. Acetylcholinesterase inhibitory activity .....	102
4.5. Statistical analyses.....	103
5. Conclusions .....	104
 <b>Chapter V. Docking Studies .....</b>	 <b>105</b>
1. Results and discussion .....	106
2. Experimental.....	110
3. Conclusions .....	111
 <b>Chapter VI. Final Conclusions and Future Work .....</b>	 <b>112</b>
 <b>Chapter VII. References .....</b>	 <b>115</b>

## List of Figures

<b>Figure 1.</b> $A\beta$ peptid and SP formation according with “amyloid cascade hypothesis”.	3
<b>Figure 2.</b> NFT formation.	4
<b>Figure 3.</b> Hallmarks of AD.	6
<b>Figure 4.</b> Chemical structure of drugs used in current therapy of AD.	7
<b>Figure 5.</b> The structure of xanthone with numbering.	9
<b>Figure 6.</b> Flavone scaffold.	10
<b>Figure 7.</b> Biosynthetic pathway of flavones.	11
<b>Figure 8.</b> Mechanism of action of ACh and molecular target of the current therapy of AD.	14
<b>Figure 9.</b> Structures of arisugacin and tacrine.	15
<b>Figure 10.</b> 3D-Pharmacophoric model of AChE inhibitors.	19
<b>Figure 11.</b> Molecular docking studies with compound <b>35</b> and AChE.	20
<b>Figure 12.</b> Structure of triptexanthoside C.	20
<b>Figure 13.</b> Structure of macluraxanthone.	21
<b>Figure 14.</b> Docking analysis for macluraxanthone with AChE at 2D (A) and 3D (B) space.	22
<b>Figure 15.</b> Structure of compound <b>38</b> .	22
<b>Figure 16.</b> Molecular docking studies for compound <b>38</b> with AChE.	23
<b>Figure 17.</b> Structure of compounds <b>39</b> and <b>40</b> .	24
<b>Figure 18.</b> Structure of compounds <b>41</b> and <b>42</b> .	25
<b>Figure 19.</b> Structure of compounds <b>43</b> and <b>44</b> .	25
<b>Figure 20.</b> Structures of $\alpha$ -mangostin ( <b>45</b> ) and $\gamma$ -mangostin ( <b>46</b> ).	27
<b>Figure 21.</b> Structures of 1,4,5-trihydroxyxanthone ( <b>50</b> ) and symphoxanthone ( <b>51</b> ).	28
<b>Figure 22.</b> Major structural features for radical scavenging activity of flavones.	30
<b>Figure 23.</b> Structure of compound <b>53</b> .	31
<b>Figure 24.</b> Possible sites for chelating metal ions on flavones.	31
<b>Figure 25.</b> Structures of luteolin ( <b>54</b> ) and apigenin ( <b>55</b> ).	32
<b>Figure 26.</b> Building blocks used for the synthesis of a small library of Mannich bases.	42
<b>Figure 27.</b> Synthesis of simple xanthenes by GSS reaction.	45
<b>Figure 28.</b> Synthesis of simple xanthenes using salicylates and trimethylsilylaryl triflates.	46
<b>Figure 29.</b> Synthesis of simple xanthenes from the reaction of o-halobenzoic acids with aryne intermediates.	47

<b>Figure 30.</b> Synthesis of simple xanthenes by palladium-catalyzed annulations.	48
<b>Figure 31.</b> Synthesis of xanthenes by ortho-acylation of phenols with 2-substituted aldehydes.	48
<b>Figure 32.</b> Synthesis of xanthenes by reaction between ortho-substituted benzaldehydes and phenols, catalyzed by nanocatalysts (CuNPs).	49
<b>Figure 33.</b> Synthesis of xanthenes under microwave conditions promoted by ytterbium triflate.	49
<b>Figure 34.</b> Several alternatives for the synthesis of xanthenes through benzophenone route.	50
<b>Figure 35.</b> Synthesis of the benzophenone through a Friedel-Crafts acylation.	50
<b>Figure 36.</b> Synthesis of xanthenes through diaryl ether route.	51
<b>Figure 37.</b> Synthesis of xanthenes from chromen-4-one and some examples of xanthone obtained by this route.	52
<b>Figure 38.</b> Synthesis of xanthone <i>via</i> domino reactions.	53
<b>Figure 39.</b> General conditions for the synthesis of 1,3,8-trihydroxyxanthone ( <b>ICX1</b> ) by Eaton's reaction.	54
<b>Figure 40.</b> General conditions for the synthesis of 1,3,8-trihydroxyxanthone ( <b>ICX1</b> ) by GSS reaction.	55
<b>Figure 41.</b> General representation of Mannich reaction.	57
<b>Figure 42.</b> General conditions for the synthesis of amino derivative of 1,3,8-trihydroxyxanthone ( <b>ICX1</b> ) by Mannich reaction.	58
<b>Figure 43.</b> By-products accompanying Mannich reaction.	59
<b>Figure 44.</b> General conditions for the synthesis of methylated derivative of 1,3,8-trihydroxyxanthone ( <b>ICX2</b> ).	60
<b>Figure 45.</b> General conditions for the synthesis of amino derivative of 1,8-dihydroxy-3-methoxyxanthone ( <b>ICX2a</b> ) by Mannich reaction.	61
<b>Figure 46.</b> Main connectivities found in the HMBC of <b>ICX2</b> and <b>ICX2a</b> .	64
<b>Figure 47.</b> Synthesis of flavone <i>via</i> $\beta$ -diketone intermediate.	67
<b>Figure 48.</b> Synthesis of flavones under microwave conditions.	67
<b>Figure 49.</b> Typical oxidative cyclization of 2-hydroxychalcone.	68
<b>Figure 50.</b> Synthesis of flavones <i>via</i> cross coupling reactions.	68
<b>Figure 51.</b> Synthesis of flavones <i>via</i> Wittig-type reactions.	69
<b>Figure 52.</b> General conditions for the synthesis of amino derivative of baicalein ( <b>ICB1</b> ) by Mannich reaction.	70
<b>Figure 53.</b> Main connectivities found in the HMBC of <b>ICB1</b> .	72

<b>Figure 54.</b> Basic structure of the aminoxanthonic derivatives previously synthesized in our research group.	82
<b>Figure 55.</b> Copper interaction with <b>ICX1</b> and its effect in UV-Vis spectrum of this compound.	86
<b>Figure 56.</b> Copper interaction with <b>ICX2</b> and its effect in UV-Vis spectrum of this compound.	86
<b>Figure 57.</b> Copper interaction with <b>ICX2a</b> and its effect in UV-Vis spectrum of this compound.	87
<b>Figure 58.</b> Copper interaction with <b>PPX1</b> , <b>PPX2</b> , <b>PPX3</b> , <b>PPX4</b> , <b>PEX1</b> and <b>PEX3</b> and its effect in UV-Vis spectrum of each compound.	89
<b>Figure 59.</b> Copper interaction with <b>B</b> and <b>ICB1</b> and its effect in UV-Vis spectrum of each compound.	91
<b>Figure 60.</b> Sequence of reactions for detection of AChE activity by the Ellman's method.	92
<b>Figure 61.</b> Reaction from detection of AChE activity by the Marston's method.	93
<b>Figure 62.</b> Conversion of 7-acetoxy-1-methyl quinolinium iodide to 7-hydroxy-1-methyl quinolinium iodide by AChE.	94
<b>Figure 63.</b> AChE (surface) and docked <b>ICB1</b> .	107
<b>Figure 64.</b> AChE active site (surface) bound to crystallographic donepezil (pdb ID: 4EY7), galantamine (pdb ID: 4EY6), and huperzine A (pdb ID: 4EY5).	109

## List of Tables

<b>Table 1.</b> Inhibitory activities of dihydroxanthones against AChE.	15
<b>Table 2.</b> Natural xanthonic derivatives as potent AChE inhibitors.	17
<b>Table 3.</b> Inhibitory activity of xanthostigmine analogues on isolated AChE.	18
<b>Table 4.</b> Antioxidant activity of new C-glucopyranosylxanthones isolated from <i>Arrabidaea samydoides</i> .	27
<b>Table 5.</b> Diarylxanthones and (poly)hydroxyxanthones analogues with antioxidant activity.	29
<b>Table 6.</b> Xanthone and flavone derivatives with dual or multitarget activity.	33
<b>Table 7.</b> Reaction conditions and purification processes for the synthesis of 1,3,8-trihydroxyxanthone ( <b>ICX1</b> ) by Eaton's reaction and Modified GSS' reaction assisted by MW.	56
<b>Table 8.</b> Retention time and purity of <b>ICX1</b> , <b>ICX2</b> and <b>ICX2a</b> .	62
<b>Table 9.</b> IR data of 1,3,8-trihydroxyxanthone ( <b>ICX1</b> ) and its derivatives <b>ICX2</b> and <b>ICX2a</b> .	63
<b>Table 10.</b> <sup>1</sup> H NMR data of 1,3,8-trihydroxyxanthone ( <b>ICX1</b> ) and its derivatives ( <b>ICX2</b> and <b>ICX2a</b> ).	64
<b>Table 11.</b> <sup>13</sup> C NMR data of 1,3,8-trihydroxyxanthone ( <b>ICX1</b> ) and its derivatives ( <b>ICX2</b> and <b>ICX2a</b> ).	65
<b>Table 12.</b> Retention time and purity of <b>ICB1</b> .	71
<b>Table 13.</b> IR data of baicalein ( <b>B</b> ) and its derivative <b>ICB1</b> .	72
<b>Table 14.</b> <sup>1</sup> H NMR data of baicalein ( <b>B</b> ) and its amino derivative ( <b>ICB1</b> ).	73
<b>Table 15.</b> <sup>13</sup> C NMR data of baicalein ( <b>B</b> ) and its amino derivative ( <b>ICB1</b> ).	73
<b>Table 16.</b> DPPH radical scavenging activity of tested compounds.	83
<b>Table 17.</b> Iron chelating activity of tested compounds.	84
<b>Table 18.</b> UV spectral shifts of <b>ICX2a</b> .	88
<b>Table 19.</b> UV spectral shifts of <b>B</b> and <b>ICB1</b> .	91
<b>Table 20.</b> AChE inhibitory activity of tested compounds.	96
<b>Table 21.</b> DPPH radical scavenging, iron chelating and AChE inhibitory activities of <b>ICX2a</b> and <b>ICB1</b> .	98
<b>Table 22.</b> Docking scores of known AChE inhibitors and <b>ICB1</b> .	106

## List of Abbreviations and Symbols

<b><math>^{13}\text{C}</math> NMR</b>	Carbon Nuclear Magnetic Resonance
<b><math>^1\text{H}</math> NMR</b>	Proton Nuclear Magnetic Resonance
<b>ABP</b>	Acyl-binding Pocket
<b>Ach</b>	Acetylcholine
<b>AChE</b>	Acetylcholinesterase
<b>AChEI</b>	Acetylcholinesterase Inhibitors
<b>AD</b>	Alzheimer's Disease
<b>AMQI</b>	7-acetoxy-1-methyl quinolinium iodide
<b>ANR</b>	Anthocyanidin reductase
<b>APP</b>	Amyloid Precursor Protein
<b>AS</b>	Active Site
<b>A<math>\beta</math></b>	Amyloid beta
<b>brd</b>	Broad doublet
<b>brt</b>	Broad triplet
<b>BuChE</b>	Butyrylcholinesterase
<b>CNS</b>	Central Nervous System
<b>CHI</b>	Chalcone Isomerase
<b>CHKR</b>	Chalcone Polyketide Reductase
<b>CHS</b>	Chalcone Synthase
<b>d</b>	Doublet
<b>DAD</b>	Diode Array Detector
<b>dd</b>	Double doublet
<b>DMSO</b>	Dimethylsulphoxide
<b>DNA</b>	Deoxyribonucleic acid
<b>DPPH</b>	Di(phenyl)-(2,4,6-trinitrophenyl)iminoazanium
<b>DTNB</b>	5,5'-dithiobis-(2-nitrobenzoic acid)
<b>EDTA</b>	Ethylenediaminetetraacetic acid
<b>EMA</b>	European Agency for the Evaluation of Medicinal Products
<b>EtOAc</b>	Ethyl Acetate
<b>FDA</b>	Food and Drug Administration
<b>FHT</b>	Flavanone 3- $\beta$ -hydroxylase
<b>FLS</b>	Flavonol Synthase
<b>FNS</b>	Flavone Synthase

<b>GSS</b>	Grover Shah and Shah
<b>HSQC</b>	Heteronuclear Single Quantum Coherence
<b>HMBC</b>	Heteronuclear Multiple Bond Correlation
<b>HPLC</b>	High-Performance Liquid Chromatography
<b>HMQUI</b>	7-hydroxy-1-methylquinolinium iodide
<b>IC<sub>50</sub></b>	Concentration of the compound that causes 50% of inhibition
<b>IFD</b>	Isoflavone Dehydratase
<b>IFS</b>	Isoflavone Synthase
<b>iNOS</b>	Inducible Nitric Oxide
<b>IR</b>	Infrared Spectroscopy
<b><i>J</i></b>	Coupling Constant
<b>ki<sup>c</sup></b>	Values of inhibition constant for competitive inhibitor
<b>ki<sup>nc</sup></b>	Values of inhibition constant for non- competitive inhibitor
<b>LDL</b>	Low-density lipoprotein
<b>LAR</b>	Leucoanthocyanidin Reductase
<b>m</b>	Multiplet
<b>MAP</b>	Microtubule - associated Protein
<b>MAO</b>	Monoamine Oxidase
<b>MAOS</b>	Microwave Assisted Organic Synthesis
<b>MCM</b>	Multiple-compound Medication
<b>MeOH</b>	Methanol
<b>MMT</b>	Multiple-medication Therapy
<b>m.p.</b>	Melting Point
<b>MTDLs</b>	Multi-target Ligands
<b>MW</b>	Microwave
<b>NFT</b>	Neurofibrillary Tangles
<b>NMDA</b>	<i>N</i> -methyl-D-aspartate
<b>NMR</b>	Nuclear Magnetic Resonance
<b>PAS</b>	Peripheral Anionic Site
<b>PHF</b>	Paired Helical Filaments
<b>RNS</b>	Reactive Nitrogen Species
<b>ROS</b>	Reactive Oxygen Species
<b>s</b>	Singlet
<b>SiO<sub>2</sub></b>	Silica
<b>SP</b>	Senile Plaques
<b>TLC</b>	Thin Layer Chromatography

<b>UV</b>	Ultraviolet
<b>UV-vis</b>	Ultraviolet-visible
<b><math>\nu</math></b>	Wavenumber
<b><math>\delta_{\text{H}}</math></b>	Proton chemical shifts
<b><math>\delta_{\text{C}}</math></b>	Carbon chemical shifts

## **Outline of the Dissertation**

The present dissertation is organized in seven main parts:

### **Chapter I. General Introduction**

In this chapter, a brief introduction of some key concepts about Alzheimer's disease, as well as the therapy that is currently used in this disease are presented in section 1.

A brief description of the chemistry of xanthones and flavones as well as their importance in Medicinal Chemistry is highlighted in sections 2 and 3.

In section 4, xanthones and flavones with anticholinesterase and antioxidant activities and/or both dual effects are reviewed.

### **Chapter II. Aims and Overview**

This chapter summarizes the main objectives of this work.

### **Chapter III. Synthesis**

The chapter is divided into two parts: one part concerning the xanthonic derivatives (section 1) and another part related to flavonic derivatives (section 2). In the section 1.1., a brief introduction about general methodologies that are available for the synthesis of xanthones is presented. In section 1.2., the results obtained for the synthesis of xanthone derivatives and their structure elucidation are described and discussed.

The section 2, starts with a short introduction about general methodologies for the synthesis of flavones. In section 2.2., the results obtained for the synthesis of the amino derivative of baicalein and its structure elucidation are present and discussed.

In section 3, the general methods, reagents and procedures used for the synthesis are described.

In section 4, some conclusions about the results obtained in the synthesis of xanthone and flavone derivatives are draw.

## **Chapter IV. Biological Activity**

Chapter four is divided into two parts: one part concerning the antioxidant activity and another part related to the AChE inhibitory activity of xanthenes and flavones.

The section related to the antioxidant activity starts with an outline of the methods that are available for evaluation of the antioxidant activity (section 1.1.). In section 1.2., the results obtained for antioxidant activity of xanthone and flavone derivatives are shown and discussed.

The section 2 is related to AChE inhibitory activity and starts with a brief introduction where the available methods to evaluate this activity are summarized. The results obtained in assays with xanthone and flavone derivatives are presented and discussed in section 2.2..

In section 3, are indicated and discussed the results concerning the compounds that showed dual activity.

In section 4, the procedures used for the biological activity evaluation are described. This chapter ends with the main achievements of the present work.

## **Chapter V. Docking Studies**

This chapter starts with a description and a discussion of the results obtained in the docking studies of the most active compound with AChE.

In section 2, the general methods applied for the molecular docking studies are indicated.

In section 3, some conclusions about the results obtained in these docking studies are draw.

## **Chapter VI. Final Conclusions and Future Work**

This chapter consists of a general conclusion of the dissertation.

## **Chapter VII. References**

The references are presented at the end of this thesis. The references followed the ACS American Chemical Society style guide.

# CHAPTER I

## GENERAL INTRODUCTION

## 1. Alzheimer's disease (AD)

In 1906, Alois Alzheimer, a German psychiatrist, was the first to describe this pathology <sup>1</sup>. AD is a neurodegenerative disease which is associated with age and it is the cause of most cases of dementia observed in elderly <sup>2,3</sup>. Two types of AD were described, differing by the number of individuals in a family who are affected by this pathology. One is called "familiar" (if several family members have AD) and the second one is referred as "sporadic" (when only one member of the family or a few people suffer from AD) <sup>4</sup>. Typically, people with this disease have a progressive synaptic dysfunction, which may lead to the death of neurons in the neocortex, limbic system and subcortical regions of the brain. These disturbances in the brain, therefore, are the cause of some symptoms, such as personality and cognitive changes and memory deficits <sup>2</sup>. As this pathology is caused by a number of factors, including genetic, environmental and endogenous usually it is designated as a multifactorial <sup>4</sup>.

More recently, a lot of research in the area of neurodegenerative diseases, particularly in AD, has been made in order to understand its pathogenesis <sup>4,5</sup>. For most scientists and pathologists the main characteristics associated with this disease are the formation of senile plaques (SP) and neurofibrillary tangles (NFT) <sup>4-6</sup>.

SP are deposits composed of amyloid beta ( $A\beta$ ) peptide and the formation of these protein aggregates is currently explained by the "amyloid cascade hypothesis". **Figure 1** illustrates the formation of  $A\beta$  peptide according with this hypothesis, as well as its neurotoxicity <sup>4,6</sup>.

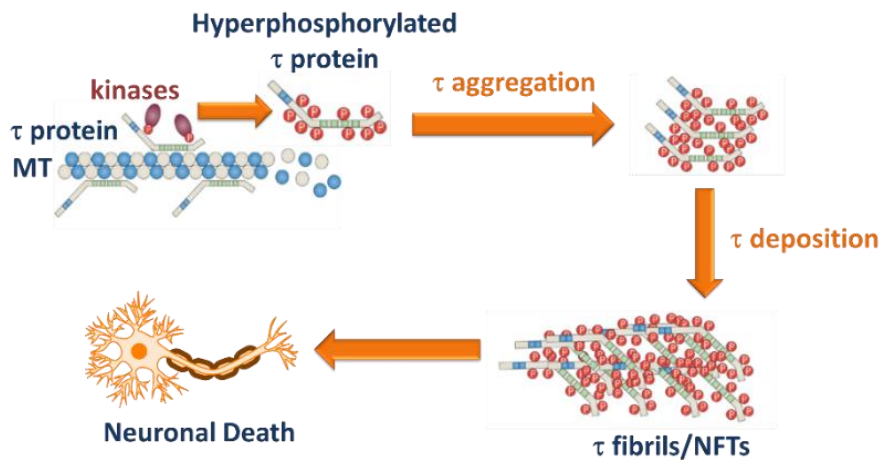


**Figure 1.** A $\beta$  peptide and SP formation according with “amyloid cascade hypothesis”. A $\beta$  peptide results from successive proteolytic cleavages by  $\beta$ -secretase and  $\gamma$ -secretase of amyloid precursor protein (APP). The neurotoxicity of A $\beta$  deposits in the SP is related to the fact that it promotes the activation of microglial cells; they can accumulate in mitochondrion promoting dysfunction leading ultimately to the neuronal death (adapted <sup>4</sup>).

NFT in AD are composed of straight filaments and paired helical filaments (PHF), which are composed of an abnormal hyperphosphorylated isoform of the microtubule-associated protein  $\tau$  (MAP) <sup>4,6,7</sup>. The formation of NFT in AD is summarized in **Figure 2**.

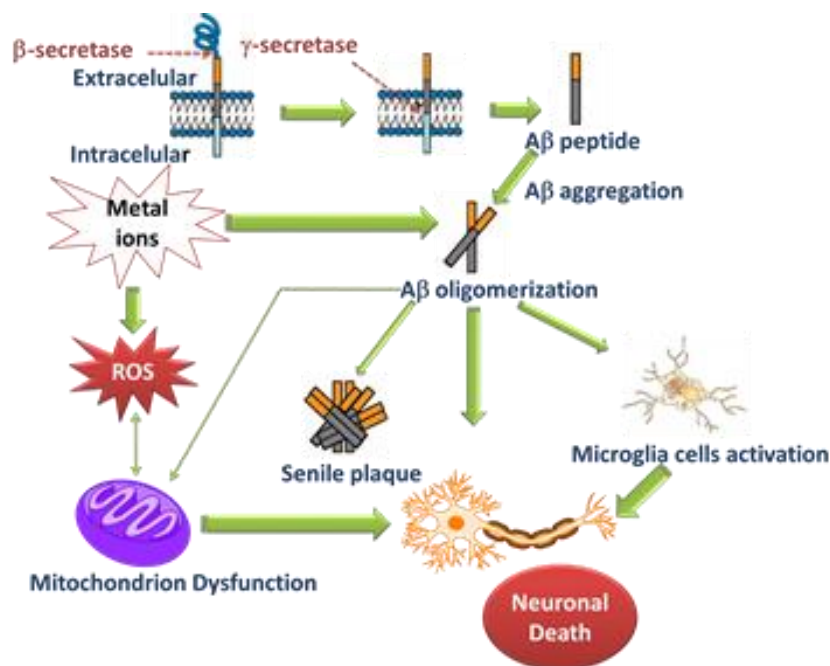


**Figure 2.** NFT formation.  $\tau$  protein has the function of stabilizing the neuronal microtubules, allowing them to play their role in cellular processes, namely the establishment of cell polarity and intracellular transport. The phosphorylation of  $\tau$  protein by protein kinases in the microtubule binding domain leads to the dissociation of this protein from microtubules and the formation of aggregates, which will culminate in the formation of NFTs. These molecular events will result in decrease of microtubules functions; disruption of neuronal transport; synaptic loss and, ultimately in cell death (adapted <sup>8</sup>).

In addition to the SP and NFP, AD is currently characterized by other hypotheses that attempt to explain the pathogenic nature of this disease. It is considered that inflammation, oxidative stress, metal ion dyshomeostasis and loss of cholinergic neural transmission contribute, in an interconnected way, to the development and the symptoms that characterize this disease <sup>4,9</sup>.

Regarding neuroinflammation, it has been considered as a hallmark of AD. In this kind of neuroinflammation, microglial cells are those which have attracted great interest from researchers <sup>4</sup>. These cells are defined as cells of the immune system of the Central Nervous System (CNS) because they constitute the population of resident macrophages in the CNS. Particularly, in AD, microglial cells play a dual role. On one hand, these cells have a neuroprotective role by degradation of Aβ by phagocytosis. On the other hand, Aβ can lead to activation of these cells, which produce several toxic substances, such as cytokines, chemokines and neurotoxins <sup>10</sup>. This proinflammatory activity attenuates the phagocytic activity of microglial cells, which contributes to neuronal degradation observed in AD. Due to the neuroprotective role of the microglial cells, the scientists considered that therapies

involving inhibition of the recruitment of monocytes and macrophages may not be adequate<sup>4,10</sup>.

Another pathogenic feature of AD is the oxidative stress. Patients with this condition have oxidative damage in all biomolecules (nucleic acids, lipids, carbohydrates and proteins)<sup>11</sup>. This oxidative damage will lead to a secondary excessive oxidative stress resulting from mitochondrial dysfunction, lack of energy supply, disruption in antioxidant defenses, and free radicals induced by A $\beta$  peptide or inflammation. The metal ions also contribute to oxidative stress, since they induce the production of reactive oxygen species (ROS) via the Fenton reaction. Specifically, copper ion with other metallic ions, in addition to promoting oxidative damage still have the ability to interfere with protein aggregation processes (A $\beta$  peptide and APP) in AD<sup>4,11,12</sup>.

Moreover, it has been found that the increase of acetylcholine (ACh) release at cholinergic synapses has favored behavioral and cognitive improvement in Alzheimer patients. These results have been achieved through the use of acetylcholinesterase inhibitors (AChEI). This enzyme, which is released into the synaptic cleft by activation of presynaptic and postsynaptic cholinergic receptors, has the function to cleave the neurotransmitter ACh into choline and acetic acid. Inestrosa *et al.* (1996) described another function of acetylcholinesterase (AChE), which is designated as "non-classical function"<sup>13</sup>. According to these researchers, this enzyme will act as a "pathological chaperone", because it will be responsible for stimulating the aggregation of A $\beta$  peptide by direct interaction of its peripheral anionic site (PAS) with the peptide fibrils<sup>4,9,13</sup>.

Finally, other enzyme that is also involved in the pathogenesis of AD is the monoamine oxidase (MAO)<sup>14,15</sup>. This enzyme is responsible for catalyzing the deamination of neurotransmitters (noradrenalin, dopamine and serotonin), and in the humans, MAO exists as two isozymes: MAO-A and MAO-B<sup>14,15</sup>. These two isozymes have different amino acidic constitution; different distribution and different substrate specificity, but both of them can be found in and outside the CNS<sup>14,15</sup>. In patients with AD, there was a high MAO activity, being that this enzyme acted as a hallmark of behavioral characteristics. It has been found that MAO is also responsible by causing cognitive dysfunction and disorders of the cholinergic neurons and it is associated with the formation of A $\beta$  peptide and NFTs in this disease<sup>14</sup>. **Figure 3** summarizes the main hallmarks of AD.

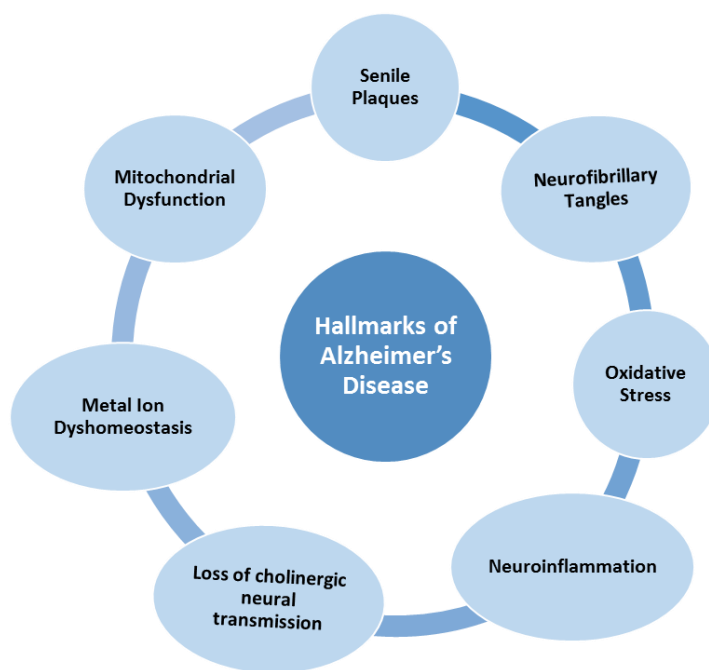


**Figure 3.** Hallmarks of AD.

### 1.1. Alzheimer's disease therapy

Considering the above hypotheses that contribute to the arising and development of AD there are several targets that may be associated with the current therapy. The most common drugs used in therapy are AChEI, inhibitors of  $\beta$ -secretase and  $\gamma$ -secretase, antioxidants, chelating agents and inhibitors of enzymes involved in the phosphorylation of  $\tau$  protein <sup>4</sup>.

Nowadays, a very common therapy for AD is based on the administration of AChEI. Tacrine, donepezil, rivastigmine and galantamine are AChEI used as drugs for the treatment of AD approved by the Food and Drug Administration (FDA) (**Figure 4**) <sup>4,16</sup>. However, only rivastigmine has been approved by the European Agency for the Evaluation of Medical Products (EMA)<sup>1</sup>. Although tacrine has been the first AChEI to be approved by the FDA, is currently rarely used due to its hepatotoxicity <sup>4,16</sup>. It should be noted that donepezil, rivastigmine and galantamine belong to the same therapeutic class, but have different pharmacodynamic and pharmacokinetic profiles. In this way, donepezil is a non-competitive reversible inhibitor of AChE; galantamine is a selective reversible inhibitor of

<sup>1</sup>[http://www.ema.europa.eu/ema/index.jsp?curl=pages/medicines/human/medicines/001183/human\\_med\\_001212.jsp&mid=WC0b01ac058001d124](http://www.ema.europa.eu/ema/index.jsp?curl=pages/medicines/human/medicines/001183/human_med_001212.jsp&mid=WC0b01ac058001d124)

AChE and a positive allosteric modulator of nicotinic receptors of pyramidal neurons and rivastigmine behaves as a slowly inhibitor of both AChE and butyrylcholinesterase (BuChE)<sup>16</sup>. Another alternative therapy to AChEI is the administration of memantine (**Figure 4**), a non-competitive antagonist of *N*-methyl-D-aspartate (NMDA) receptor. This also represents an effective therapy for the treatment of AD because in this pathology, an excessive glutamate release is associated with an intense activation of the NMDA receptor with consequent long - lasting influx of  $\text{Ca}^{2+}$  into neurons. In turn, this intracellular accumulation of  $\text{Ca}^{2+}$  leads to the activation of a cascade of events that contribute to increased cell death<sup>4,16</sup>.

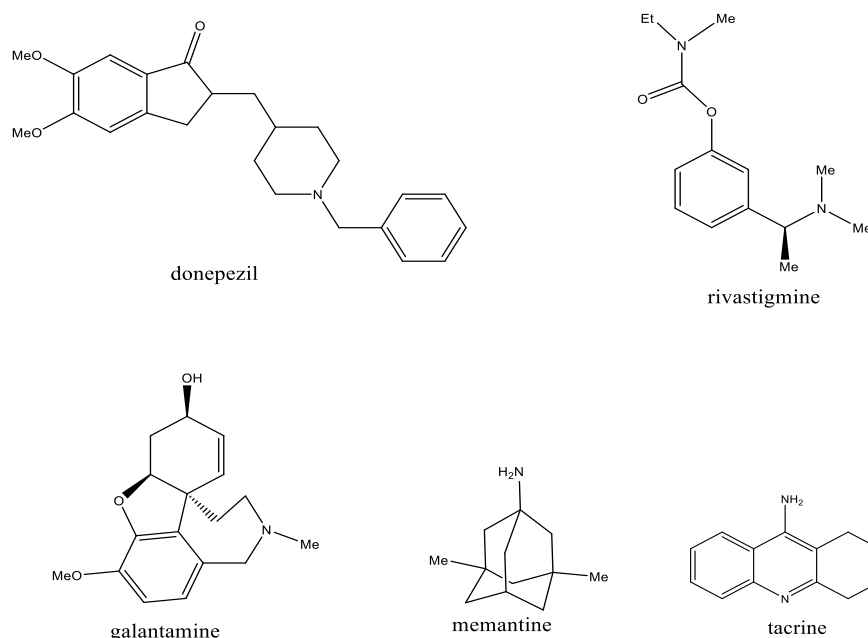


**Figure 4.** Chemical structure of drugs used in current therapy of AD.

Due to the multifactorial nature of AD, an effective therapy does not involve a single agent acting on a single target. Concerning this concept, three types of therapies that enhance the efficiency of treatments have been reported: “multiple-medication therapy” (MMT), “multiple-compound medication” (MCM) and “multi-target-directed ligands” (MTDLs)<sup>4,17</sup>. The first approach (MMT) consists in a therapy, where two or three drugs acting on different molecular targets are administered separately in different pharmaceutical formulations<sup>4,17</sup>. The MCM approach refers to the administration of a single pharmaceutical formulation which comprises several active substances with different molecular targets<sup>4,17</sup>. The last approach (MTDLs) involves the administration of a single chemical entity which

can simultaneously modulate multiple molecular targets <sup>4,17,18</sup>. MCM therapy can be considered as more advantageous than MMT therapy, since it allows a simple dosage application. MTDLs approach has demonstrated to be more suitable for treating complex diseases, such as neurodegenerative diseases, because the referred compounds show the ability to interact with multiple molecular targets responsible for the pathogenesis of the disease <sup>4,17,18</sup>.

## 2. Xanthone derivatives

### 2.1. Chemistry of xanthenes

In 1855, Schmidt, a German scientist, has isolated a crystalline compound from the pericarp rind of the mangosteen fruit. Due to its yellow color, the scientist has designated the compound by xanthone, which derives from the Greek word "xanthos" (yellow). Xanthenes are secondary metabolites that may be found in certain families of higher plants, lichens and fungi <sup>19,20</sup>.

Chemically, xanthenes are a class of oxygenated heterocyclic compounds with a dibenzo- $\gamma$ -pyrone scaffold (**Figure 5**) <sup>21,22</sup>.

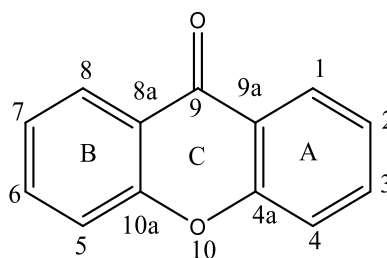


**Figure 5.** The structure of xanthone with numbering.

This class of secondary metabolites can be derived from different biosynthetic pathways. The biosynthetic pathways of xanthenes have been widely discussed by different authors for forty years and have been reported in several reviews <sup>23-28</sup>. In general, it is proposed that xanthenes from higher plants derived from a mixed acetate-shikimate pathway and xanthenes from fungi and lichens are acetate-derived <sup>22-24</sup>.

The natural xanthenes can be classified into six groups according to their substitution pattern: simple oxygenated xanthenes, xanthone glycosides, prenylated xanthenes, xanthonolignoids, bisxanthenes and miscellaneous xanthenes <sup>20,21</sup>.

In addition to natural xanthenes, there are a large variety of xanthenes of synthetic origin. Xanthenes obtained by synthesis may hold from simple substituents (hydroxy, methoxy, methyl, carboxy) to more complex substitution patterns (epoxide, azole, methylenedibutylolactone, aminoalcohol, sulfamoyl, methylthiocarboxylic acid and dihydropyridine) <sup>21</sup>.

### 3. Flavone derivatives

#### 3.1. Chemistry of flavones

In 1895, von Kostanecki and Tambor were the first to coin the term “flavones”<sup>29</sup> for natural products isolated from different kind of fruits and vegetables<sup>30</sup>.

Chemically, flavones are a class of flavonoids based on the backbone of 2-phenylchromen-4-one (2-phenyl-1-benzopyran-4-one), which have a three-rings referred as A, B and C (**Figure 6**)<sup>30,31</sup>.

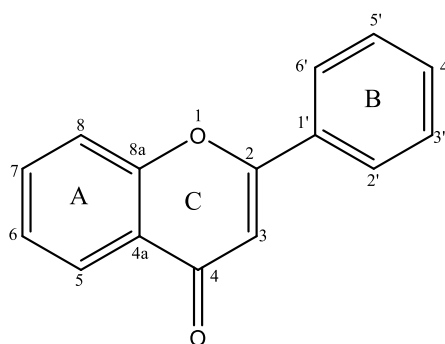


**Figure 6.** Flavone scaffold.

Flavones and all other flavonoids derived mainly from a biosynthetic pathway, where the crucial reaction is the condensation of three molecules of malonyl-CoA with one molecule of *p*-coumaroyl-CoA to give a chalcone intermediate (**Figure 7**). From this intermediate is formed flavanone. Derived from the flavanone structure, all other classes of flavonoids, including flavones, can be generated (**Figure 7**)<sup>29,30</sup>.

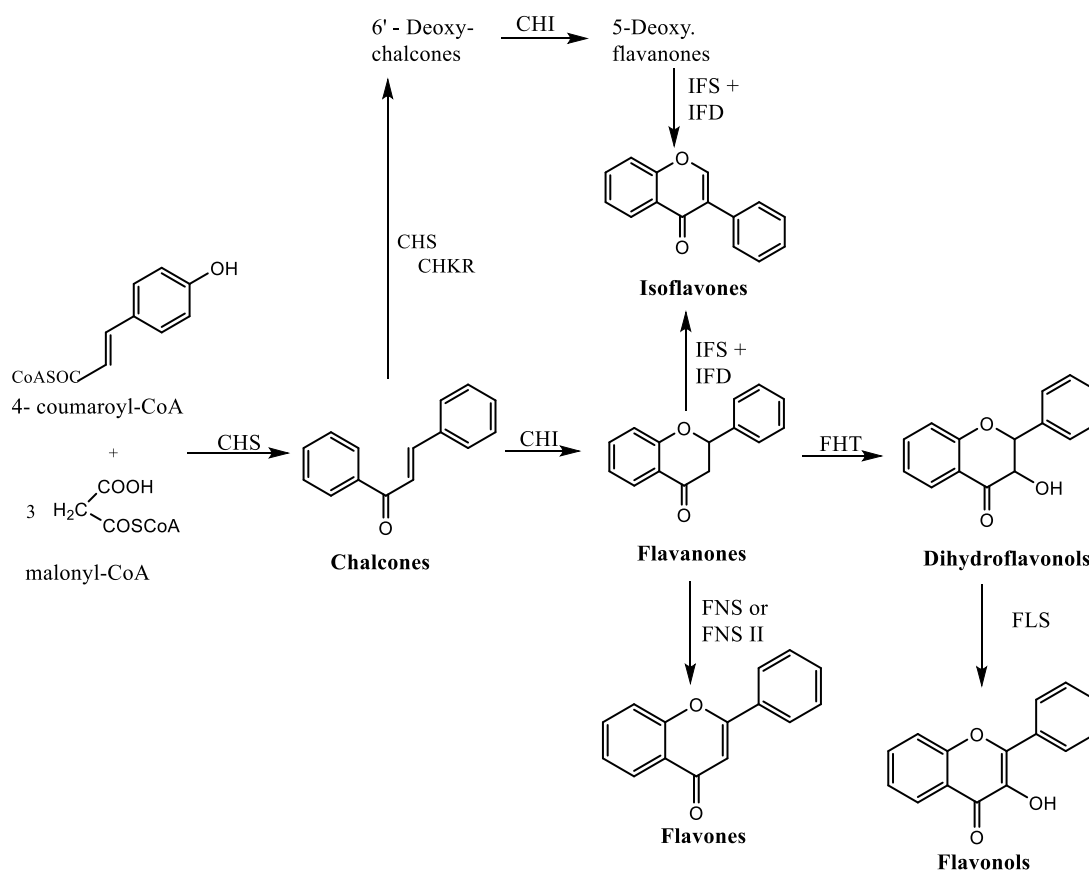


**Figure 7.** Biosynthetic pathway of flavones. Enzymes that are involved in this pathway are abbreviated as follows: CHS, chalcone synthase; CHKR, chalcone polyketide reductase; CHI, chalcone isomerase; FHT, flavanone 3- $\beta$ -hydroxylase; FNS, flavone synthase; FLS, flavonol synthase; LAR, leucoanthocyanidin reductase; ANR, anthocyanidin reductase; IFS, isoflavone synthase; IFD, isoflavone dehydratase (adapted <sup>29</sup>).

Natural flavones have different substitution patterns and they are classified into several subgroups according to hydroxylation, O-methylation, C-methylation, isoprenylation, methylenedioxy or O- and C-glycosides substitution <sup>29</sup>. This structural diversity of flavones is responsible for the wide variety of biological activities that this class of flavonoids presents <sup>32</sup>. Due to this, several research groups have taken flavone as lead compound for the synthesis of new derivatives with different functional groups at different positions on the flavone moiety <sup>30</sup>. For various natural and synthetic flavones, a variety of pharmacological activities have been evaluated and demonstrated, such as anti-inflammatory, anti-oestrogenic, anti-allergic, antioxidant, vascular, antitumor, cytotoxic, antimicrobial, antidiabetic, antiasthmatic and anti-ulcer activities <sup>30,31</sup>. Flavone moiety can be designated 'skeleton key' because it is an important core in many compounds that act

at different targets. In this context, flavones can be also considered a privileged structure in drug development, because flavone derivatives, depending of their substitution patterns, can reveal various biological / pharmacological activities, since they can act on several molecular targets that are involved in the pathology of different diseases <sup>30,33</sup>.

#### 4. Xanthone and flavone derivatives related with Alzheimer's disease

Xanthonones and flavones can be considered as privileged structures since their derivatives are capable of interacting with several different targets <sup>20,30,31,34</sup>.

Xanthonic and flavonic derivatives (natural and synthetic) that act on molecular targets of neurodegenerative diseases have been widely studied and explored <sup>34-39</sup>. Recently, researchers have given special attention to these derivatives as potential agents for the treatment of AD <sup>38</sup>. Some xanthonones and flavones have been shown to inhibit AChE and MAO enzymes <sup>37,38,40-44</sup>; to chelate metal ions <sup>45,46</sup>; to scavenge ROS <sup>38,47-49</sup> and to inhibit the aggregation of A $\beta$  peptides <sup>50-53</sup>.

Despite all these activities, the association between AChE inhibition and antioxidant activity has been considered as an attractive strategy for the development of new agents that can combat AD <sup>38,39,44</sup>. Accordingly, more relevance will be given to xanthonic and flavonic derivatives with anticholinesterase and antioxidant activities, as well as those with dual activity.

##### 4.1. Xanthone and flavone derivatives with anticholinesterase activity

According to the cholinergic hypothesis, patients with AD have a loss of cholinergic synaptic transmission which is also associated with low levels of ACh in the brain. This hypothesis is explained in **Figure 8**, as well as the action of AChEIs that are used in current therapy of AD <sup>9</sup>. However, these drugs have several disadvantages (**Figure 8**) and consequently, scientists have searched for more potent and selective compounds which are capable of inhibiting AChE.

Particularly, in recent years, xanthonic derivatives that inhibit AChE have been explored <sup>54,55</sup>.

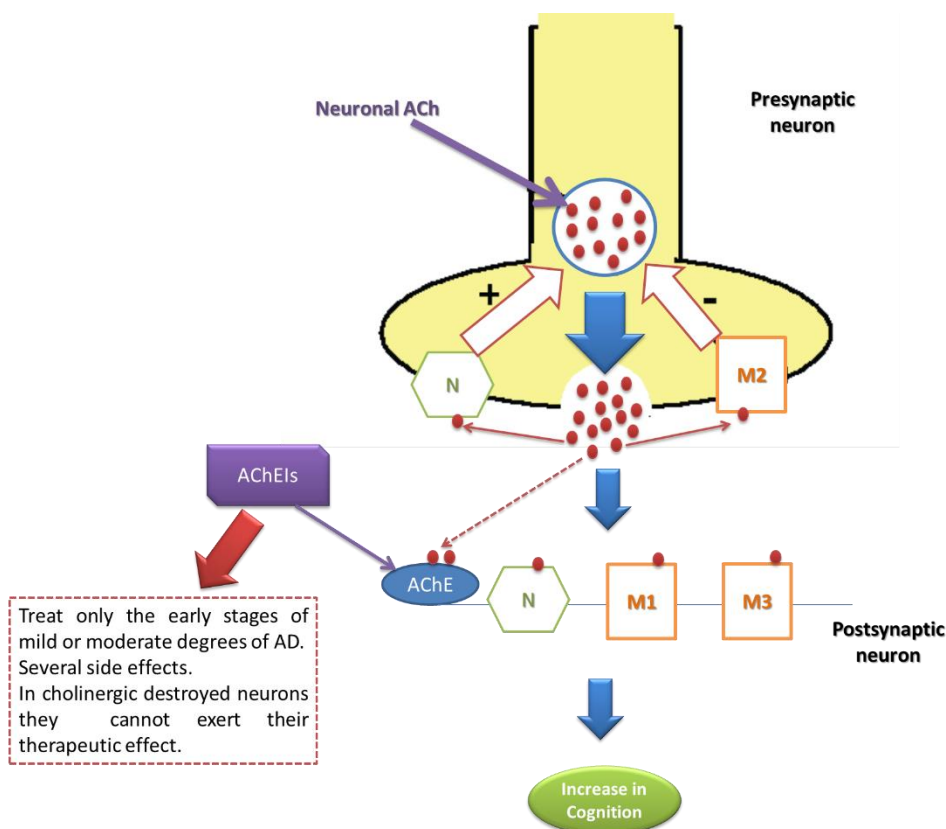


**Figure 8.** Mechanism of action of ACh and molecular target of the current therapy of AD. ACh that is released in the synaptic cleft will activate muscarinic (M1, M2 and M3) and nicotinic (N) receptors in presynaptic and postsynaptic neurons which results in increasing cognition. AChE whose function is to remove the ACh released into the synaptic cleft is the molecular target for AChEIs used in the current therapy of AD. However, AChEIs have various disadvantages, such as these drugs are able only to treat the early stages of mild or moderate degrees of AD; have several side effects and when cholinergic neurons are destroyed they tend to lose their therapeutic effect (adapted <sup>4</sup>).

Degen *et al.* (1999) developed their research in the area of AD, searching for new compounds based on arisugacin and on the conventional inhibitor tacrine (**Figure 9**). These scientists reported the synthesis of some dihydroxanthones, using the structures of arisugacin and tacrine as models (**Figure 9**) and respective evaluation of their inhibitory activity against AChE <sup>54</sup>. These results are listed in **Table 1**.

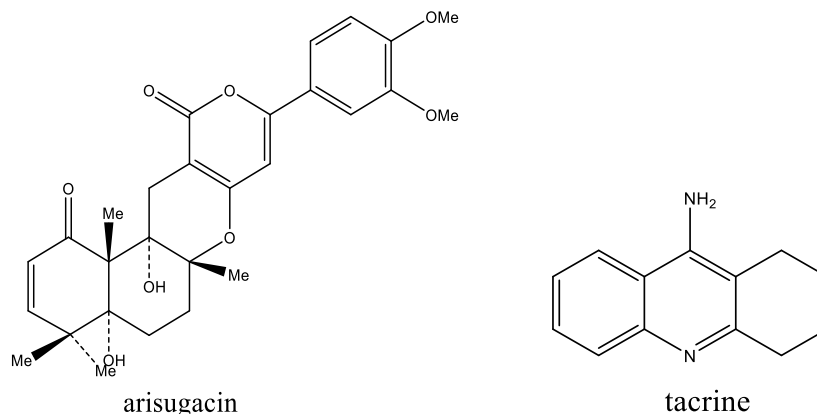


**Figure 9.** Structures of arisugacin and tacrine.

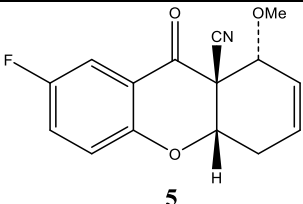
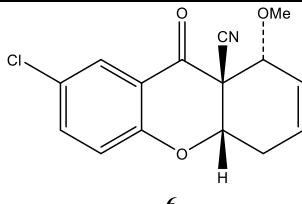
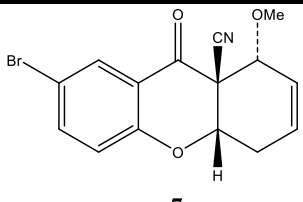
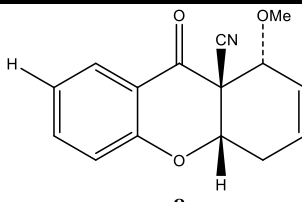
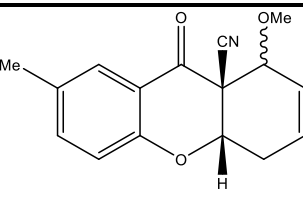
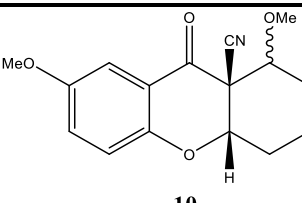
Considering compounds **1-4** that differ only in one aromatic ring, it can be seen that xanthone **1** has the most steric bulkiness, whereas compounds **3** and **4** have bridged bicyclic structures in one of the aromatic rings. The compound **1** has a double bond and a bulky group compared to compound **2**. However, compound **2** showed a lower  $IC_{50}$ , being the more potent AChE inhibitor <sup>54</sup>.

Regarding compounds **5-10**, that differ on the substituent on C-7, it was also verified that the derivatives **5** and **6** that have strong electron withdrawing groups (F, Cl) in one ring are those having a higher inhibitory activity against AChE <sup>54</sup>.

**Table 1.** Inhibitory activities of dihydroxanthones against AChE (adapted <sup>54</sup>).

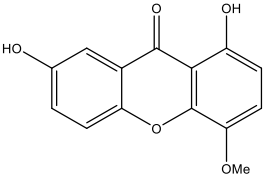
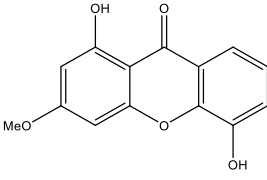
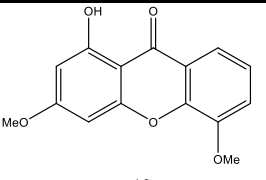
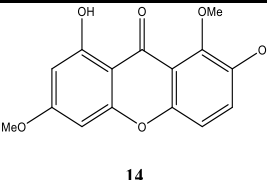
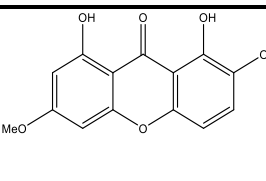
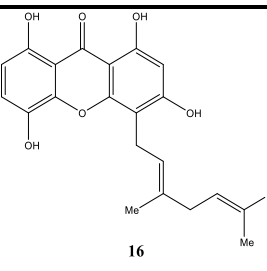
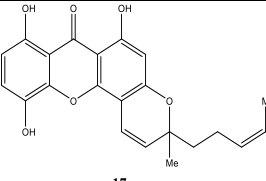
Dihydroxanthonic Derivatives	$IC_{50}$ ( $\mu M$ )	Dihydroxanthonic Derivatives	$IC_{50}$ ( $\mu M$ )
<p style="text-align: center;"><b>1</b></p>	$\geq 2.0$	<p style="text-align: center;"><b>2</b></p>	0.32
<p style="text-align: center;"><b>3</b></p>	$\geq 2.0$	<p style="text-align: center;"><b>4</b></p>	0.58

**Table 1** (*continuation*)

Dihydroxanthonic Derivatives	IC <sub>50</sub> (μM)	Dihydroxanthonic Derivatives	IC <sub>50</sub> (μM)
 <p style="text-align: center;"><b>5</b></p>	0.28	 <p style="text-align: center;"><b>6</b></p>	0.24
 <p style="text-align: center;"><b>7</b></p>	1.42	 <p style="text-align: center;"><b>8</b></p>	1.12
 <p style="text-align: center;"><b>9</b></p>	0.79	 <p style="text-align: center;"><b>10</b></p>	0.82

In 2004, Brühlmann *et al.* related the search of potent non-alkaloid inhibitors of AChE. In this study, a wide variety of natural products, including xanthenes, was used. Among the active xanthenes, xanthone **17** proved to be the most active compound (**Table 2**). From these results, Brühlmann *et al.* (2004) concluded that the xanthonic scaffold would not be the single condition for this kind of activity. In addition, the inhibitory activity was also influenced by the substitution pattern (hydroxylation and methoxylation) in the tricyclic hydroxy-methoxy-xanthenes (**11**, **12**, **13**, and **14**). The presence of an additional pyran ring linked to the xanthonic nucleus possessing a hydrophobic side chain like in xanthone **17** also appears to be a factor which improved the anticholinesterase activity <sup>41</sup>.

**Table 2.** Natural xanthonic derivatives as potent AChE inhibitors (adapted <sup>41</sup>).

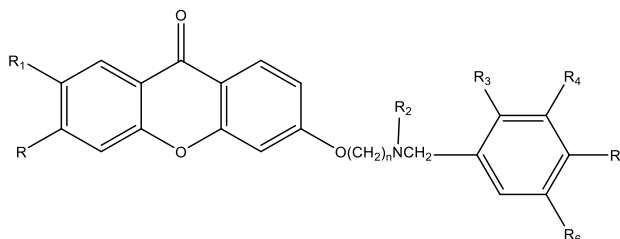
Xanthonic Derivatives	K <sub>i</sub> <sup>c</sup> [μM]	K <sub>i</sub> <sup>nc</sup> [μM]	Xanthonic Derivatives	K <sub>i</sub> <sup>c</sup> [μM]	K <sub>i</sub> <sup>nc</sup> [μM]
 11	15.1 ± 0.9	44 ± 10	 12	16.0 ± 1.8	53 ± 12
 13	4.3 ± 0.5	15.4 ± 0.1	 14	12.0 ± 0.5	28.7 ± 1.5
 15	n.d.	n.d.	 16	n.d.	26.8 ± 5.4
 17	n.d.	1.9 ± 1.4			

k<sub>i</sub><sup>c</sup> = values of inhibition constant for competitive inhibition; k<sub>i</sub><sup>nc</sup>=values of inhibition constant for non-competitive inhibition; Not determined (n.d.).

In 2007, Piazzzi *et al.* have discovered a new class of AChE inhibitors, using xanthostigmine (**34**) as lead compound. The anticholinesterase activity was evaluated for diverse non-carbamic xanthostigmine analogues (**Table 3**). The results obtained allowed to get some structure-activity assumptions. First, removal of the carbamic function from xanthostigmine allowed obtaining a reversible inhibitor (compound **18**). Moreover, it was found that changing the size of the alkoxy side chain also influenced the anticholinesterase activity of these analogues (compounds **18-27**). Finally, the substitution of the methyl group

on the amino function by an ethyl group did not change the ability of the compound **33** to inhibit the AChE <sup>56</sup>.

**Table 3.** Inhibitory activity of xanthostigmine analogues on isolated AChE (adapted <sup>56</sup>).



Compound	<i>n</i>	R	R <sub>1</sub>	R <sub>2</sub>	R <sub>3</sub>	R <sub>4</sub>	R <sub>5</sub>	R <sub>6</sub>	IC <sub>50</sub> (μM)
<b>18</b>	3	H	H	Me	H	H	H	H	2.68 ± 0.09
<b>19</b>	4	H	H	Me	H	H	H	H	6.25 ± 0.85
<b>20</b>	5	H	H	Me	H	H	H	H	7.78 ± 0.54
<b>21</b>	6	H	H	Me	H	H	H	H	2.89 ± 0.23
<b>22</b>	7	H	H	Me	H	H	H	H	2.82 ± 0.61
<b>23</b>	8	H	H	Me	H	H	H	H	10.3 ± 6.50
<b>24</b>	9	H	H	Me	H	H	H	H	152
<b>25</b>	10	H	H	Me	H	H	H	H	388
<b>26</b>	11	H	H	Me	H	H	H	H	626
<b>27</b>	12	H	H	Me	H	H	H	H	908
<b>28</b>	7	OMe	H	Me	H	H	H	H	7.84 ± 0.51
<b>29</b>	7	OMe	OMe	Me	H	H	H	H	2.32 ± 0.13
<b>30</b>	3	H	H	Me	OMe	H	H	H	3.40 ± 0.51
<b>31</b>	7	H	H	Me	OMe	H	H	H	2.18 ± 0.16
<b>32</b>	7	H	H	Me	H	OMe	H	H	40.0 ± 3.80
<b>33</b>	7	H	H	Et	OMe	H	H	H	3.15 ± 0.20
<b>34</b>	3	H	H	Me	H	H	H	OCONHMe	0.00030 ± 0.0001

Based on eighty xanthostigmine analogues that had already been reported as inhibitors of AChE <sup>56-59</sup>, Gupta and Mohan (2011) developed a 3D-pharmacophore model based in the virtual screening for the identification of selective inhibitors of AChE. In this

study, the pharmacophoric model **Hypo 1** was identified as the best quantitative pharmacophore model (**Figure 10**).

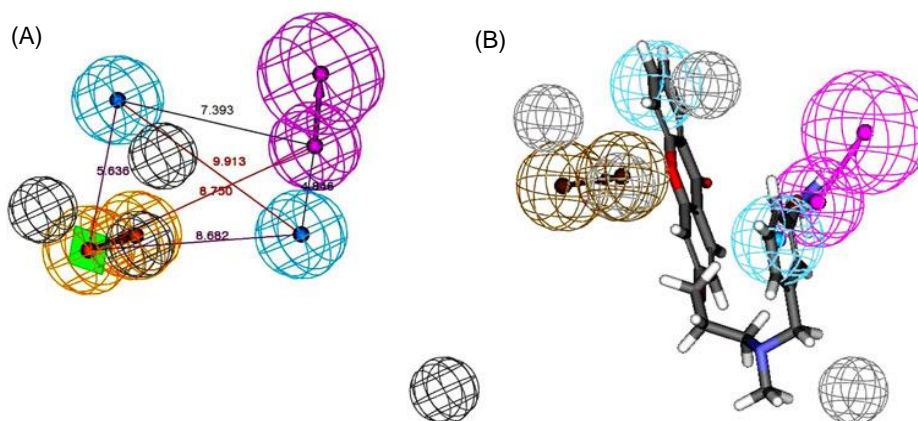


**Figure 10.** 3D-Pharmacophoric model of AChE inhibitors. **(A)** The best quantitative pharmacophoric model, **Hypo1**. **(B)** **Hypo1** with compound **35** ( $IC_{50} = 0.3$  nM) <sup>60</sup>.

After validation of the model, a sequential virtual screening procedure was performed based on **Hypo 1** pharmacophore in order to find AChE inhibitors that were able to bind to its active site (AS) and PAS <sup>60</sup>. From this molecular docking studies, the xanthostigmine analogue **35** emerged has the most active inhibitor. **Figure 11** shows the results obtained for the molecular docking studies with compound **35**. As shown in **Figure 11**, these studies reveal an hydrogen interaction between the quaternary nitrogen atom and Tyr334 of AChE; a water-mediated interaction between the NH of the amide group of compound **35** and Gln74 and a  $\pi$ - $\pi$  interaction between the aromatic moiety of the xanthone and Trp279 of the PAS of AChE. Thus, the xanthone derivative **35** is a potent inhibitor of AChE and can also interact with the PAS and AS of AChE. These results therefore suggested that this compound was also able to interfere with the aggregation of A $\beta$  peptide <sup>60</sup>.

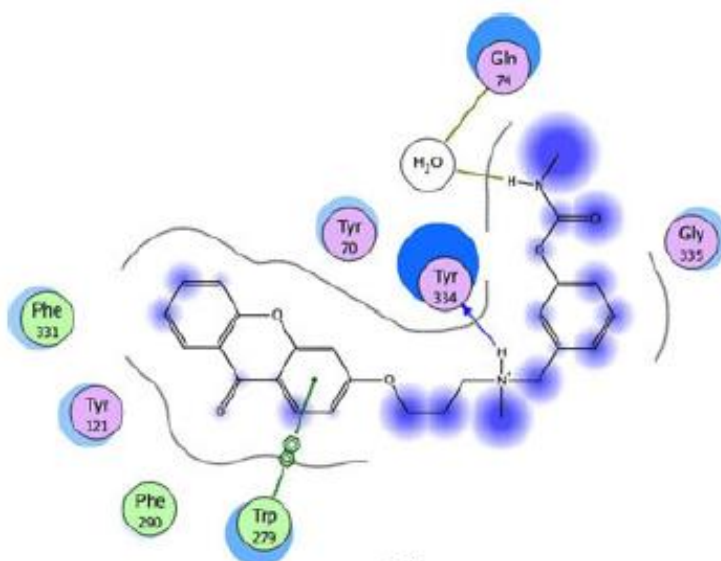
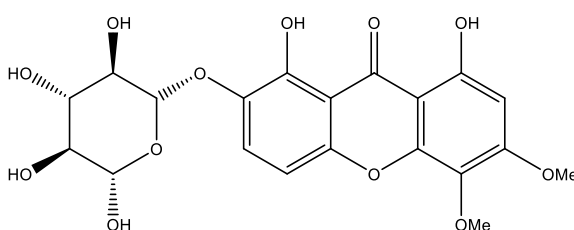


**Figure 11.** Molecular docking studies with compound **35** and AChE <sup>60</sup>.

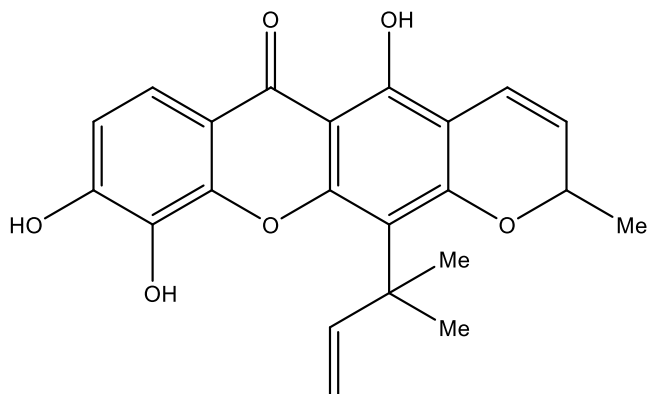
Urbain *et al.* (2008) isolated xanthenes from *Gentianella amarella ssp. acuta*, and tested their inhibitory activity against AChE. All xanthenes had a low inhibitory activity, except triptexanthoside C (**36**) (**Figure 12**), which inhibited AChE with  $IC_{50} = 13.8 \pm 1.6 \mu M$  <sup>42</sup>.



triptexanthoside C (**36**)

**Figure 12.** Structure of triptexanthoside C.

In 2009, Khan *et al.* evaluated the anticholinesterase activity of the macluraxanthone (**37**) (**Figure 13**). In this study, macluraxanthone was the compound that demonstrated a greater ability to inhibit AChE ( $IC_{50} = 8.47 \mu M$ ) in a non-competitive manner <sup>61</sup>.



macluraxanthone (37)

**Figure 13.** Structure of macluraxanthone.

Molecular docking studies with this xanthone showed that the most energetically favorable binding mode of the macluraxanthone to the binding site of AChE has a free binding energy of  $-15.49$  kcal/mol<sup>61</sup>. In this study, the interactions between macluraxanthone and the several subsites of AChE (PAS, AS and acyl-binding pocket (ABP)) at 2D and 3D space were also analyzed (**Figure 14**)<sup>61</sup>.

As a result of this analysis, it was observed that two oxygen atoms of macluraxanthone (HO-5 and HO-6) were responsible for establishing bounds with important amino acid residues of the PAS (Tyr124 and Tyr72). Moreover, the existence of several hydrophobic interactions with aminoacidic residues of the subsites PAS, AS and ABP of AChE was also observed (**Figure 14**)<sup>61</sup>.

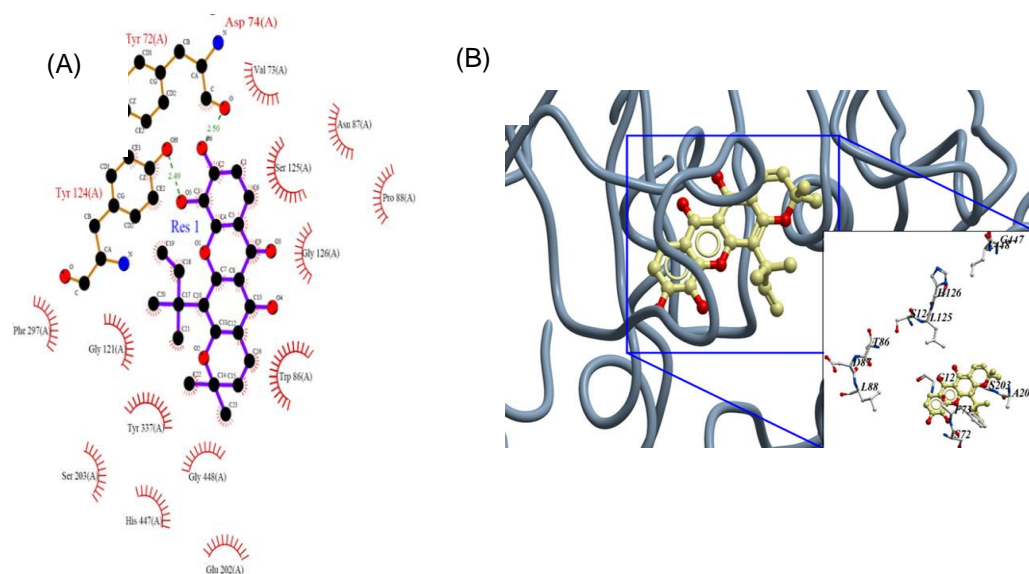


**Figure 14.** Docking analysis for macluraxanthone with AChE at 2D (A) and 3D (B) space. The 3D ribbon represents the enzyme, the yellow stick model is the most favorable binding mode of macluraxanthone, and the gray-sticks with numberings represent the interacting amino acid residues of the enzyme <sup>61</sup>.

More recently, Qin *et al.* (2013) synthesized various analogs of the 1,3-dihydroxyxanthone by Mannich reaction of this building block with secondary amines and formaldehyde and evaluated the anticholinesterase activity of the derivatives. The results showed that 2-((diethylamino)methyl)-1-hydroxy-3-(3-methylbut-2-enyloxy)-9*H*-xanthen-9-one (**38**) (Figure 15) was found to be one of the most active compound ( $IC_{50} = 2.60 \pm 0.13 \mu M$ ) <sup>34</sup>.

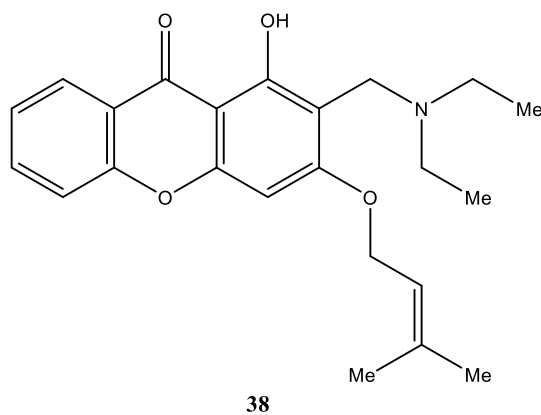


**Figure 15.** Structure of compound **38**.

This research group in order to determine the type of inhibition of this xanthonic compound also made enzyme kinetics studies and molecular docking studies by using the 3D crystal structures of human AChE (PDB code: 1EVE). Firstly, the analysis of enzyme kinetics demonstrated that compound **38** showed a mixed inhibition, in other words, it is able to bind to the AS and the PAS of AChE. Secondly, molecular docking studies showed the free binding energy corresponding to the most favorable binding mode of compound **38** and the bindings that are established between compound **38** and the active site of AChE. These results demonstrated that the most favorable binding mode of compound **38** had a free binding energy of -7.14 kcal/mol and therefore, this binding mode was used for docking simulations (**Figure 16A**). As shown in **Figure 16B**, it can be seen that the compound **38** extends into the deep cavity of the binding pocket of the enzyme, occupying the central hydrophobic region of the binding pocket of AChE composed of Tyr70, Tyr121, Trp279 and Phe290 residues. It was also observed that this xanthonic derivative extends for PAS which is situated near the Trp84 residue of the AS of the enzyme. Particularly, the aromatic ring of compound **38** establishes  $\pi$ - $\pi$  interactions with Trp279 residue of the PAS of AChE (**Figure 16C**). Thus, these observations enabled to confirm that compound **38**, in fact, showed a kind of mixed inhibition <sup>34</sup>.

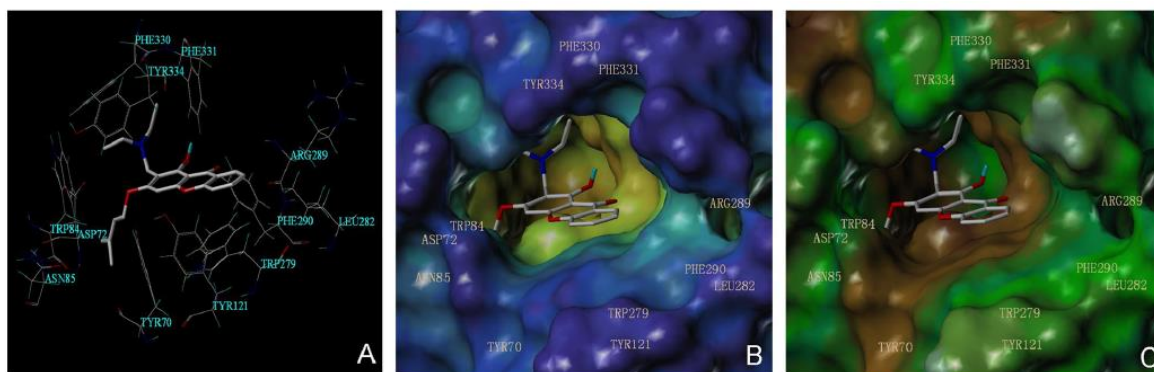


**Figure 16.** Molecular docking studies for compound **38** with AChE. (A) Interactions of compound **38** with active site of AChE. (B) The MOLCAD surface modeling with cavity depth potential of binding pocket of AChE. (C) The MOLCAD surface of the binding pocket with lipophilic potential <sup>34</sup>.

Diverse flavone derivatives have also revealed interesting AChE inhibitory activity <sup>62,63</sup>.

In 2011, Uriarte-Puevo and Calvo reviewed the AChE inhibitory activity of 128 flavonoids (natural and synthetic): 41 flavones, 21 flavanones, 35 flavonols, 25 isoflavones and 6 chalcones (see **Figure 7**) <sup>44</sup>. Among the reported flavonoids, flavones and isoflavones

were the compounds which showed higher activity against AChE. This suggests that the presence of a carbonyl group at C-4 appears to be important to AChE inhibitory activity. It can also be noted that flavones had greater AChE inhibitory activity than flavanones, indicating that the double bond at C2-C3 influences the inhibition of this enzyme <sup>44</sup>.

Considering all the studied flavones, 6,7-dimethoxy-2-[4-(piperidin-1-ylmethyl)-phenyl]-4*H*-chromen-4-one (**39**) ( $IC_{50} = 0.034 \mu M$ ) and 6,7-dimethoxy-2-[4-(pyrrolidin-1-ylmethyl)-phenyl]-4*H*-chromen-4-one (**40**) ( $IC_{50} = 0.055 \mu M$ ) (synthetic compounds) were the most active compounds (**Figure 17**). These results reveal that the substituents like pyrrolidin-1-ylmethyl or piperidin-1-ylmethyl at C-4' and the presence of methoxyl groups at C-6 or C-7 seem to favor the AChE inhibitory capacity of flavones <sup>44,55</sup>.

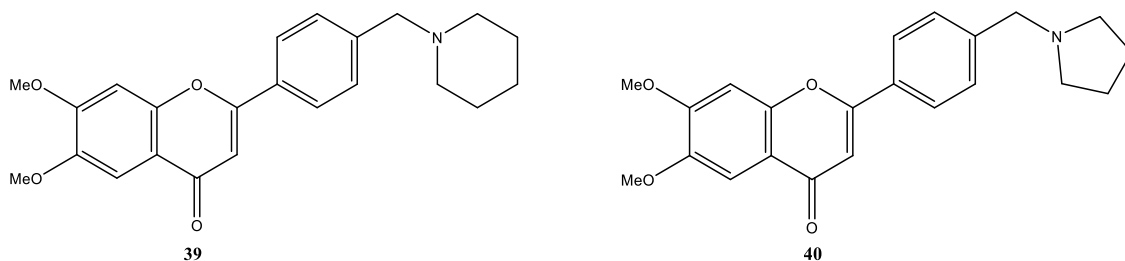


**Figure 17.** Structure of compounds **39** and **40**.

Concerning natural flavone glycosides, isolinariins A (**41**) and B (**42**) isolated from *Linaria reflexa*, revealed to be potent AChE inhibitors showing  $IC_{50}$  values of  $0.27 \mu M$  and  $0.30 \mu M$ , respectively. These results suggested that rhamnoglycoside moiety may exert an essential role in the interaction of the compound with AChE (**Figure 18**) <sup>44,64</sup>.

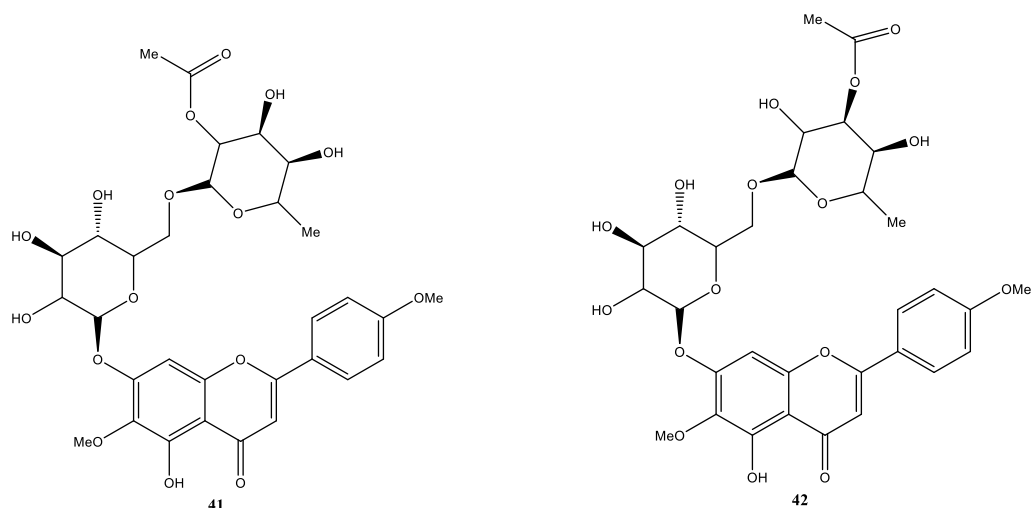


**Figure 18.** Structure of compounds **41** and **42**.

More recently, Duan *et al.* (2014) synthesized new Mannich base derivatives of 2'-hydroxy-3,4,4',6'-tetramethoxychalcone and 5-hydroxy-7,3',4'-trimethoxyflavone and evaluated their AChE inhibitory activities. The results showed that Mannich base analogues of flavone were more active than Mannich base derivatives of chalcone. Particularly, compounds **43** and **44** were the most active compounds with  $IC_{50}$  values of 0.54 and 1.39  $\mu$ M, respectively (**Figure 19**). These data highlighted the importance of the presence of *N,N*-diethyl or alicyclic amine (pyrrolidinyll ring) at C-6 of the flavone skeleton for enhance AChE inhibitory capacity <sup>65</sup>.

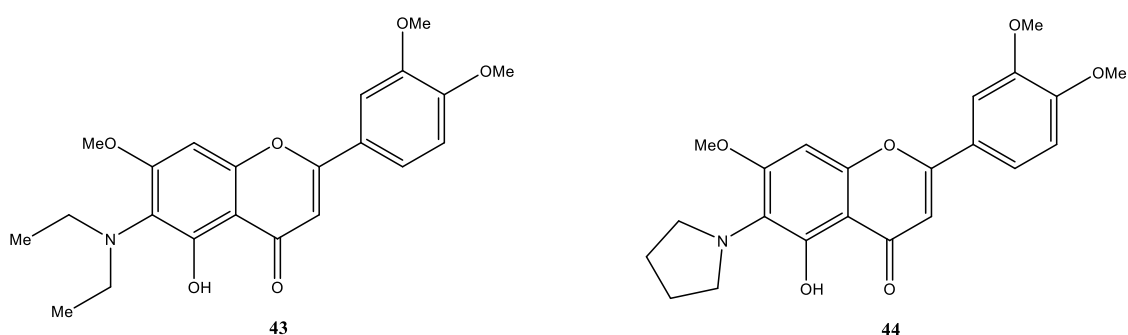


**Figure 19.** Structure of compounds **43** and **44**.

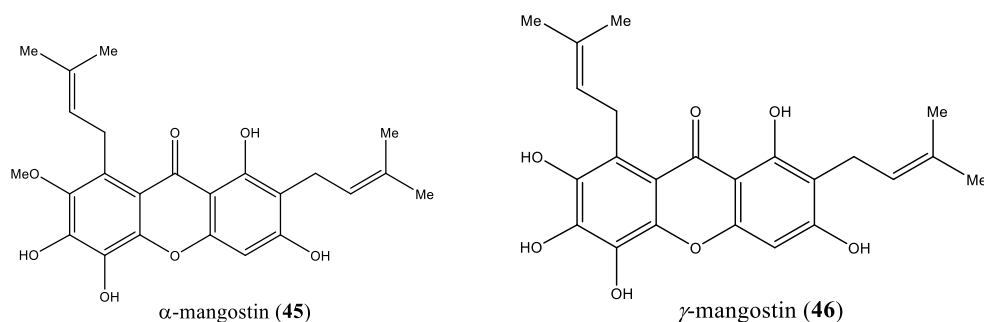
#### 4.2. Xanthone and flavone derivatives with antioxidant activity

AD is also associated with oxidative stress, which is responsible for causing various disturbances in the organism, such as inflammation, mitochondrial dysfunction and alterations of antioxidant defenses. Thus, in recent years, compounds with high antioxidant activity have been searched as possible drugs to be used in AD <sup>4</sup>. Antioxidants are compounds that have the function of inhibiting at low concentrations the oxidation of molecules in a biological system <sup>66</sup>. The antioxidants may, therefore, eliminate or prevent certain degenerative processes by several mechanisms, such as free radicals scavenging <sup>4,66</sup>. Among a variety of antioxidants, natural and synthetic xanthenes and flavones derivatives have been widely studied in recent years.

Xanthenes have shown a high capacity to scavenge a variety of ROS and reactive nitrogen species (RNS); inhibit oxidant enzymes activity <sup>36,49,67-69</sup> and induce antioxidant enzymes activity <sup>70,71</sup>.

Over the years, many researchers have studied the antioxidant activity of xanthonic derivatives isolated from several plants. In the Review “Xanthenes as Potential Antioxidants”, natural xanthenes that have revealed antioxidant activity are recorded <sup>36</sup>.

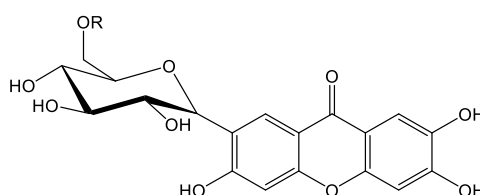
According to this review, the majority of xanthenes which possess antioxidant activity were isolated from different parts of *Garcinia* plants <sup>36</sup>. Among the bioactive secondary metabolites isolated from *Garcinia* sp., prenylated xanthenes,  $\alpha$ -mangostin (**45**) and  $\gamma$ -mangostin (**46**) (**Figure 20**) have been extensively reported for their diversity biological activities, including antioxidant activity <sup>72-75</sup>. Jung *et al.* (2006) reported that  $\gamma$ -mangostin was a more potent scavenger of peroxynitrite than  $\alpha$ -mangostin. These results, therefore, suggest that the presence of O-dihydroxyl system at C-6 and C-7 in  $\gamma$ -mangostin will be essential for this activity <sup>36,76</sup>.

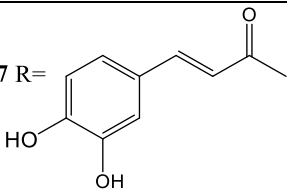
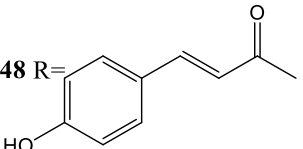


**Figure 20.** Structures of  $\alpha$ -mangostin (**45**) and  $\gamma$ -mangostin (**46**).

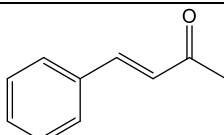
It was also found that glycosylated xanthenes showed antioxidant activity<sup>36</sup>. In 2003, Pauletti *et al.*, isolated three new C-glucopyranosylxanthenes (**Table 4**) from *Arrabidaea samydoides* and evaluated their antioxidant capacity<sup>77</sup>. The results of this study demonstrated that compounds **47** and **48** have the best antioxidant activity, whereas compound **49** has a lower antioxidant activity. It was also highlighted that compound **47** has a stronger ability to scavenge free radicals<sup>77</sup>. Considering the structure-activity relationship of these xanthonic compounds, it can be concluded that the increase of the number of catechol or hydroxyl groups in the structure leads to a higher free radical scavenging activity<sup>77</sup>.

**Table 4.** Antioxidant activity of new C-glucopyranosylxanthenes isolated from *Arrabidaea samydoides*.

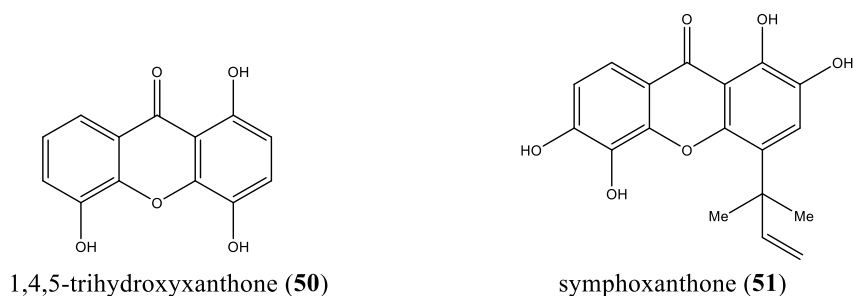


Compound	IC <sub>50</sub> ( $\mu$ M)
<b>47</b> R= 	17.81
<b>48</b> R= 	25.45

**Table 4** (continuation)

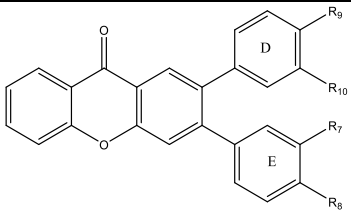
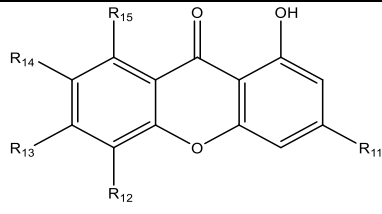
Compound	IC <sub>50</sub> ( $\mu$ M)
49 R= 	31.36

Among all xanthonic derivatives isolated from *Garcinia subelliptica*, 1,4,5-trihydroxyxanthone and symphoxanthone (**Figure 21**) were those that had a higher superoxide anion radical scavenging activity. This suggests that catechol group or 1,4-dihydroquinone moiety are important for the scavenger activity of these xanthes <sup>36,78,79</sup>.

**Figure 21.** Structures of 1,4,5-trihydroxyxanthone (**50**) and symphoxanthone (**51**).

In addition to the natural xanthes, several synthetic xanthes have demonstrated antioxidant activity. Some examples of synthetic xanthes with this biological activity, namely diarylxanthes and (poly)hydroxyxanthes, are presented in **Table 5** <sup>36</sup>.

**Table 5.** Diarylxanthenes and (poly)hydroxyxanthenes analogues with antioxidant activity.

Diarylxanthenes	(poly)Hydroxyxanthenes
 <p><b>52</b> R7 = R8 = R9 = R10 = H</p>	 <p><b>53a</b> R11=R12=R13=R14=R15=H</p>
<b>52b</b> R7= R8 = R10 = H; R9 = OH	<b>53b</b> R11=OH, R12=R13=R14=R15=H
<b>52c</b> R7 = R8 = H; R9 = R10 = OH	<b>53c</b> R11=R12=R14=R15=H, R13=OH
<b>52d</b> R7 = OH; R8 = R9 = R10 = H	<b>53d</b> R11=R12=OH, R13=R14=R15=H
<b>52e</b> R7 = R9 = OH; R8 = R10 = H	<b>53e</b> R12=R14=R15=H, R11=R13=OH
<b>52f</b> R7 = R8 = R10 = OH; R9 = H	<b>53f</b> R12=R3=R15=H, R11=R14=OH
<b>52g</b> R7 = R8 = OH; R9 = R10 = H	<b>53g</b> R12=R13=R14=H, R11=R15=OH
<b>52h</b> R7 = R8 = R9 = OH; R10 = H	
<b>52i</b> R7 = R8 = R9 = R10 = OH	

For all these xanthenes, the antioxidant activity was dependent on the number and position of hydroxyl groups. Particularly, the antioxidant activity of diarylxanthenes was influenced by the number and position of hydroxyl groups in D and E rings. Also, the presence of the catechol group in the D ring proved to be more important than the presence of this group in the E ring (compounds **52c** and **52f** showed a higher scavenger activity than compounds **52h** and **52g**)<sup>49,80</sup>.

Taking into account all these studies, in general, it can be concluded that xanthenes possessing a higher number of hydroxyl groups on xanthonic skeleton, show increased antioxidant capacity. Moreover, another important structural characteristic that contributes to its antioxidant activity is the presence of catechol moiety on the xanthone nucleus<sup>39</sup>.

In addition to the xanthenes, flavones also have the ability to act in oxidative stress through its antioxidant and protective activities<sup>81</sup>. This biological activity of flavones has been extensively studied and, in recent years, several articles have reported flavones as strong antioxidants<sup>30,38,81</sup>. Like other antioxidants (including xanthenes), flavones can exert this activity by different mechanisms: prevention of initiation of oxidation by inhibiting superoxide anion formation, degrading hydrogen peroxide and chelating or reducing metal ions; or as chain breaking antioxidants through scavenging free radicals<sup>82</sup>.

Particularly, flavones scavenge free radicals (ROS and RNS) through two different ways: transfer of hydrogen atom from the flavone to the free radical or transfer of an electron from the flavone to the free radical<sup>81</sup>.

Recently, Catarino *et al.* (2015) reviewed the major structural features of flavones that enhance their ability to scavenge free radicals. According to this review, the main structural requirements for this antioxidant activity are: the 2,3-olefinic bond in conjugation with 4-keto functional group in C ring; the catechol moiety in B ring and the hydroxyl group at C-5 (**Figure 22**)<sup>81</sup>.

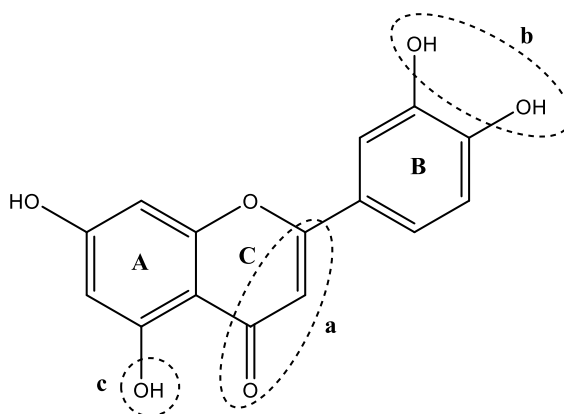
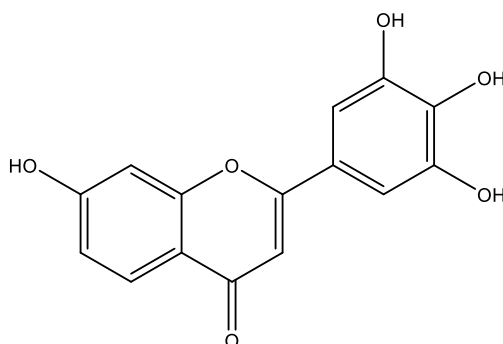


**Figure 22.** Major structural features for radical scavenging activity of flavones (adapted<sup>81</sup>).

In 2010, Hyun *et al.* studied the relationship between the number of hydroxyl groups on the flavone scaffold and its ability to scavenge free radicals. The researchers found that the increase of the number of hydroxyl groups is associated to the increase of the radical scavenging activity, being this effect particularly enhanced if two or more adjacent hydroxyl groups are present in the flavone nucleus. Therefore, 7,3',4',5'-tetrahydroxyflavone (**53**) was the most potent DPPH scavenger among the tested compounds (**Figure 23**)<sup>83</sup>.

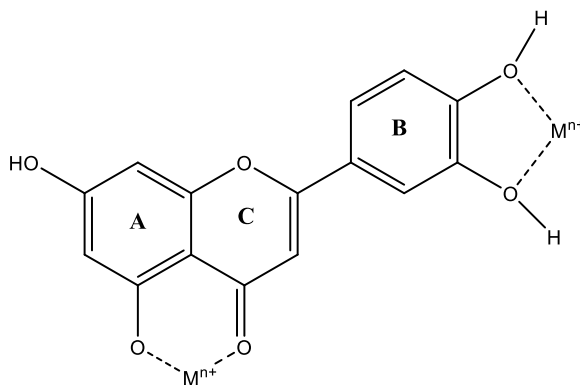
A recent study performed by Treesuwan *et al.* (2015), in order to elucidate the importance of the hydroxyl groups on the antioxidant activity of flavones, confirmed the requirements demonstrated by Hyun *et al.*<sup>84</sup>.



7,3',4',5'-tetrahydroxyflavone (53)

**Figure 23.** Structure of compound 53.

Flavones also act as antioxidant agents by chelating metal ions ( $\text{Fe}^{2+}$  and  $\text{Cu}^{2+}$ ). The interactions of flavones with these catalytically active metals play an important role, because they prevent the formation of oxidizing species and reactive hydroxyl radicals that can be generated through Fenton reactions<sup>81</sup>. In this framework, several studies indicated that the association between the hydroxyl group at C-5 (A ring) and the 4-keto group, as well as the presence of *ortho*-hydroxyl groups are important roles for flavone chelating activity (**Figure 24**)<sup>31,81</sup>.

**Figure 24.** Possible sites for chelating metal ions on flavones (adapted<sup>31</sup>).

Another mode of antioxidant action of flavones is through inhibiting enzymes responsible for the production of RNS and ROS, such as inducible nitric oxide synthase (iNOS) and xanthine oxidase. In fact, some flavones like luteolin (54) and apigenin (55) (**Figure 25**) can inhibit iNOS<sup>85-87</sup>. In addition, luteolin proved to be a potent inhibitor of xanthine oxidase<sup>31,81</sup>. In 1997, Rastelli *et al.* reported a model for flavones-xanthine oxidase interaction, based on the structural similarity of flavone with substrates or inhibitors of this

enzyme <sup>88</sup>. Details of this model may be found in the original article <sup>88</sup>, as well as in two review articles <sup>31,81</sup>. Besides this, other authors have proposed that the hydroxyl groups at C-6 and C-7 and the presence of catechol moiety or 3',4',5'-pyrogallol functionality on the flavone nucleus are important requirements for xanthine oxidase inhibition by flavones <sup>31,89</sup>.

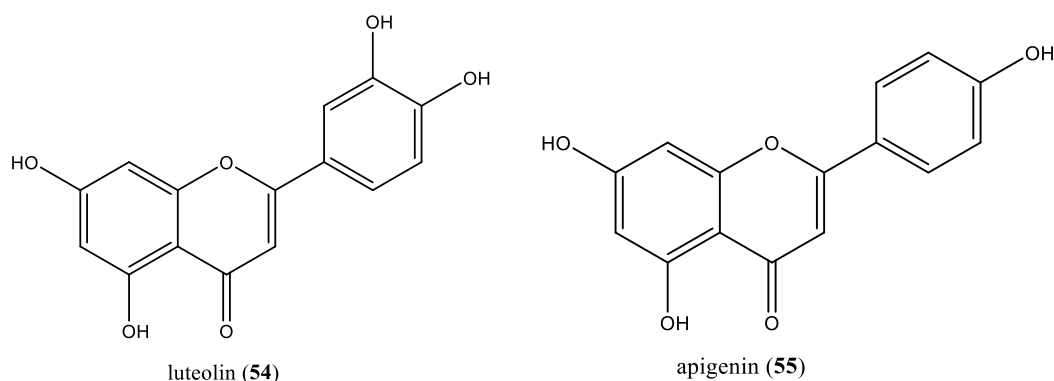


**Figure 25.** Structures of luteolin (54) and apigenin (55).

#### 4.3. Xanthone and flavone derivatives with dual activity

It is known that many factors are involved in the etiology of AD. Thus, the ideal therapy for this disease probably will include the administration of drugs that can act by multiple mechanisms, including AChE and BuChE inhibition and antioxidant activity <sup>4,34</sup>.

As previous described, in the context of AD, xanthenes and flavones can show various biological activities, such as ROS scavenging, and MAO and AChE inhibitory activities. Consequently, in recent years a great deal of effort has been devoted to find multi-target xanthone and flavone derivatives which can be used to treat AD <sup>37,38</sup>. In addition to AChE, BuChE is described as a pseudocholinesterase, since this enzyme distributed in the nervous system and plasma, can hydrolyze several choline esters, such as acetylcholine and butyrylcholine <sup>90</sup>. Recently, researchers have found that patients with AD have high level of this enzyme, that could also be responsible for the lower levels of acetylcholine associated with AD. Thus, BuChE may also be used as a target for the treatment of AD and xanthenes that are capable of inhibiting AChE and BuChE simultaneously, can act like anti-Alzheimer multipotent agents <sup>90</sup>.

Among the xanthone and flavone derivatives that had been described as AChE inhibitors in subchapter 4.1. some had also been reported as BuChE inhibitors. For

example, xanthenes **1-10** (**Table 1**) synthesized and tested by Degen *et al.* (1999) were able to inhibit both enzymes<sup>54</sup>. Among the xanthostigmine analogues synthesized by Piazzini *et al.* (2007), compounds **21**, **22**, **31** and **34** (**Table 3**) were the most active xanthenes against AChE and BuChE<sup>56</sup>. Moreover, Quin *et al.* (2013) evaluated the activity of the synthesized xanthonic derivatives against AChE and BuChE. Among the various compounds, xanthone **38** (**Figure 15**) showed the highest inhibitory activity against both enzymes<sup>34</sup>. In addition to xanthenes previously referred, flavones **69**, **70**, apigenin (**55**), kuwanon C (**67**) and morusin (**68**) were also described as AChE and BuChE inhibitors (**Table 6**)<sup>44,62,91</sup>.

Xanthone and flavone derivatives can also be considered as multitarget agents for AD not also for their activity as AChE and BuChE inhibitors but also by other mechanisms, namely those listed in **Table 6**.

**Table 6.** Xanthone and flavone derivatives with dual or multitarget activity.

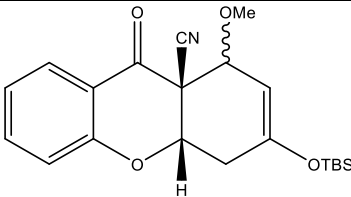
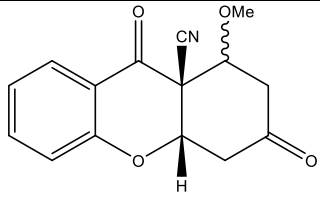
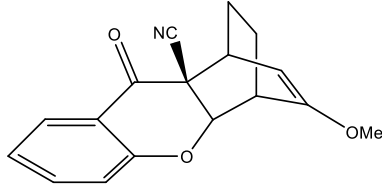
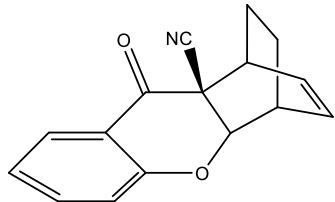
Compounds	Dual or Multitarget Activity
<b>Xanthone Derivatives</b>  <b>1</b>	AChE and BuChE inhibitor <sup>54</sup>
 <b>2</b>	AChE and BuChE inhibitor <sup>54</sup>
 <b>3</b>	AChE and BuChE inhibitor <sup>54</sup>
 <b>4</b>	AChE and BuChE inhibitor <sup>54</sup>

Table 6 (continuation)

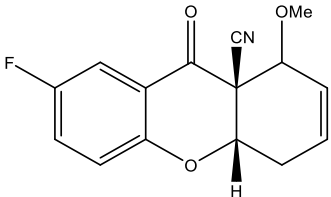
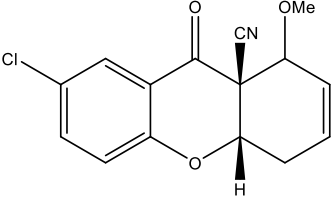
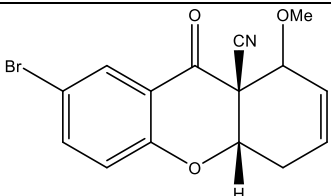
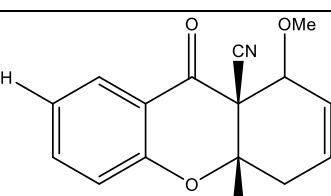
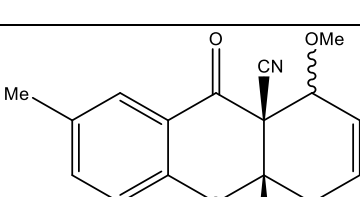
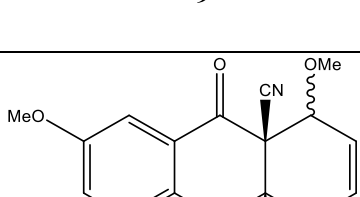
Compounds Xanthone Derivatives	Dual or Multitarget Activity
 <p style="text-align: center;"><b>5</b></p>	AChE and BuChE inhibitor <sup>54</sup>
 <p style="text-align: center;"><b>6</b></p>	AChE and BuChE inhibitor <sup>54</sup>
 <p style="text-align: center;"><b>7</b></p>	AChE and BuChE inhibitor <sup>54</sup>
 <p style="text-align: center;"><b>8</b></p>	AChE and BuChE inhibitor <sup>54</sup>
 <p style="text-align: center;"><b>9</b></p>	AChE and BuChE inhibitor <sup>54</sup>
 <p style="text-align: center;"><b>10</b></p>	AChE and BuChE inhibitor <sup>54</sup>

Table 6 (continuation)

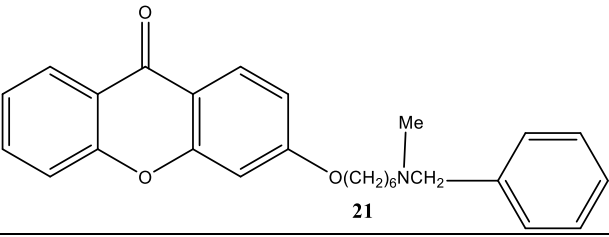
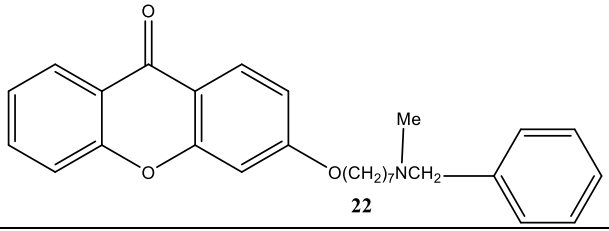
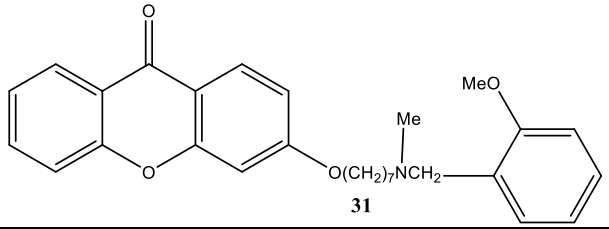
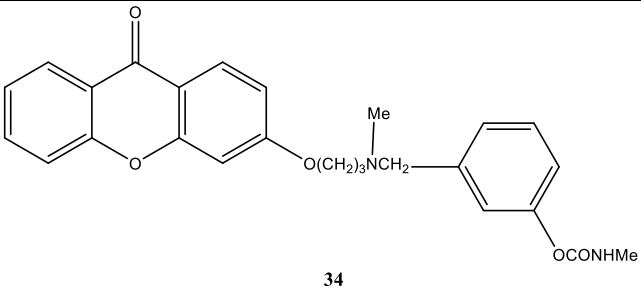
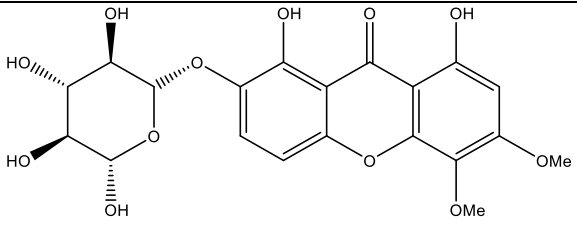
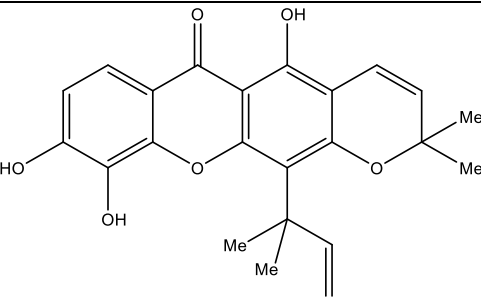
Compounds Xanthone Derivatives	Dual or Multitarget Activity
 <p style="text-align: center;"><b>21</b></p>	AChE and BuChE inhibitor <sup>56</sup>
 <p style="text-align: center;"><b>22</b></p>	AChE and BuChE inhibitor <sup>56</sup>
 <p style="text-align: center;"><b>31</b></p>	AChE and BuChE inhibitor <sup>56</sup>
 <p style="text-align: center;"><b>34</b></p>	AChE and BuChE inhibitor <sup>56</sup>
 <p style="text-align: center;">triptexanthoside C (<b>36</b>)</p>	MAO and AChE inhibitor <sup>42</sup>
 <p style="text-align: center;">macluraxanthone (<b>37</b>)</p>	AChE inhibitor <sup>92</sup> and antioxidant activity (hydroxyl, superoxide anion and DPPH radicals scavenging) <sup>61,93</sup>

Table 6 (continuation)

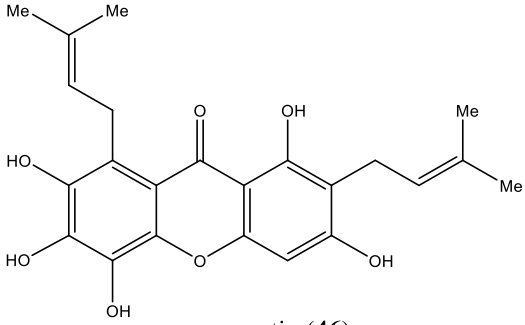
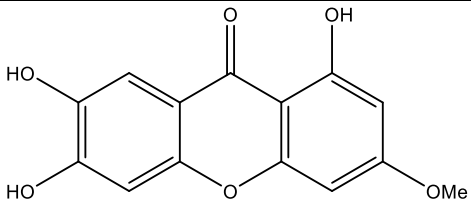
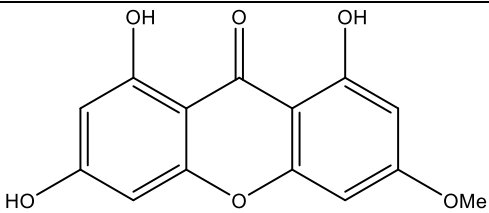
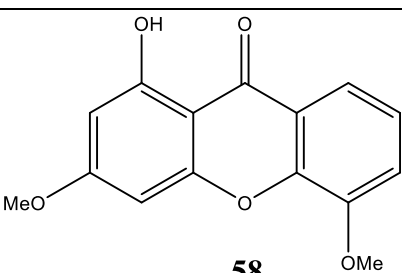
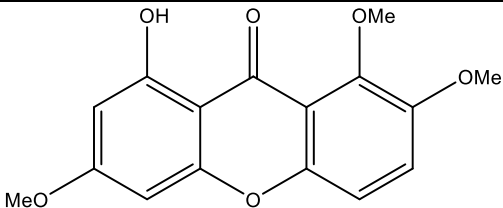
Compounds Xanthone Derivatives	Dual or Multitarget Activity
 <p style="text-align: center;"><b>γ-mangostin (46)</b></p>	<p>AChE inhibitor <sup>34,75</sup> and antioxidant activity (superoxide anion, peroxynitrite, hydroxyl and DPPH radicals scavenging) <sup>36,72,76</sup></p>
 <p style="text-align: center;"><b>56</b></p>	<p>MAO inhibitor and antioxidant activity (DPPH radical scavenging) <sup>37</sup></p>
 <p style="text-align: center;"><b>57</b></p>	<p>MAO inhibitor and antioxidant activity (DPPH radical scavenging) <sup>37</sup></p>
 <p style="text-align: center;"><b>58</b></p>	<p>MAO and AChE inhibitor <sup>38</sup></p>
 <p style="text-align: center;"><b>59</b></p>	<p>MAO and AChE inhibitor <sup>38</sup></p>

Table 6 (continuation)

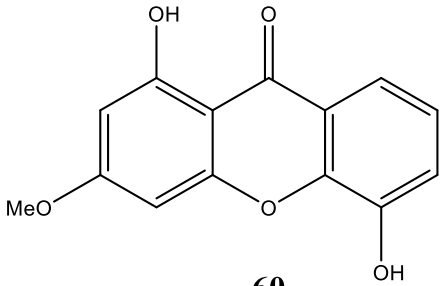
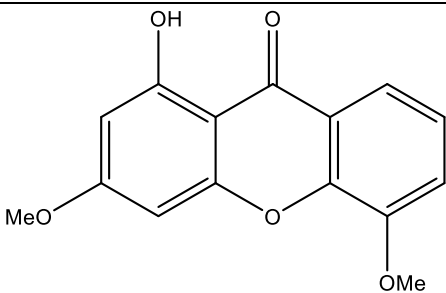
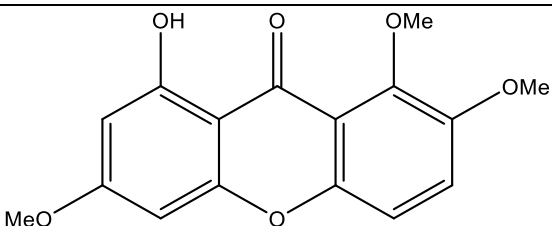
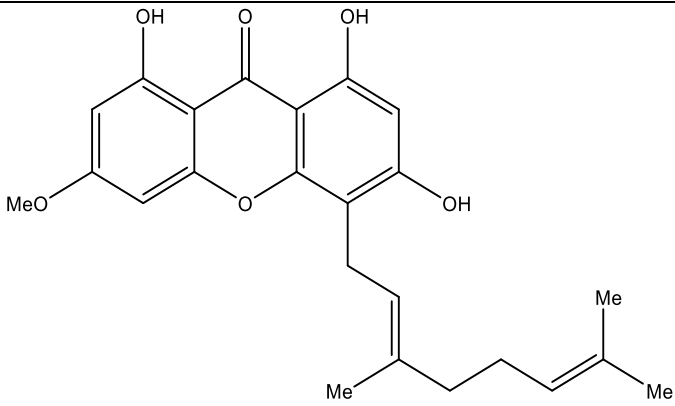
Compounds Xanthone Derivatives	Dual or Multitarget Activity
 <p style="text-align: center;"><b>60</b></p>	MAO and AChE inhibitor <sup>38</sup>
 <p style="text-align: center;"><b>61</b></p>	MAO and AChE inhibitor <sup>41</sup>
 <p style="text-align: center;"><b>62</b></p>	MAO and AChE inhibitor <sup>41</sup>
 <p style="text-align: center;"><b>63</b></p>	MAO and AChE inhibitor <sup>41</sup>

Table 6 (continuation)

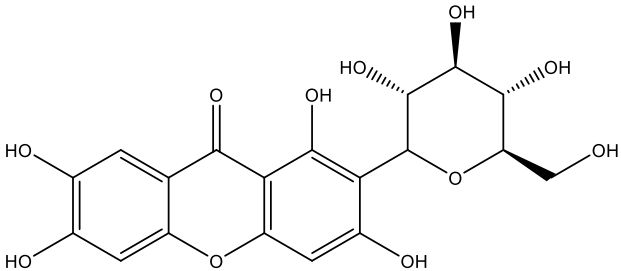
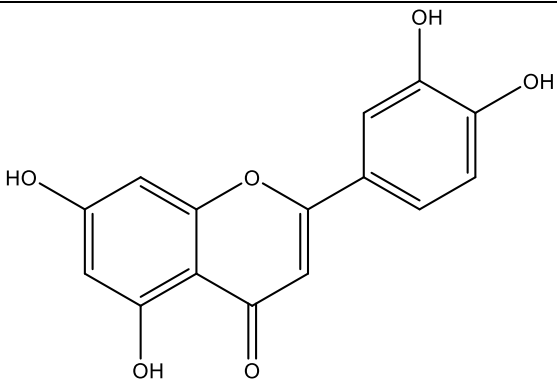
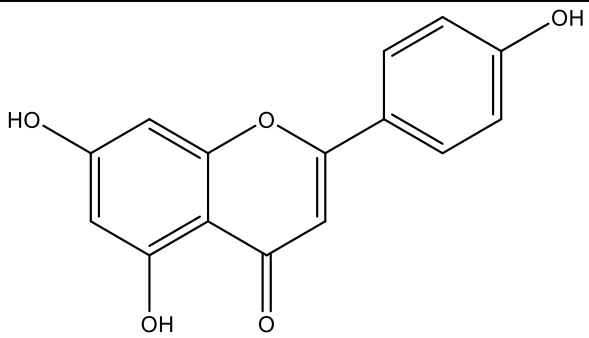
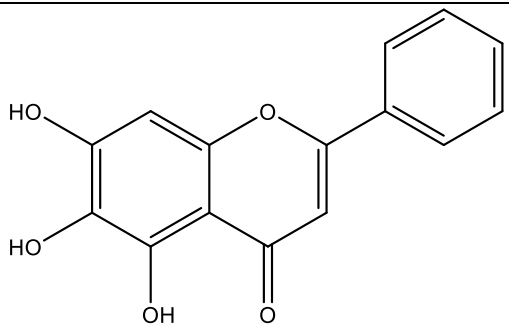
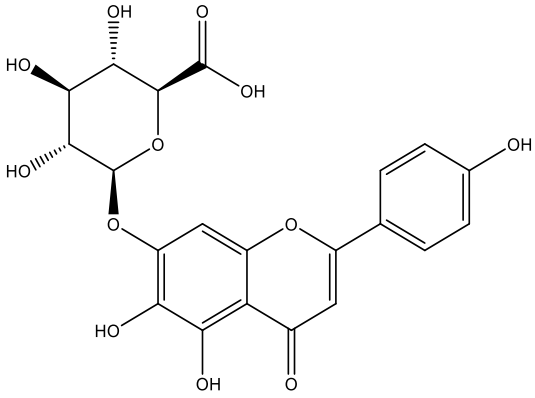
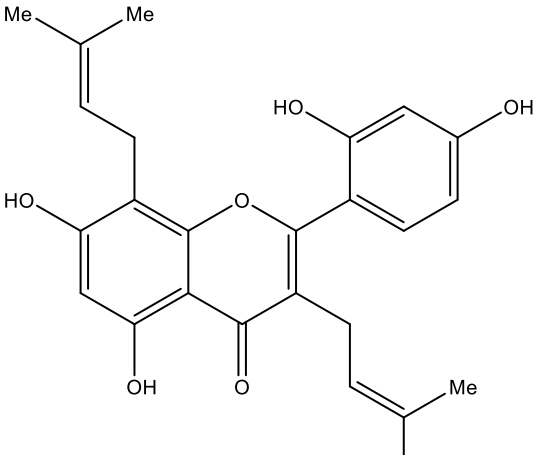
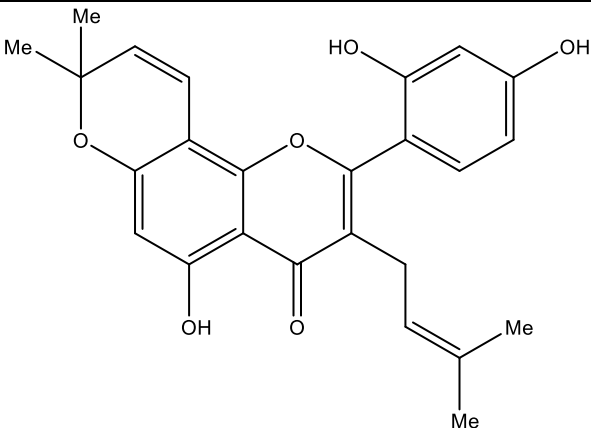
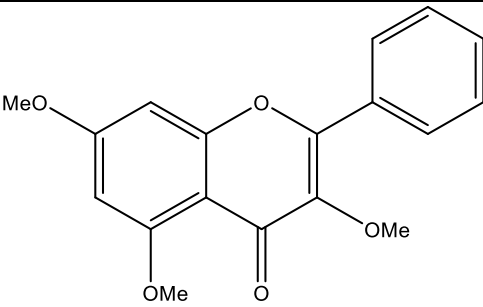
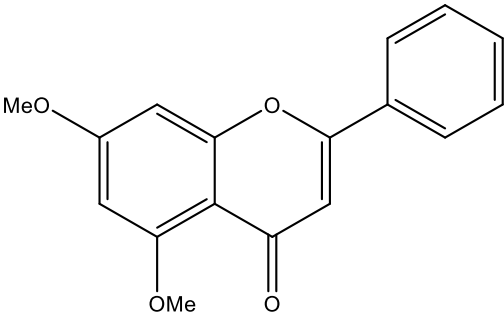
Compounds Xanthone Derivatives	Dual or Multitarget Activity
 <p style="text-align: center;">mangiferin (64)</p>	<p>AChE inhibitor <sup>94</sup> and antioxidant activity (superoxide anion, DPPH radical and hydrogen peroxide scavenging; cytochrome c reduction; protection against lipid peroxidation, oxidation of proteins and DNA fragmentation) <sup>95-97</sup></p>
Flavone Derivatives	
 <p style="text-align: center;">luteolin (54)</p>	<p>AChE <sup>55</sup> and MAO inhibitor <sup>98</sup> and antioxidant activity (nitric oxide, hydrogen peroxide, superoxide anion, peroxynitrite, DPPH and ABTS radicals scavenging; metal chelating activity; prevention of lipid peroxidation) <sup>85,99-101</sup></p>
 <p style="text-align: center;">apigenin (55)</p>	<p>AChE <sup>55</sup>, BuChE <sup>91</sup> and MAO inhibitor <sup>43</sup> and antioxidant activity (nitric oxide, superoxide anion, peroxynitrite and hydroxyl radicals scavenging; metal chelating activity; prevention of LDL oxidation and inhibition of iNOS) <sup>85,102-106</sup></p>
 <p style="text-align: center;">baicalein (65)</p>	<p>AChE inhibitor <sup>107</sup>, anti-A<math>\beta</math> aggregation effect <sup>108</sup> and antioxidant activity (nitric oxide, superoxide anion, hydrogen peroxide, peroxynitrite, hydroxyl and DPPH radicals scavenging; metal chelating activity; prevention of lipid peroxidation; inhibition of xanthine oxidase) <sup>52,109-112</sup></p>

Table 6 (continuation)

Compounds Flavone Derivatives	Dual or Multitarget Activity
 <p style="text-align: center;">scutellarin (66)</p>	<p>AChE <sup>44</sup> and MAO inhibitor <sup>113</sup>, anti-A<math>\beta</math> aggregation effect <sup>113</sup> and antioxidant activity (nitric oxide, hydrogen peroxide, superoxide anion, hydroxyl and DPPH radicals scavenging) <sup>114-116</sup></p>
 <p style="text-align: center;">kuwanon C (67)</p>	<p>AChE <sup>44</sup> and BuChE <sup>91</sup> inhibitor and antioxidant activity (nitric oxide and DPPH and ABTS radicals scavenging; inhibition of iNOS) <sup>117-119</sup></p>
 <p style="text-align: center;">morusin (68)</p>	<p>AChE <sup>44</sup> and BuChE <sup>91</sup> inhibitor and antioxidant activity (nitric oxide, superoxide anion and DPPH and ABTS radicals scavenging; inhibition of iNOS) <sup>117-120</sup></p>
 <p style="text-align: center;">69</p>	<p>AChE and BuChE inhibitor <sup>62</sup></p>

**Table 6** (*continuation*)

Compounds Flavone Derivatives	Dual or Multitarget Activity
 <p style="text-align: center;"><b>70</b></p>	<p style="text-align: center;">AChE and BuChE inhibitor <sup>62</sup></p>

As can be seen in **Table 6**, some xanthenes can inhibit both AChE and MAO enzymes (compounds **36** and **58-63**). Flavones luteolin (**54**), apigenin (**55**) and scutellarin (**66**) simultaneously exhibit anticholinesterase, antioxidant and MAO inhibitory activities.

Over the years, it has been found other xanthone and flavone derivatives with dual antioxidant and anticholinesterase activities (compounds **37**, **46**, **54**, **55**, **64-68**). Additionally, baicalein (**65**) and scutellarin (**66**) had anti-A $\beta$  aggregation effect, as well as antioxidant and anticholinesterase activities. These xanthenes and flavones due to their biological activities can also be considered as multipotent agents against AD.

# CHAPTER II

## AIMS AND OVERVIEW

The main purpose of this dissertation was to obtain xanthone and flavone derivatives as dual agents (anticholinesterase and antioxidants) with potential in treatment for AD.

Inspired by the potential of natural hydroxylated xanthenes and flavones as antioxidant agents and that Mannich base analogues of these scaffolds can enhance and/or provide the anticholinesterase activity, like already described above, we aimed to synthesize bioactive Mannich bases of hydroxylated xanthenes and flavones, using natural products as substrates, either by molecular modification or total synthesis. To accomplish this goal, one natural xanthone and flavone were selected as building blocks: 1,3,8-trihydroxyxanthone (**ICX1**) and baicalein (**B**) (**Figure 26**).

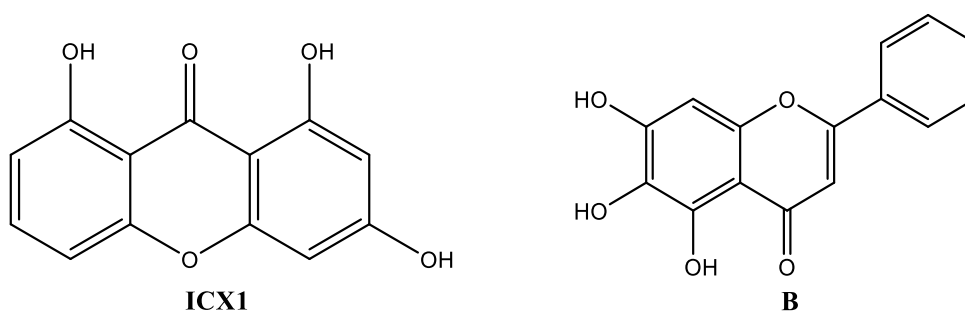


**Figure 26.** Building blocks used for the synthesis of a small library of Mannich bases.

1,3,8-Trihydroxyxanthone (**ICX1**) and baicalein (**B**) were chosen as building blocks, since the natural hydroxylated xanthenes and flavones have already demonstrated to have antioxidant activity<sup>30,36</sup>. Many studies showed that these natural compounds are powerful antioxidants against free radicals and ROS<sup>38,39</sup>. These species when generated in excess can damage the biomolecules and they are, therefore involved in the etiology of several diseases such as AD<sup>44</sup>. Particularly, several studies have shown that baicalein (**B**), isolated from different species of *Scutellaria* (examples: *Scutellaria baicalensis*; *Scutellaria rivularis*; *Scutellaria lateriflora*)<sup>121-123</sup>, has antioxidant activity by scavenging ROS and RNS and chelating metal ions like iron and copper<sup>30,112,122,124</sup>. 1,3,8-Trihydroxyxanthone (**ICX1**), isolated from *Garcinia cantleyana var. cantleyana*<sup>125</sup> was able to protect LDL from oxidation induced by Cu<sup>2+</sup> and to inhibit the transition metal-induced production of free radicals by chelating Cu<sup>2+</sup><sup>125</sup>.

Once more, the choice for these building blocks was motivated by the facts that baicalein (**B**) has also demonstrated the ability to inhibit AChE<sup>44,107</sup> and that a series of xanthone Mannich base derivatives have been described as promising anticholinesterase agents<sup>34</sup>.

These evidences prompt us to consider 1,3,8-trihydroxyxanthone (**ICX1**) and baicalein (**B**) as interesting building blocks for the design and synthesis of a small library of Mannich base derivatives with potential dual mode of action (antioxidant and AChEI) for AD.

Other aims of this research work were:

- to apply classical methodologies for the total synthesis of 1,3,8-trihydroxyxanthone (**ICX1**), namely GSS and Eaton's reactions;
- to obtain new compounds with promising dual mode of action for AD;
- to elucidate the structure of the obtained derivatives through several spectroscopic techniques, namely IR and NMR ( $^1\text{H}$ ,  $^{13}\text{C}$ , HSQC and HMBC);
- to evaluate the antioxidant and AChE inhibitory activities of the synthesized Mannich base derivatives, as well as the activity of a small library of other structure related aminoxanthone derivatives previously synthesized in our research group;
- to perform molecular docking studies of the most active compound with AChE.

# CHAPTER III

## SYNTHESIS

## 1. Xanthonic derivatives

### 1.1. Introduction

#### 1.1.1. Synthesis of xanthenes: general methodologies

The natural xanthenes have a variety of substitution patterns that lead to the diversity of biological/pharmacological activities attributed to this class of secondary metabolites (privileged structures). However, their biosynthetic pathways can be considered as limiting factor for structural variations in natural xanthenes. Thus, in recent years, strategies for synthesis of xanthenes have received much attention in order to obtain novel xanthonic derivatives with important biological/pharmacological activities <sup>126</sup>.

Michael and Kostanecki (1883 and 1891) developed the first method for the synthesis of xanthenes, which is based on the distillation of a mixture of *o*-hydroxybenzoic acid and acetic anhydride <sup>127</sup>.

Over the years alternative methods were developed being three of them widely used: synthesis of xanthenes in one step; the synthesis of xanthenes *via* benzophenone and through a diaryl ether <sup>126,128</sup>.

The Grover, Shah and Shah (GSS) reaction is a methodology that allows obtaining the xanthone scaffold from a single step. In this strategy, the xanthone is obtained by the reaction of a salicylic acid derivative with a polyphenolic compound catalyzed by zinc chloride / phosphoryl chloride, an acid catalyst (**Figure 27**) <sup>129</sup>.

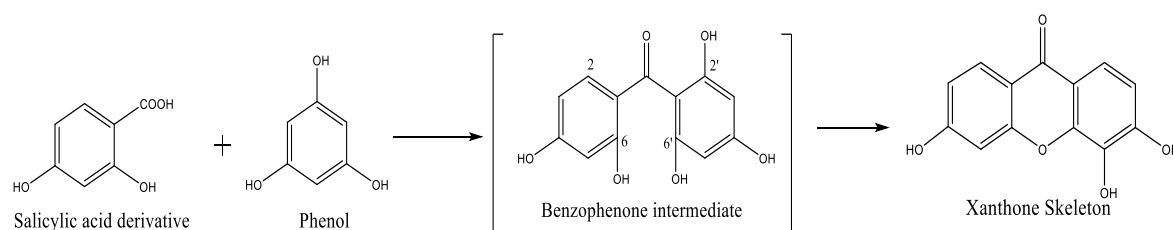


**Figure 27.** Synthesis of simple xanthenes by GSS reaction (adapted <sup>126</sup>).

More recently, other methods that involve the synthesis of xanthone from a single step were created <sup>128</sup>. In 2005, Zhao *et al.* developed, for the first time, a synthesis

methodology that involves the reaction of salicylate esters with an aryne intermediary (**Figure 28**)<sup>130</sup>. The choice of the solvent in this strategy is a very important factor and it has been reported that tetrahydrofuran is the most suitable solvent for this method, since it allows obtaining the xanthone with high selectivity and high yields<sup>128,130</sup>.

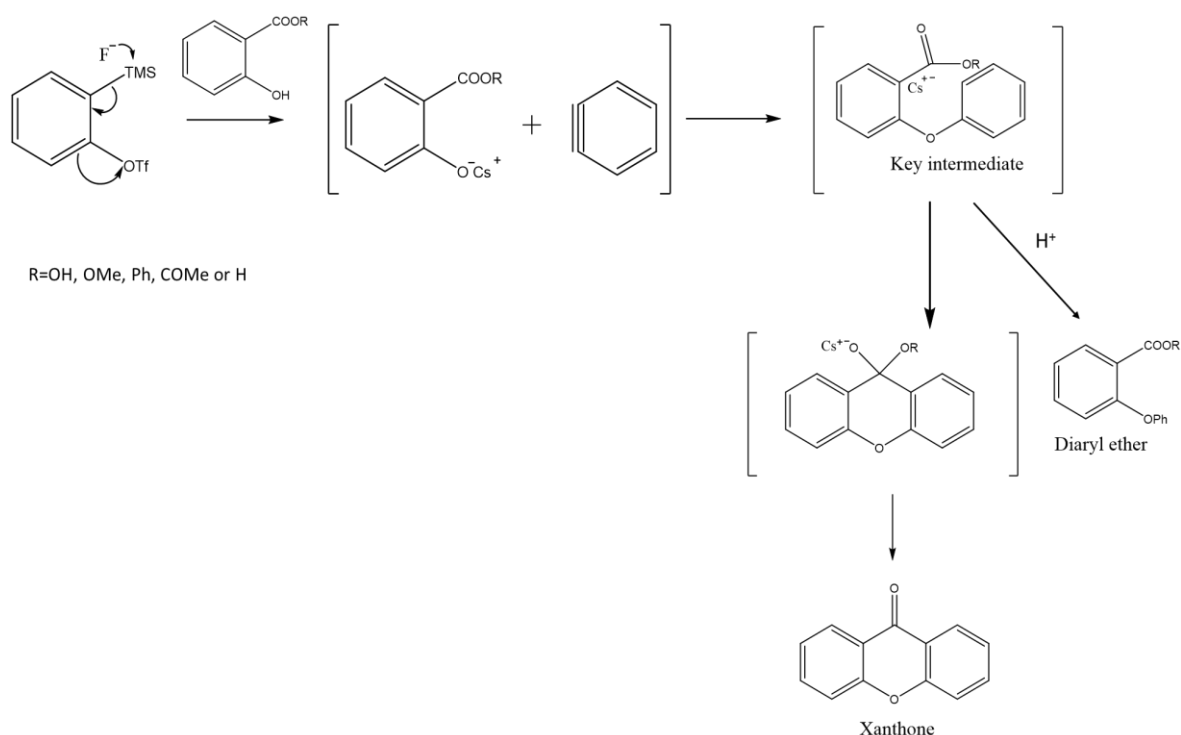


**Figure 28.** Synthesis of simple xanthenes using salicylates and trimethylsilylaryl triflates (adapted<sup>128</sup>).

In 2010, Dubrovskiy and Larock proposed a change to this methodology, where xanthenes would be produced by the reaction of *o*-halobenzoic acids with aryne intermediates (**Figure 29**)<sup>131</sup>.

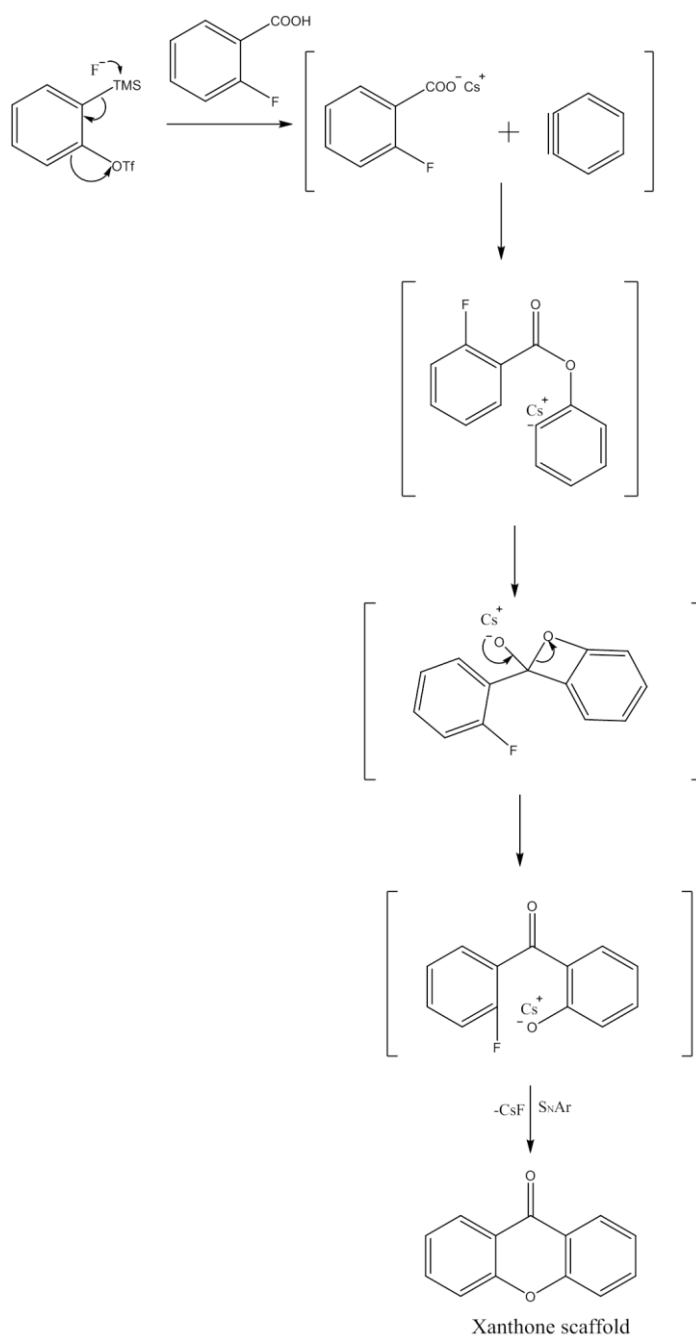


**Figure 29.** Synthesis of simple xanthones from the reaction of *o*-halobenzoic acids with aryne intermediates (adapted <sup>128</sup>).

Other methodology allowing the synthesis of xanthones in one step was developed by Wang *et al.* in 2009. This method of synthesis involves the reaction of salicylaldehyde and 1,2-dibromobenzene derivatives, where the annulations are catalyzed *via* palladium (**Figure 30**) <sup>132</sup>.

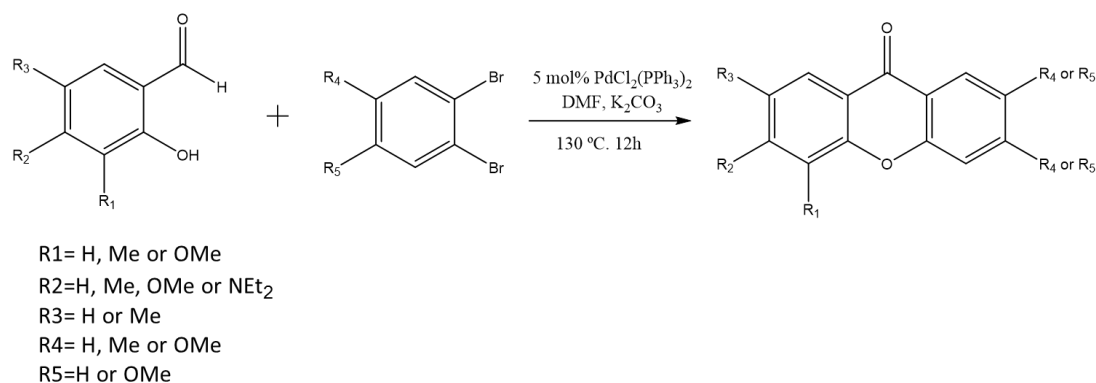


**Figure 30.** Synthesis of simple xanthenes by palladium-catalyzed annulations (adapted <sup>128</sup>).

Other strategy in the context of one-step synthesis of xanthenes was developed by Hu *et al.* in 2012. These researchers used phenols and various aryl aldehydes as starting materials and  $\text{CuCl}_2$  as a catalyst in the presence of triphenylphosphine (**Figure 31**). Although it was obtained xanthenes with high yields, this methodology has some limitations, including the fact that the phenols have to be activated and the reaction times are very high <sup>133</sup>.

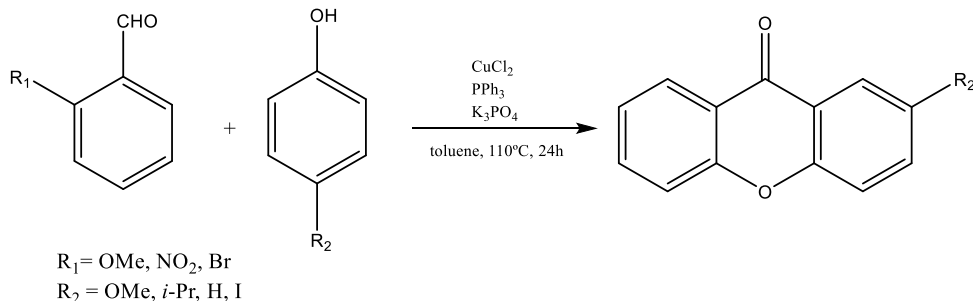


**Figure 31.** Synthesis of xanthenes by *ortho*-acylation of phenols with 2-substituted aldehydes (adapted <sup>133</sup>).

In fact, the use of copper catalysts in reactions in organic chemistry has associated economic advantages, but also allows more “green” reactions in the context of green chemistry. Therefore, in recent years, it has been tried to develop efficient copper-based catalysts which may be used in various reactions <sup>134</sup>.

In this framework and in order to improve the methodology developed by Hu *et al.*, Menendez *et al.*, in 2014, established the synthesis of xanthenes based on the reaction between *ortho*-substituted benzaldehydes and phenols, catalyzed by magnetic nanocatalyst that consists of CuNPs on silica coated maghemite (**Figure 32**) <sup>134</sup>. With this

synthetic strategy and with these catalysts, it was possible to obtain xanthenes with high yields and overcome the limitations associated with more classic methodologies <sup>134</sup>.

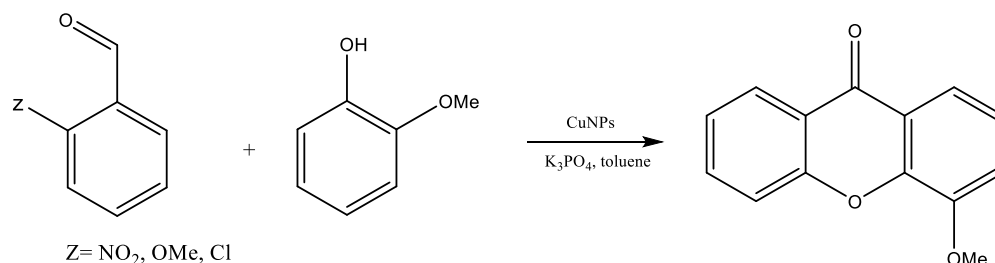


**Figure 32.** Synthesis of xanthenes by reaction between ortho-substituted benzaldehydes and phenols, catalyzed by nanocatalysts (CuNPs) (adapted <sup>134</sup>).

Additionally, in 2015, Genovese *et al.*, proposed the synthesis of xanthenes under microwave conditions and using ytterbium triflate as acid catalyst <sup>135</sup>. In this approach, substituted 2-hydroxybenzoic acids react with phenols in the presence of Yb(OTf)<sub>3</sub> hydrate by microwave irradiation to afford the xanthone in high yields (**Figure 33**) <sup>135</sup>.

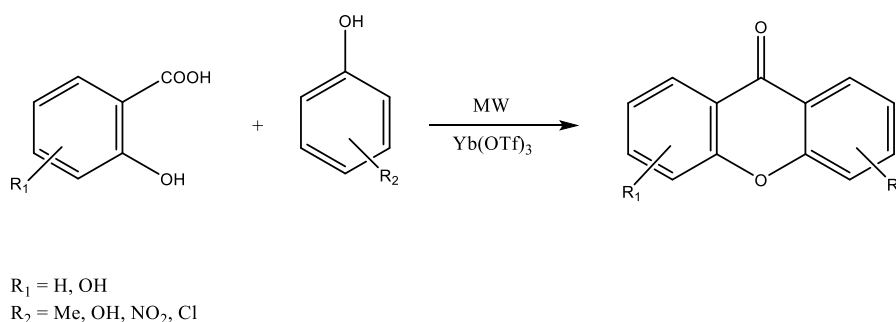


**Figure 33.** Synthesis of xanthenes under microwave conditions promoted by ytterbium triflate (adapted <sup>135</sup>).

In addition to these synthetic strategies that involve a single step, multi-step methodologies were created <sup>128</sup>. Among the various strategies developed, one that is frequently used is the benzophenone route. This route, basically involves the synthesis of benzophenone followed by its cyclization <sup>126</sup>. Several strategies to synthesize benzophenone intermediate and its cyclization can be seen in **Figure 34**.

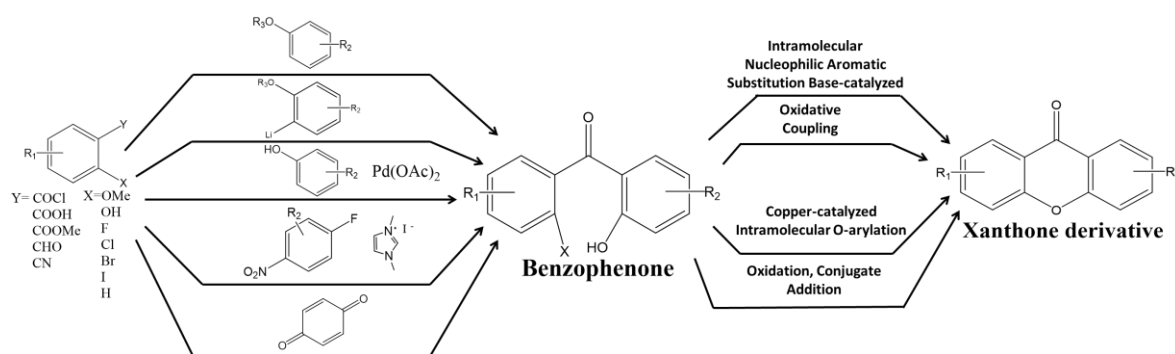


**Figure 34.** Several alternatives for the synthesis of xanthenes through benzophenone route (adapted<sup>128</sup>).

Among all these strategies that can be used for the synthesis of benzophenone, the most common is the Friedel-Crafts acylation of a phenol or a protected phenol-derivative in presence of an acyl chloride, catalyzed by aluminum chloride (**Figure 35**) <sup>136</sup>.

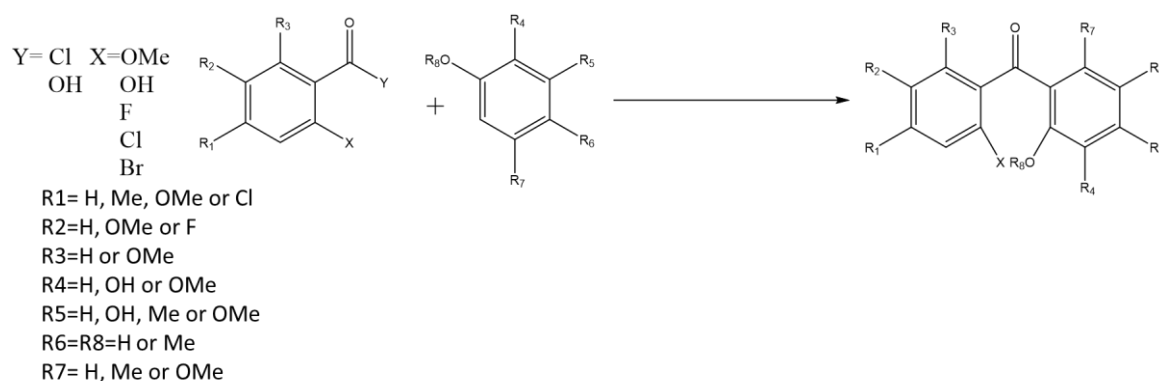


**Figure 35.** Synthesis of the benzophenone through a Friedel-Crafts acylation (adapted <sup>128</sup>).

Another methodology for the synthesis of the xanthone scaffold is that which follows the diaryl ether route. This route that uses diaryl ether as key intermediate, also involves two main steps: the synthesis of diaryl ether and subsequent cyclization. All strategies for synthesis and cyclization of the intermediate are summarized in **Figure 36**<sup>126,128</sup>.

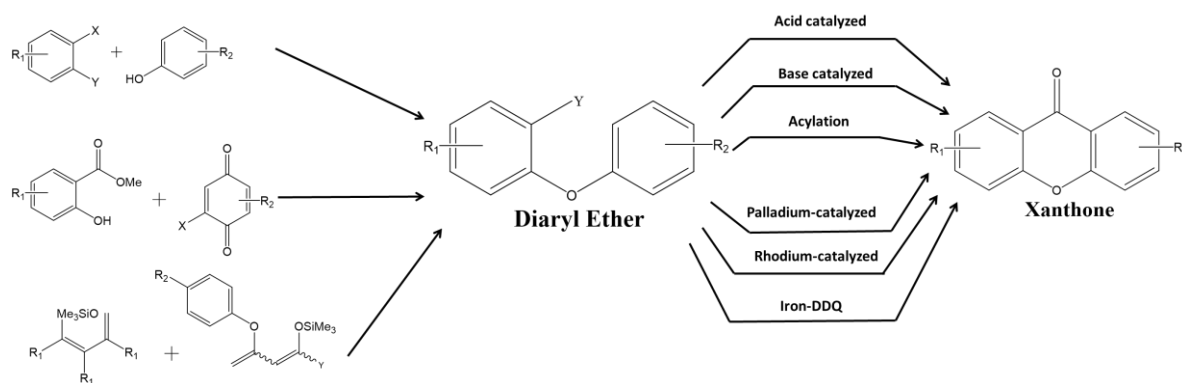


**Figure 36.** Synthesis of xanthenes through diaryl ether route (adapted <sup>128</sup>).

All the synthetic strategies described so far involve basically two aryl derivatives as building blocks, and the xanthone scaffold was obtained by the formation of an ether and ketone linkage <sup>128</sup>. However, other strategies using chromen-4-ones as building blocks were developed. This strategy has the advantage of allowing the synthesis of xanthenes with more complex substitution patterns. Depending on the substituents at positions 2 and 3 of the chromen-4-ones, different reactions can be used to obtain xanthone (**Figure 37**) <sup>128</sup>.

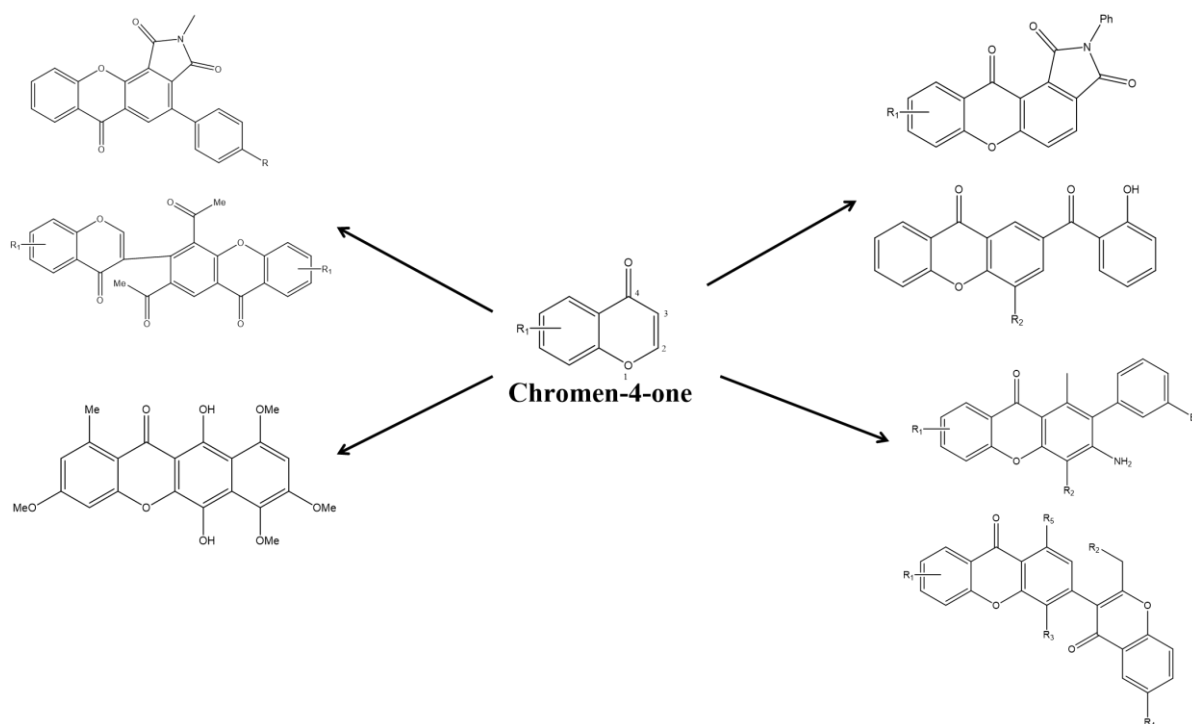


**Figure 37.** Synthesis of xanthenes from chromen-4-one and some examples of xanthone obtained by this route (adapted <sup>128</sup>).

El-Desoky *et al.*, in 2014, reported the synthesis of xanthone nucleus through domino reactions of 3-vinylchromone <sup>137</sup>. Domino reactions are a synthetic strategy that consist of two or more bond- forming reactions in which the subsequent transformation result as a consequence of the functionality obtained in the previous step, affording the synthesis of complex molecules <sup>137</sup>. Particularly, in the methodology developed by these researchers, various heterocyclic nuclei, including xanthone, were obtained using a domino protocol starting from 3-vinylchromone (**Figure 38**) <sup>137</sup>.

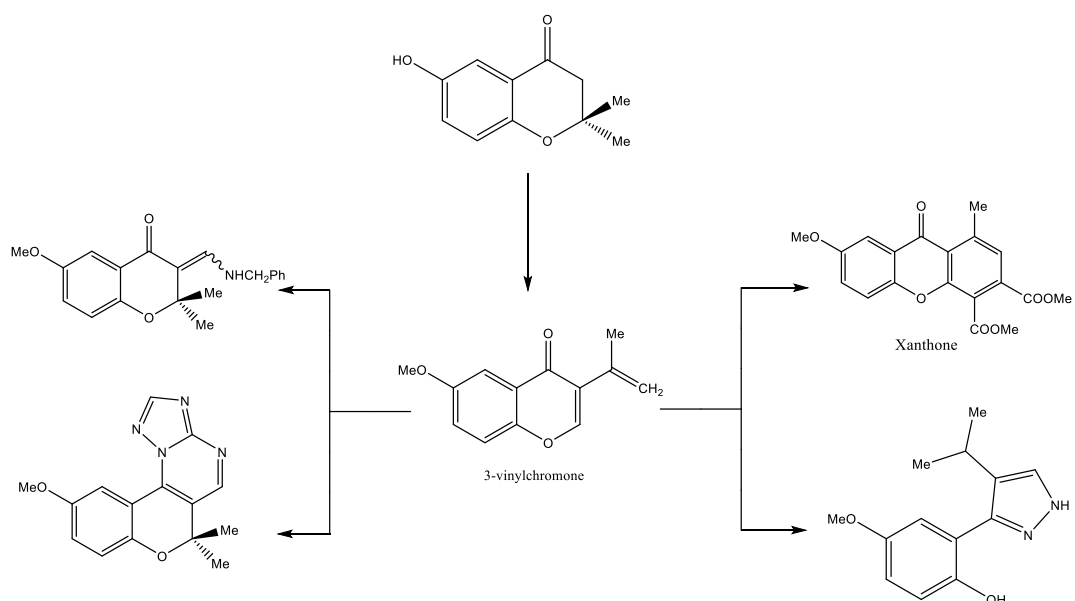


**Figure 38.** Synthesis of xanthone *via* domino reactions (adapted <sup>137</sup>).

## 1.2. Results and discussion

### 1.2.1. Synthesis

#### 1.2.1.1. 1,3,8- Trihydroxyxanthone (ICX1)

In recent years, a large number of methodologies for the synthesis of simple oxygenated xanthonic derivatives have been developed <sup>128</sup>. Among the various synthetic methodologies that are available, in this work, the building block 1,3,8-trihydroxyxanthone (**ICX1**) was obtained by one-pot synthesis using two different strategies: Eaton's reaction and GSS reaction.

In accordance with literature <sup>126</sup> and the experience of our research group, the synthesis of hydroxylated xanthenes by GSS demands a difficult work up, when compared with the Eaton's reaction. Therefore, **ICX1** was firstly synthesized by Eaton's reaction.

In the Eaton's reaction, **ICX1** was obtained by the condensation of 2,6-dihydroxybenzoic acid with phloroglucinol in the presence of a mixture of phosphorus pentoxide - methanesulfonic acid (Eaton's reagent) as condensing agent (**Figure 39**).

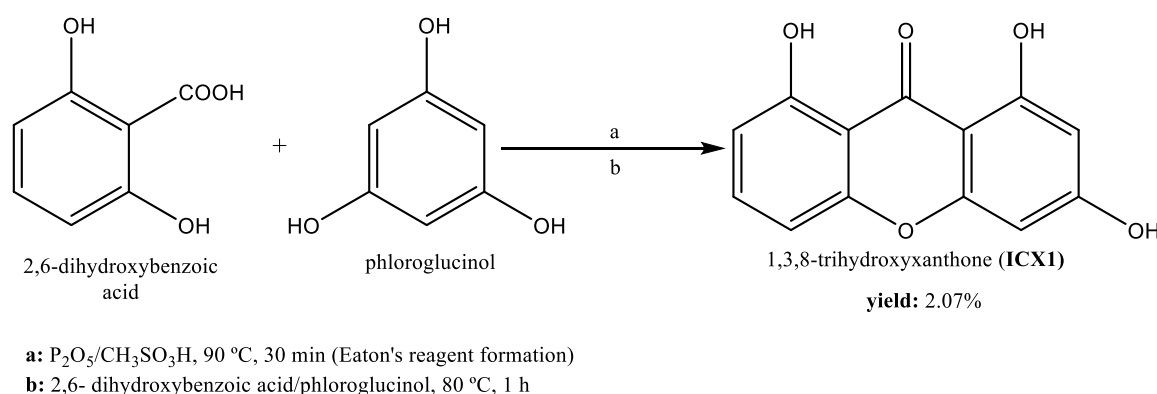


**Figure 39.** General conditions for the synthesis of 1,3,8-trihydroxyxanthone (**ICX1**) by Eaton's reaction.

The yield obtained in this reaction was very low (2.07%), being this mainly due to the formation of a by-product with a similar retention factor, making the purification of the desired xanthone by flash column chromatography or thin layer chromatography (TLC) very difficult.

Therefore, **ICX1** was also synthesized by GSS. In this reaction, **ICX1** was obtained by the condensation of 2,6-dihydroxybenzoic acid with phloroglucinol in the presence of zinc chloride in phosphorus oxychloride, instead of Eaton's reagent (**Figure 40**). Although this condensation agent has been shown to be efficient for the synthesis of hydroxylated xanthones, this synthetic methodology has some limitations and low yields<sup>126,128</sup>. Taking these into account, some experimental modifications to the classic GSS reaction were performed including the stepwise addition of reactants and the use of microwave assisted organic synthesis (MAOS), instead of conventional thermal heating (classical synthesis). Particularly, in the original GSS methodology, a mixture of an hydroxybenzoic acid, a phenol, fused zinc chloride and phosphorus oxychloride was heated together on a water bath. Instead, in the GSS reaction modified by our research group, firstly a mixture of fused zinc chloride and phosphorus oxychloride was irradiated by MW at 400 W for 10 min at 60 °C; then, the hydroxybenzoic acid was added and the mixture was subjected to MW irradiation at 400 W for 10 min at 60 °C and finally, the appropriated phenol was added and the mixture was once more submitted to MW at 400 W for 60 min at 60 °C. The synthetic route, the reaction conditions and the yield for **ICX1** are shown in **Figure 40**.

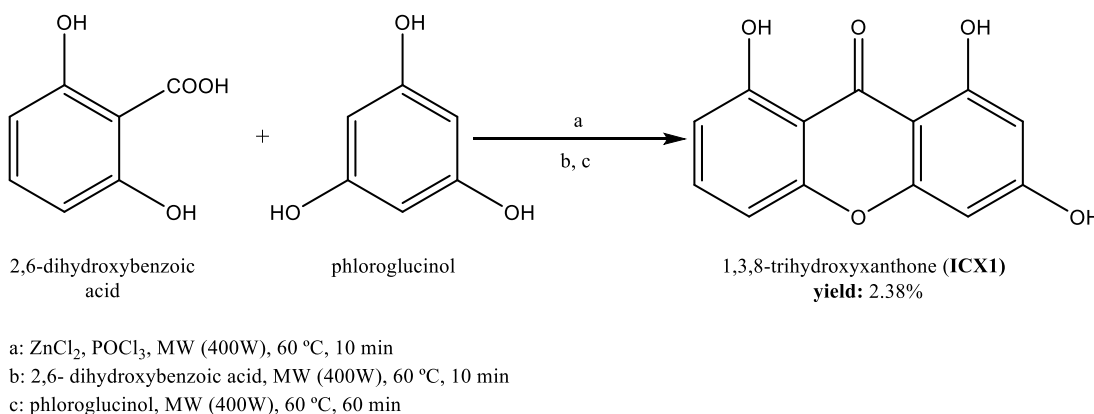


**Figure 40.** General conditions for the synthesis of 1,3,8-trihydroxyxanthone (**ICX1**) by GSS reaction.

According to **Figure 40**, the yield of this reaction was very low (2.38%). These results were not expected, since this GSS methodology had been applied in this research group for the synthesis of other hydroxylated xanthenes with higher yields <sup>138</sup>.

This low yield could be explained by the fact that this reaction has been incomplete, and more than one product have been formed, making the purification steps quite complicated and time consuming. Particularly, an amount of 2,6-dihydroxybenzoic acid that remained in the reaction mixture proved to be extremely difficult to remove by a simple flash column chromatography. Therefore, to optimize the purification process, prior to column chromatography an extraction with a saturated solution of NaHCO<sub>3</sub> 5% was performed in order to eliminate 2,6-dihydroxybenzoic acid.

**Table 7** summarizes the reaction conditions and purification processes used for the synthesis of 1,3,8-trihydroxyxanthone (**ICX1**) by the two different reactions. In general, both approaches showed short reaction times (Eaton's reaction: 1 h 30 min; modified GSS reaction by MW: 1 h 20 min) and low yields. Although purification of **ICX1** in both reactions was time consuming, this process was more complex in the GSS reaction. In fact, in this methodology, three different procedures had been performed: extraction with CH<sub>2</sub>Cl<sub>2</sub> in order to remove a brown slimy material; extraction with saturated solution of NaHCO<sub>3</sub> 5% to eliminate benzoic acid and a flash column chromatography to get **ICX1**. In contrast, in Eaton's reaction, **ICX1** was only obtained using flash chromatography as purification method. In conclusion, according to these results, Eaton's reaction seems to be more suitable than GSS for the synthesis of **ICX1**, because it was a cleaner approach, which required less purification procedures.

**Table 7.** Reaction conditions and purification processes for the synthesis of 1,3,8-trihydroxyxanthone (**ICX1**) by Eaton's reaction and Modified GSS reaction assisted by MW.

	Eaton's reaction	Modified GSS reaction assisted by MW
<b>Reaction Conditions</b>	<b>a:</b> P <sub>2</sub> O <sub>5</sub> /CH <sub>3</sub> SO <sub>3</sub> H, 90 °C, 30 min (Eaton's reagent formation) <b>b:</b> 2,6- dihydroxybenzoic acid/phloroglucinol, 80 °C, 1 h	<b>a:</b> ZnCl <sub>2</sub> , POCl <sub>3</sub> , MW (400W), 60 °C, 10 min <b>b:</b> 2,6- dihydroxybenzoic acid, MW (400W), 60 °C, 10 min <b>c:</b> phloroglucinol, MW (400W), 60 °C, 60 min
<b>Purification Processes</b>	flash column chromatography.	extraction with CH <sub>2</sub> Cl <sub>2</sub> ; extraction with saturated solution of NaHCO <sub>3</sub> 5%; flash column chromatography.
<b>Yields</b>	2.07%	2.38%

### 1.2.1.2. Amino derivatives of 1,3,8-trihydroxyxanthone

The 1,3,8-trihydroxyxanthone **ICX1** was used as building block for the synthesis of the correspondent amino derivatives, by the Mannich reaction.

The Mannich reaction who accidentally took place for the first time in 1912, is nowadays one of the most important strategies that is used in organic chemistry for the aminomethylation of compounds and formation of new C-C bonds. Over the years, its products (Mannich bases) have shown a variety of biological activities, and therefore this synthetic approach has been widely used in the medicinal pharmaceutical chemistry for drug design <sup>139,140</sup>.

Basically, the classic Mannich reaction consists of a three-component condensation, which involves several substrates having at least one active hydrogen atom, an aldehyde (usually formaldehyde) and an amine reagent to give a class of compounds called Mannich bases (**Figure 41**).

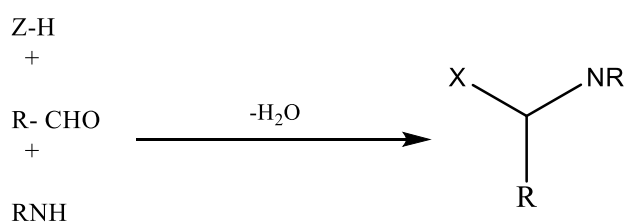


**Figure 41.** General representation of Mannich reaction (adapted <sup>140</sup>).

The reaction conditions range according to the substrate (may belong to a diverse class of compounds), the amine and the aldehyde that are used <sup>141</sup>. Thus, there are a large number of combinations amine / substrate which can be used in this reaction, being one of the reasons for the wide applicability of this synthetic strategy <sup>140-142</sup>. Additionally, in the Mannich reaction there are three different procedures for the addition of the reactants <sup>141</sup>. The most common procedure consists of mixing all the chemical species involved in the reaction, while the second approach involves first the reaction of the amine with the aldehyde, and then the addition of substrate <sup>141</sup>. Alternatively, in some cases, it is performed the condensation of substrate and aldehyde, and then the methylated derivative formed is isolated and reacted with the respective amine <sup>141</sup>.

Particularly, in our work, for the aminomethylation of **ICX1**, diethylamine was allowed to react with formaldehyde in methanol for 1 hour and then a solution of **ICX1** was added to the reaction mixture (**Figure 42**).

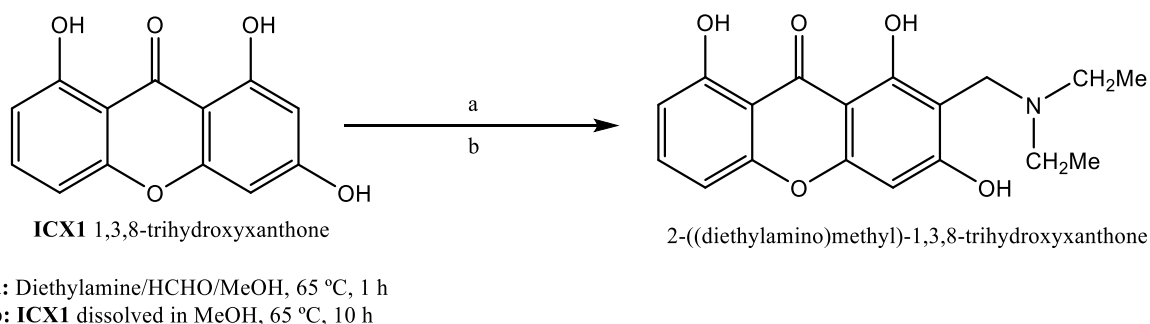


**Figure 42.** General conditions for the synthesis of amino derivative of 1,3,8-trihydroxyxanthone (**ICX1**) by Mannich reaction.

Despite being used the same reaction conditions reported in literature for the phenolic Mannich reactions<sup>141</sup>, and particularly for hydroxylated xanthenes<sup>34</sup>, this synthetic approach failed to produce the desired amino derivative of **ICX1**. More specifically, it has been found that this Mannich reaction was not complete and led to the formation of a wide variety of by-products which made impossible to obtain the desired aminoxanthonic derivative.

In order to afford this derivative, successive attempts of purification were carried out. Firstly, crystallization was performed with a mixture of chloroform / methanol, but it did not result. Then, we made a flash column chromatography using chloroform / acetone as eluent. No pure fractions were obtained, and therefore, the fractions that contained the same chromatographic profile were joined. Subsequently, flash column chromatography and preparative TLC were performed for the fractions with positive revelation with ferric chloride. Although all these purification steps have been performed, the desired amino derivative of **ICX1** was not isolated.

Despite these results not being expected, they are supported by the literature. A major disadvantage of Mannich reactions is the formation of by-products that could cause difficulties in the purification of the final product, being necessary to develop more specific protocols<sup>141,142</sup>. In fact, several secondary reactions have been identified as the main routes which may be involved in the production of undesired by-products in Mannich reactions<sup>141</sup>. These main pathways are shown in **Figure 43**.

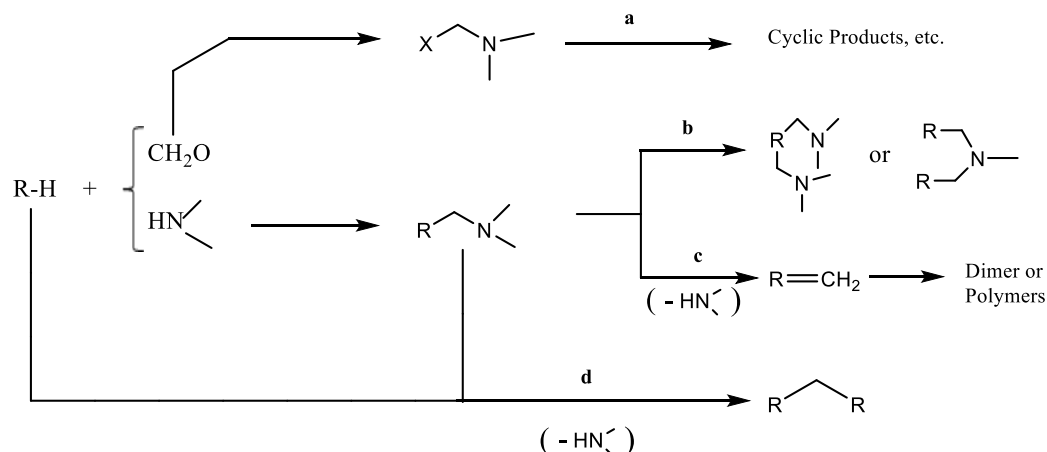


**Figure 43.** By-products accompanying Mannich reaction (adapted <sup>141</sup>).

According to this review, the pathway **a**) occurs when the amine used as reactant is very stable and the substrate is poorly reactive, resulting in the formation of by-products that derive exclusively from the amine reactant. The route **b**) shows a typical reaction that results in a further aminomethylation, which leads to the formation of a Mannich base. This Mannich base may behave as an amine or substrate, depending on the functionality present in the starting materials of the reaction. The pathway **c**) represents a situation in which can occur a deaminomethylation of the Mannich base and it may be generated dimers or polymers as by-products. Finally, the route **d**) shows the synthesis of methylene-bis-derivatives of substrate as by-products of some Mannich reactions <sup>141</sup>.

Additionally, our results may be also explained by the fact that the aminomethylation have not only occurred at C-2. Taking into account the structure of building block **ICX1**, it can be verified that this is the most nucleophilic aromatic position, but C-4 and C-7 are also activated and, consequently, the aminomethylation could happen at those positions, generating other amino derivatives of **ICX1**. Thus, is possible that this may have also contributed to the formation of more by-products.

### 1.2.1.3. Methylated derivative of 1,3,8-trihydroxyxanthone (ICX2)

The synthetic approach used for the synthesis of methylated derivative **ICX2** was based on the reaction of 1,3,8-trihydroxyxanthone (**ICX1**) with methyl iodide in presence of anhydrous potassium carbonate and anhydrous acetone<sup>34</sup>. The reaction conditions and the results obtained in the synthesis of **ICX2** are present in **Figure 44**.

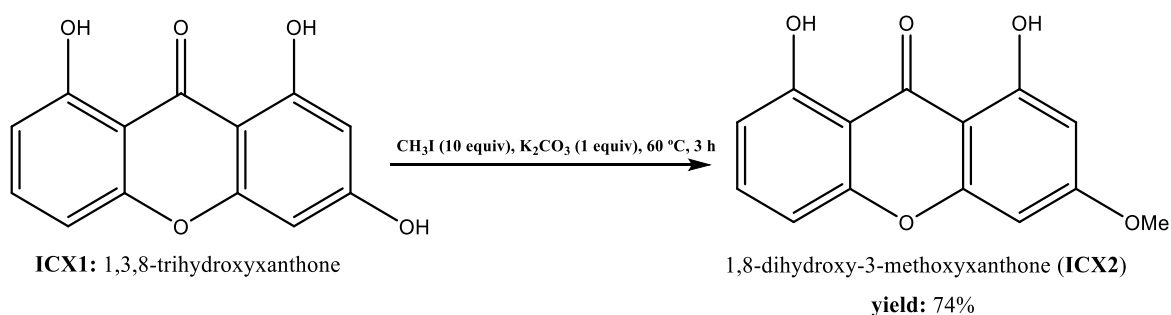
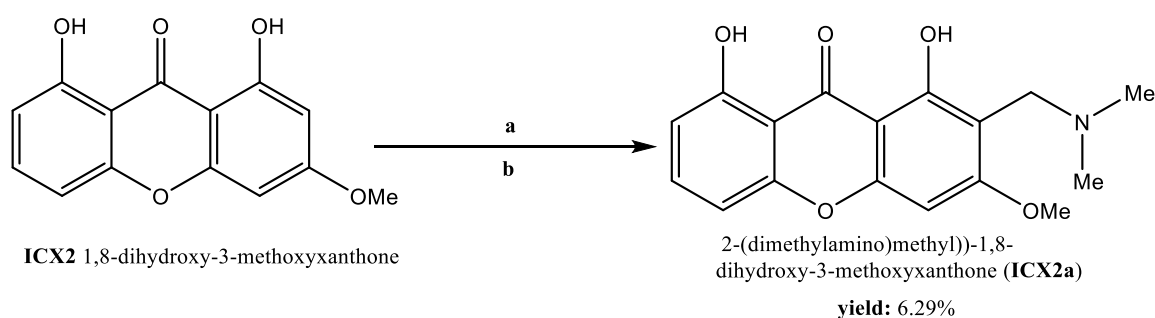


**Figure 44.** General conditions for the synthesis of methylated derivative of 1,3,8-trihydroxyxanthone (**ICX2**).

This synthetic strategy demonstrated to be efficient for the synthesis of **ICX2**, being this derivative obtained in high yield (74%). In addition, as expected, the obtained results indicated that O-methylation of **ICX1** occurs only at the hydroxyl group on the position 3, since a weak base was used in this reaction.

### 1.2.1.4. Amino derivative of 1,8-dihydroxy-3-methoxyxanthone (ICX2a)

The methylated derivative of 1,3,8-trihydroxyxanthone (**ICX2**) was used as building block for the synthesis of aminoxanthone **ICX2a** by the Mannich reaction. The general experimental conditions and its results are indicated in **Figure 45**.



**a:** Dimethylamine (4.35 equiv)/HCHO (6.63 equiv)/CH<sub>3</sub>COOH, room temperature, 1 h

**b:** addition of **ICX2**, room temperature, 6 days

**Figure 45.** General conditions for the synthesis of amino derivative of 1,8-dihydroxy-3-methoxyxanthone (**ICX2a**) by Mannich reaction.

The synthetic conditions were quite different from those used for the synthesis of amino derivatives of **ICX1** (section 1.2.1.2.). In accordance with the procedure described by Qin *et al.* (2013) for the synthesis of amino derivatives of 1-hydroxy-3-methoxyxanthone, in this Mannich reaction, instead of methanol as solvent, acetic acid was used as acid catalyst<sup>34</sup>. These acidic conditions are often used in this kind of reactions in order to favor the reaction, by facilitating the formation of iminium cation and / or to improve the stability of the product formed<sup>141</sup>.

Even under these conditions, the reaction time was high (6 days) and the yield for **ICX2a** was low (6.29%). This low yield could be justified by the fact of this reaction has been incomplete and its work-up has been difficult and time-consuming. Particularly, the purification of **ICX2a** by flash column chromatography was difficult because some by-products formed in this reaction had a similar polarity to the desired compound and, consequently, were isolated with **ICX2a**.

### 1.2.2. Evaluation of xanthenes purity

The purity of each compound was determined by HPLC-DAD, using a C18 stationary phase and a mixture of methanol:water:acetic acid (70:30:1 v/v/v) as mobile phase, and the results obtained are presented in **Table 8**.

**Table 8.** Retention time and purity of **ICX1**, **ICX2** and **ICX2a**.

Compound	Retention time (min)	Purity (%)
<b>ICX1</b>	12.2	97.4
<b>ICX2</b>	27.6	98.9
<b>ICX2a</b>	2.8	99.5

According to **Table 8**, it can be verified that all synthesized compounds show a purity higher than 95% by HPLC-DAD method.

### 1.2.3. Structure elucidation

The structure elucidation of all xanthone derivatives was established on the basis of IR and NMR techniques.  $^{13}\text{C}$  NMR assignments were determined by heteronuclear single quantum coherence (HSQC) and heteronuclear multiple bond correlation (HMBC) experiments.

The IR data of 1,3,8-trihydroxyxanthone (**ICX1**) and its derivatives (**ICX2** and **ICX2a**) were in accordance with the performed molecular modification (**Table 9**). The IR spectra of compounds **ICX1**, **ICX2** and **ICX2a** showed the presence of absorption bands corresponding to the C=O ( $1663\text{--}1653\text{ cm}^{-1}$ ), aromatic C=C ( $1605\text{--}1470\text{ cm}^{-1}$ ) and C-O ( $1296\text{--}1293\text{ cm}^{-1}$ ). The presence of methyl groups in the derivatives **ICX2** and **ICX2a** was suggested by the observation of bands at  $2959\text{--}2852\text{ cm}^{-1}$  characteristic of aliphatic C-H. As the precursor (**ICX1**), for derivatives **ICX2** and **ICX2a**, a large band of stretching vibration at  $3600\text{--}3400\text{ cm}^{-1}$  (hydroxyl groups) was visualized, revealing that the methylation did not occur at all hydroxyl groups of **ICX1**. Additionally, the presence of an aliphatic amine in the

xanthone **ICX2a** was suggested by the observation of a stretching vibration band at 1230  $\text{cm}^{-1}$ .

**Table 9.** IR data of 1,3,8-trihydroxyxanthone (**ICX1**) and its derivatives **ICX2** and **ICX2a**.

Groups	$\nu$ ( $\text{cm}^{-1}$ )		
	ICX1	ICX2	ICX2a
OH	3500-3400	3500-3400	3600-3400
Aliphatic C-H	–	2959 2925 2852	2923 2853
C=O	1663	1662	1653
Aromatic C=C	1601 1565 1514 1483	1603 1568 1505 1470	1605 1558 1539 1490
C-O	1293	1294	1296
C-N	–	–	1230

The  $^1\text{H}$  and  $^{13}\text{C}$  NMR data of 1,3,8-trihydroxyxanthone (**ICX1**) and its derivatives (**ICX2** and **ICX2a**) are reported in **Table 10** and **Table 11**.

The  $^1\text{H}$  NMR spectra of 1,3,8-trihydroxyxanthone (**ICX1**) showed signals of two hydrogen-bonded hydroxyl group at  $\delta_{\text{H}}$  11.89 s and  $\delta_{\text{H}}$  11.81 s, revealing the presence of two hydroxyl groups linked to C-1 and C-8. The presence of a broad triplet at  $\delta_{\text{H}}$  7.68 (H-6) coupled with two double doublets at  $\delta_{\text{H}}$  7.00 (H-5) and  $\delta_{\text{H}}$  6.79 (H-7) reveals the presence of three aromatic protons on consecutive carbon atoms on B ring. In addition, the signals of two doublets at  $\delta_{\text{H}}$  6.38 (H-4) and  $\delta_{\text{H}}$  6.21 (H-2) confirmed the presence of two *meta* coupled aromatic protons in A ring. The low chemical shifts of these two doublets in comparison to that observed for H-5, H-6 and H-7 are in accordance to the expected for aromatic protons on *ortho/para* positions to hydroxyl groups. The  $^{13}\text{C}$  NMR data confirmed the structure proposed for this compound. All spectroscopic data are in agreement with those found in the literature <sup>143</sup>.

As the precursor (**ICX1**), the  $^1\text{H}$  NMR spectra of derivatives **ICX2** and **ICX2a** showed that both have retained the hydrogen-bonded hydroxyl group at C-1 ( $\delta_{\text{H}}$  12.09-11.99 s) and

C-8 ( $\delta_{\text{H}}$  12.09- 11.92 s) and three aromatic protons at  $\delta_{\text{H}}$  7.56-7.55 brt (H-6),  $\delta_{\text{H}}$  6.87- 6.86 *dd* or *brd* (H-5), and  $\delta_{\text{H}}$  6.78 *dd* or *brd* (H-7). For derivative **ICX2**, two *meta* coupled aromatic protons at  $\delta_{\text{H}}$  6.35 *d* (H-2) and  $\delta_{\text{H}}$  6.42 *d* (H-4) are also observed, confirming the presence of hydrogen atoms on H-2 and H-4. Instead of these two double doublets, only one singlet at  $\delta_{\text{H}}$  6.44 (H-4) is observed in  $^1\text{H}$  NMR of **ICX2a** and characteristic signals of a dimethylamine ( $\delta_{\text{H}}$  2.37 s;  $\delta_{\text{C}}$  44.96) attached to C-2 through a methylene bridge ( $\delta_{\text{H}}$  3.64 s;  $\delta_{\text{C}}$  49.97) are observed in the  $^1\text{H}$  and  $^{13}\text{C}$  spectra, suggesting the presence of a 2-(dimethylamino)methyl side chain.

The position of the methyl and dimethylaminomethyl side chains in derivatives **ICX2** and **ICX2a** was confirmed by the correlations found in the HMBC indicated in **Figure 46**.

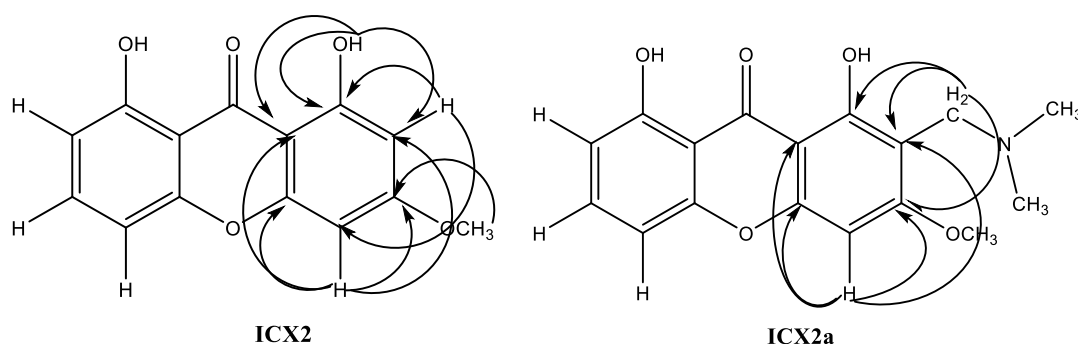


**Figure 46.** Main connectivities found in the HMBC of **ICX2** and **ICX2a**.

**Table 10.**  $^1\text{H}$  NMR data of 1,3,8-trihydroxyxanthone (**ICX1**) and its derivatives (**ICX2** and **ICX2a**).

	<b>ICX1</b>	<b>ICX2</b>	<b>ICX2a</b>
<b>H-1</b>	11.89 (OH, s)	11.99 (OH, s)	12.09 (OH, s)
<b>H-2</b>	6.21 ( <i>d</i> , $J = 2.1$ )	6.35 ( <i>d</i> , $J = 2.3$ )	—
<b>2- CH<sub>2</sub>N</b>	—	—	3.64 (s)
<b>N(CH<sub>3</sub>)<sub>2</sub></b>	—	—	2.37 (s)
<b>H-3</b>	—	—	—
<b>3- OCH<sub>3</sub></b>	—	3.89 (s)	3.94 (s)
<b>H-4</b>	6.38 ( <i>d</i> , $J = 2.1$ )	6.42 ( <i>d</i> , $J = 2.3$ )	6.44 (s)
<b>H-5</b>	7.00 ( <i>dd</i> , $J = 8.4, 0.9$ )	6.87 ( <i>dd</i> , $J = 8.4, 0.8$ )	6.86 ( <i>brd</i> , $J = 8.3$ )
<b>H-6</b>	7.68 ( <i>brt</i> , $J = 8.4$ )	7.56 ( <i>brt</i> , $J = 8.4$ )	7.55 ( <i>brt</i> , $J = 8.3$ )
<b>H-7</b>	6.79 ( <i>dd</i> , $J = 8.4, 0.9$ )	6.78 ( <i>dd</i> , $J = 8.4, 0.8$ )	6.78 ( <i>brd</i> , $J = 8.3$ )
<b>H-8</b>	11.81 (OH, s)	11.92 (OH, s)	12.09 (OH, s)

Values in parts *per* million ( $\delta_{\text{H}}$ ). Measured in DMSO- $\text{d}_6$  (**ICX1**) and  $\text{CDCl}_3$  (**ICX2** and **ICX2a**) at 300.13 MHz.  $J$  values (Hz) are presented in parentheses.

**Table 11.**  $^{13}\text{C}$  NMR data of 1,3,8-trihydroxyxanthone (**ICX1**) and its derivatives (**ICX2** and **ICX2a**).

	<b>ICX1</b>	<b>ICX2</b>	<b>ICX2a</b>
<b>C-1</b>	162.16	162.97	161.39
<b>C-2</b>	98.70	97.41	103.5
<b>2- CH<sub>2</sub>N</b>	—	—	49.97
<b>N(CH<sub>3</sub>)<sub>2</sub></b>	—	—	44.96
<b>C-3</b>	167.06	167.35	165.79
<b>3- OCH<sub>3</sub></b>	—	55.93	56.34
<b>C-4</b>	94.48	93.10	90.05
<b>C-4a</b>	157.51	157.78	157.69
<b>C-5</b>	107.10	106.96	107.85
<b>C-6</b>	137.18	136.80	136.58
<b>C-7</b>	110.60	110.89	110.90
<b>C-8</b>	160.27	161.31	161.39
<b>C-8a</b>	106.88	106.96	106.79
<b>C-9</b>	183.26	184.63	184.33
<b>C-9a</b>	101.00	102.70	102.70
<b>C-10a</b>	155.49	156.14	155.96

Values in parts *per* million ( $\delta_{\text{C}}$ ). Measured in DMSO- $\text{d}_6$  (**ICX1**) and  $\text{CDCl}_3$  (**ICX2** and **ICX2a**) at 75.47 MHz.

Assignments were confirmed by HSQC and HMBC experiments.

## 2. Flavone derivatives

### 2.1. Introduction

#### 2.1.1. General methodologies for the synthesis of flavones

The natural flavones exhibit a diversity of biological activities as mentioned above. However, the structural diversity of flavones, and consequent their biological activities are limited by their biosynthetic pathways. In this context, in recent years, it has been developed several strategies to synthesize flavones, in order to obtain flavonic derivatives with the desired biological / pharmacological activities <sup>32</sup>.

Currently, there are several methodologies that can be used for the synthesis of flavones, which can be divided into two groups: one type of strategies that involves  $\beta$ -diketones as penultimate intermediates and other type that uses chalcones as penultimate intermediate <sup>32</sup>.

Considering the first approach for the synthesis of flavones, the Baker-Venkataraman rearrangement is the most used strategy, consisting in conversion of *o*-hydroxyacetophenone into phenolic ester, which suffers an intramolecular Claisen condensation to form a  $\beta$ -diketone. Then, occurs the cyclization of the  $\beta$ -diketone to give the flavone scaffold **Figure 47** <sup>32,144,145</sup>.

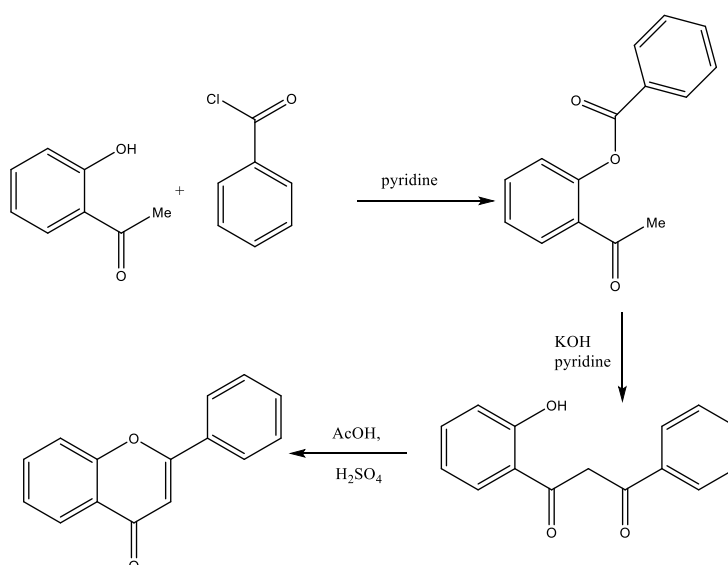


**Figure 47.** Synthesis of flavone via  $\beta$ -diketone intermediate (adapted <sup>32</sup>).

Over the years, researches tried to develop strategies for the one-step synthesis of flavones from  $\beta$ -diketones <sup>32</sup>. In 1951, Mentzer and Pillion synthesized flavones through one-step process, in which a phenol reacts with  $\beta$ -ketoesters under conventional heating <sup>32</sup>. However with this methodology, flavones were obtained in low yields <sup>32</sup>. In order to improve this strategy, in 2005, Seijas *et al.* have proposed a one-step synthesis of flavones under microwave irradiation and without using solvents <sup>146</sup>. In this methodology, phloroglucinol reacts with  $\beta$ -ketoesters under microwave conditions to afford flavones with high yields (**Figure 48**) <sup>146</sup>.

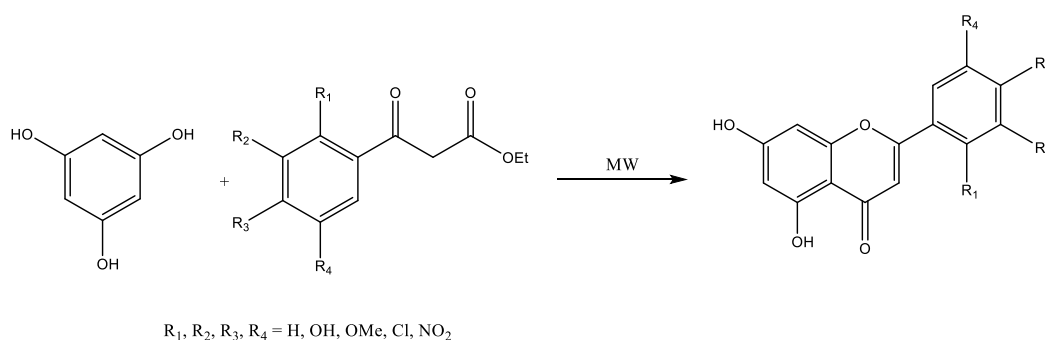


**Figure 48.** Synthesis of flavones under microwave conditions (adapted <sup>147</sup>).

The second strategy available for the synthesis of flavones uses chalcones as intermediates, which are also natural precursors of flavones. In this approach, chalcones

are synthesized through Claisen-Schmidt reaction of acetophenones with benzaldehydes. Then, chalcones can lead to flavone scaffold directly or through flavanone. The common method that is used to promote the cyclization of the chalcone to give the flavone is an oxidative ring closure with bromine and base (**Figure 49**)<sup>32</sup>.

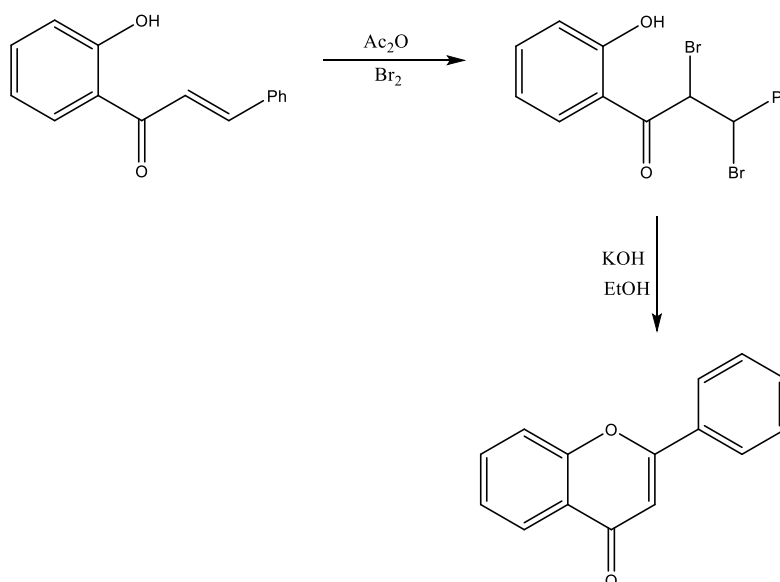


**Figure 49.** Typical oxidative cyclization of 2-hydroxychalcone (adapted<sup>32</sup>).

Moreover, flavones can also be obtained by cross-coupling reactions. Considering the methodology developed by Liang *et al.*, flavones were obtained by sequential carbonylative coupling of *o*-iodophenols with terminal acetylenes (**Figure 50**)<sup>147</sup>. This synthetic strategy has undergone some modifications, including the use of microwave irradiation or the use of ionic liquids<sup>30,32</sup>.

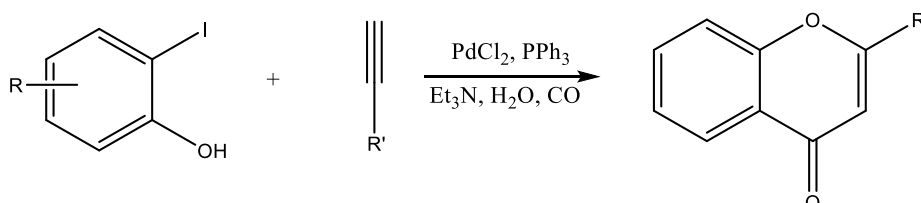


**Figure 50.** Synthesis of flavones via cross coupling reactions (adapted<sup>32</sup>).

Another approach available for the synthesis of flavones is Wittig-type reaction<sup>32</sup>. According to the methodology reported by Kumar and Bodas, firstly, the silyl ester of *O*-acyl(aroyl)salicylic acids reacts with (trimethylsilyl)-methylenetriphenylphosphorane to give

the acylphosphorane (**Figure 51**)<sup>148</sup>. Then, acylphosphorane undergoes ring closure *via* the intramolecular Wittig reaction on the ester carbonyl to afford the flavone (**Figure 51**)<sup>148</sup>.

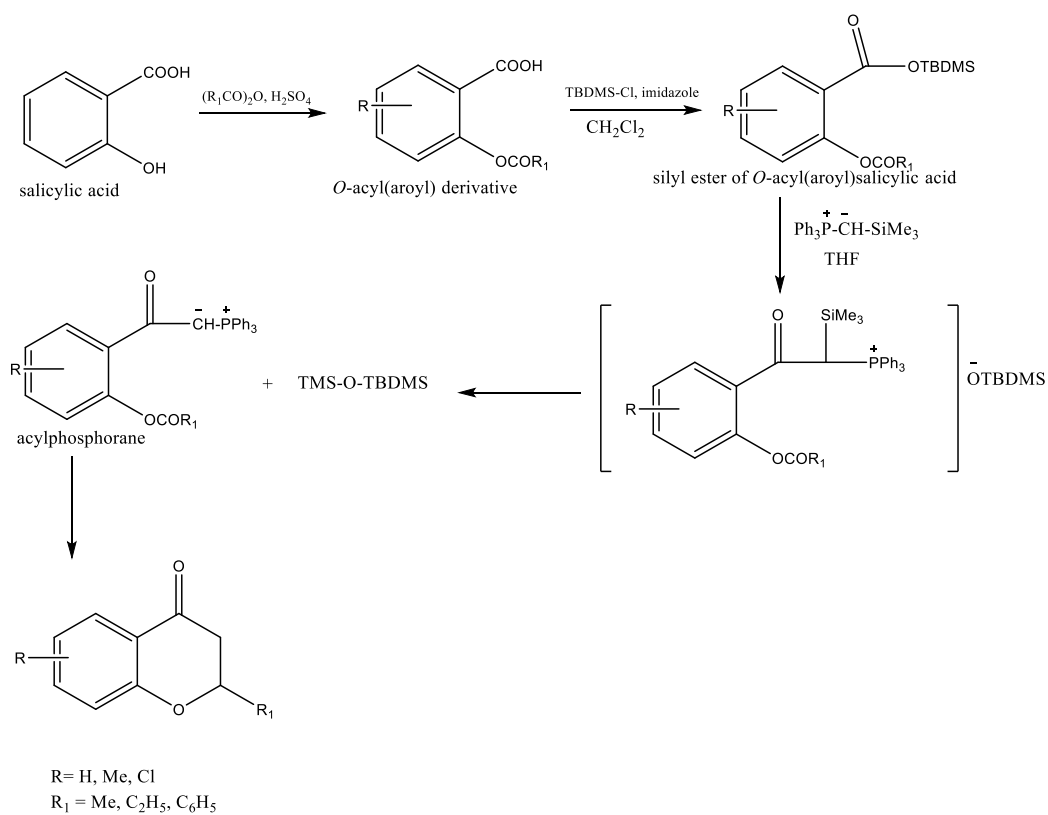


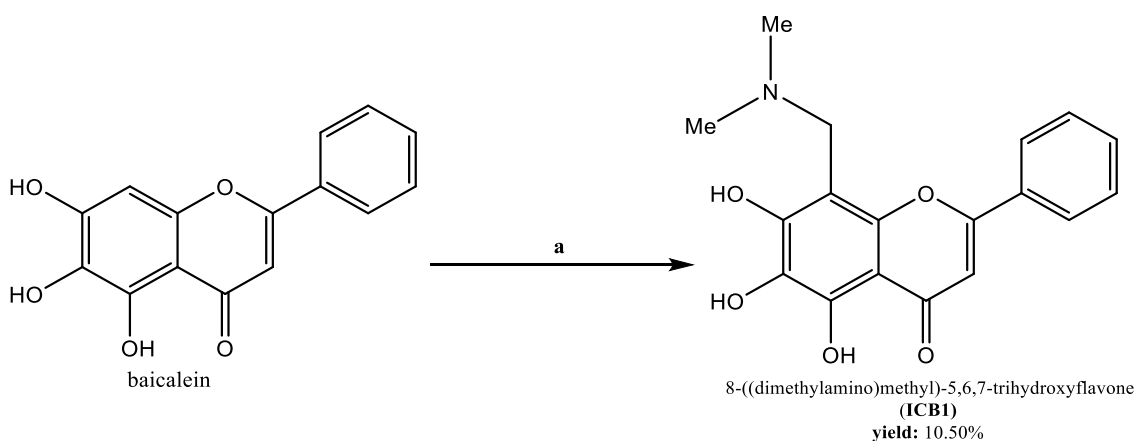
**Figure 51.** Synthesis of flavones *via* Wittig-type reactions (adapted<sup>148</sup>).

## 2.2. Results and discussion

### 2.2.1. Synthesis

#### 2.2.1.1. Amino derivative of baicalein (ICB1)

The synthetic approach used for the synthesis of the amino derivative of baicalein **ICB1** was also a Mannich reaction type. The synthetic route, the reaction conditions and the results are summarized in **Figure 52**.



**a:** dimethylamine (2.70 equiv)/HCHO (1.32 equiv)/MeOH, room temperature, 1 h 30 min

**Figure 52.** General conditions for the synthesis of amino derivative of baicalein (**ICB1**) by Mannich reaction.

In this Mannich reaction, unlike those described above, the reaction was performed as described by Zhang *et al.* (2008) for the synthesis of same compound, i. e., formaldehyde and dimethylamine were added to a baicalein methanolic solution. In contrast to that reported by Zhang *et al.* (2008), the  $^1\text{H}$  NMR of the crude product that was expected to be the desired amino derivative **ICB1** revealed a mixture of compounds. Therefore, an additionally flash column chromatography was necessary to achieve its purification. For this reason, the obtained yield was relatively low (10.50%) when compared to the previously reported by Zhang *et al.* (2008) <sup>149</sup>.

Despite this, our results show that this Mannich reaction was efficient for the synthesis of **ICB1** and the aminomethylation occurs at the most nucleophilic aromatic position (C-8) of baicalein.

### 2.2.2. Evaluation of the flavone purity

The purity of baicalein amino derivative **ICB1** was determined by HPLC-DAD, using a C18 stationary phase and a mixture of methanol:water:acetic acid (70:30:1 v/v/v) as mobile phase, and the results obtained are presented in **Table 12**.

**Table 12.** Retention time and purity of **ICB1**.

Compound	Retention time (min)	Purity (%)
<b>ICB1</b>	2.6	94.3

According to **Table 12**, it can be verified that **ICB1** shows a purity of 94.3%.

### 2.2.3. Structure elucidation

The structure elucidation of **ICB1** was established on the basis of IR and NMR techniques.  $^{13}\text{C}$  NMR assignments were determined by HSQC and HMBC experiments.

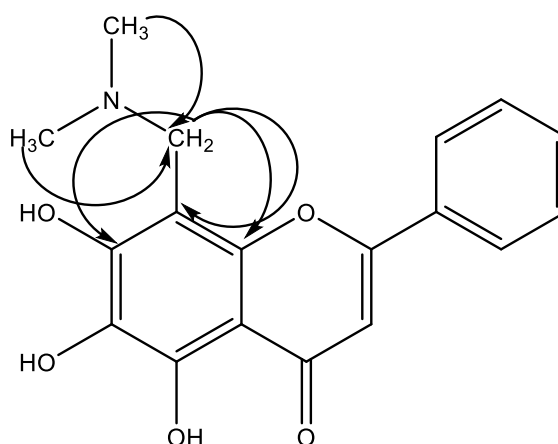
The IR data of baicalein (**B**) and its amino derivative (**ICB1**) are presented in **Table 13**. As the precursor, the IR spectra of **ICB1** showed the presence of absorption bands corresponding to hydroxyl ( $3500\text{--}3250\text{ cm}^{-1}$ ), C=O ( $1667\text{ cm}^{-1}$ ), aromatic C=C ( $1608\text{--}1468\text{ cm}^{-1}$ ) and C-O ( $1287\text{ cm}^{-1}$ ) groups. Additionally, bands at  $2955\text{ cm}^{-1}$  and  $2919\text{ cm}^{-1}$  suggested the presence of alkyl groups and a band at  $1247\text{ cm}^{-1}$  was in accordance to the presence of an aliphatic amine.

**Table 13.** IR data of baicalein (**B**) and its derivative **ICB1**.

Groups	$\nu$ (cm <sup>-1</sup> )	
	<b>B</b>	<b>ICB1</b>
<b>OH</b>	3500-3300	3500-3250
<b>Aliphatic</b>		
<b>C-H</b>	—	2955
<b>C=O</b>	1651	1667
<b>Aromatic</b>		
<b>C=C</b>	1609	1608
	1573	1572
	1498	1536
	1462	1468
<b>C-O</b>	1287	1287
<b>C-N</b>	—	1247

The <sup>1</sup>H and <sup>13</sup>C NMR data of baicalein (**B**) and its amino derivative (**ICB1**) are reported in **Table 14** and **Table 15**. The NMR data for **ICB1** are in agreement with literature<sup>150</sup>.

The <sup>1</sup>H NMR spectrum of derivative **ICB1** showed the presence of an hydrogen-bonded hydroxyl group at C-5 ( $\delta_{\text{H}}$  12.52 s), as well as a non-substituted B ring (H-3',4',5':  $\delta_{\text{H}}$  7.54-7.52 m; H-2',6':  $\delta_{\text{H}}$  7.84-7.82 m) as the building block (**B**). Instead of the singlet at  $\delta_{\text{H}}$  6.60 s (H-8) observed for baicalein (**B**), characteristic signals of a dimethylamine ( $\delta_{\text{H}}$  2.45 s;  $\delta_{\text{C}}$  44.47) attached to C-8 by a methylene bridge ( $\delta_{\text{H}}$  4.01 s;  $\delta_{\text{C}}$  55.39) are observed in the <sup>1</sup>H NMR and <sup>13</sup>C NMR spectra of **ICB1**. The position of this dimethylaminomethyl side chain in derivative **ICB1** was supported by the correlations observed in the HMBC spectrum (**Figure 53**).

**Figure 53.** Main connectivities found in the HMBC of **ICB1**.

**Table 14.**  $^1\text{H}$  NMR data of baicalein (**B**) and its amino derivative (**ICB1**).

	<b>B1</b>	<b>ICB1</b>
<b>H-3</b>	6.64 (s)	6.63 (s)
<b>H-5</b>	12.72 (OH, s)	12.52 (OH, s)
<b>H-6</b>	—	—
<b>H-7</b>	—	—
<b>H-8</b>	6.60 (s)	—
<b>N(CH<sub>3</sub>)<sub>2</sub></b>	—	2.45 (s)
<b>CH<sub>2</sub>N</b>	—	4.01 (s)
<b>H-2',6'</b>	7.92-7.88 (m)	7.84- 7.82 (m)
<b>H-3',4',5'</b>	7.60-7.52 (m)	7.54-7.52 (m)

Values in parts *per* million ( $\delta_H$ ). Measured in  $\text{CDCl}_3$  at 300.13 MHz.

**Table 15.**  $^{13}\text{C}$  NMR data of baicalein (**B**) and its amino derivative (**ICB1**).

	<b>B1</b>	<b>ICB1</b>
<b>C-2</b>	163.0	162.60
<b>C-3</b>	104.2	104.31
<b>C-4</b>	182.0	182.53
<b>C-4a</b>	104.4	105.18
<b>C-5</b>	146.5	145.43
<b>C-6</b>	128.7	119.78
<b>C-7</b>	152.8	153.65
<b>C-8</b>	93.7	98.54
<b>8-CH<sub>2</sub>N</b>	—	55.39
<b>N(CH<sub>3</sub>)<sub>2</sub></b>	—	44.47
<b>C-8a</b>	150.0	147.17
<b>C-1'</b>	130.9	131.43
<b>C-2',6'</b>	125.6	126.02
<b>C-3',5'</b>	128.5	129.10
<b>C-4'</b>	131.1	132.05

Values in parts *per* million ( $\delta_C$ ). Measured in  $\text{CDCl}_3$  at 75.47 MHz.

Assignments were confirmed by HSQC and HMBC experiments.

### 3. Experimental

#### 3.1. General Methods

All the reagents and solvents were purchased from Sigma Aldrich and were used without further purification. Solvents were evaporated using rotary evaporator under reduced pressure (Buchi Waterchath B-480).

MW reactions were performed using a glassware setup for atmospheric-pressure reactions and a 100 mL reactor (internal reaction temperature measurements with a fiber-optic probe sensor) and were carried out using an Ethos MicroSYNTH 1600 Microwave Labstation from Milestone.

All reactions were monitored by TLC carried out on precoated plates (silica gel, 60 F 254 Merck) with 0.2 mm of thickness. The visualization of the chromatograms was under UV light at 254 and 365 nm.

The purifications of compounds were performed by flash column chromatography using Macherey-Nagel silica gel 60 (0.04-0.063 mm) or by preparative TLC using Merck silica gel 60 (GF254) plates.

Melting points were obtained in a Köfeler microscope and are uncorrected.

IR spectra were measured on a KBr microplate in a FTIR spectrometer Nicolet iS10 from Thermo Scientific with Smart OMNI-Transmisson accessory (Software OMNIC 8.3).

$^1\text{H}$  and  $^{13}\text{C}$  NMR spectra were performed in the Departamento de Química, Universidade de Aveiro, and were taken in  $\text{CDCl}_3$  (Deutero GmbH) at r.t. or  $\text{DMSO-d}_6$  (Deutero GmbH) at r.t., on Bruker Avance 300 instruments (300.13 MHz for  $^1\text{H}$  and 75.47 MHz for  $^{13}\text{C}$ ).

Analytical HPLC-DAD analyses were performed on a SpectraSYSTEM (Thermo Fisher Scientific, Inc, USA) equipped with a P4000 pump, an AS3000 autosampler and a diode array detector UV8000. The separation was carried out on a 250 x 4.6 mm i.d. FortisBIO C18 (5  $\mu\text{m}$ ) (FortisTM Technologies Ltd, Cheshire, UK). ChromQuest 5.0 (version 3.2.1) software (Thermo Fisher Scientific Inc.) managed chromatographic data. Methanol (HPLC grade) was obtained from Carlo Erba Reagents, (Val de Reuil, Italy), acetic acid (HPLC grade) was obtained from Romil Pure Chemistry (Cambridge, UK) and HPLC grade water (Simplicity® UV Ultrapure Water System, Millipore Corporation, USA). Prior to use, mobile phase solvents were degassed in an ultrasonic bath for 15 min.

### 3.2. Synthesis of xanthone derivatives

#### 3.2.1. Synthesis of 1,3,8-trihydroxyxanthone (ICX1)

##### Method A: Eaton's reaction

A mixture of phosphorus pentoxide (1.00 g, 3.50 mmol) and methanesulfonic acid (15 mL) was heated on a steam bath (90 °C) until a clear solution was obtained (30 minutes). Then, a mixture of phoroglucinol (0.38 g, 3 mmol) and 2,6-dihydroxybenzoic acid (0.46 g, 3 mmol) was added to the reaction mixture. This mixture was stirred at reflux (80 °C) for 1 h and the progress of the reaction was monitored by TLC. Then, the resulting mixture was slowly poured into crushed ice and allowed to stand overnight in the fridge. The solid was collected by filtration, washed with water and dried in oven (60 °C). The crude product was purified by flash column chromatography (SiO<sub>2</sub>, petroleum ether : EtOAc (9:1 v/v)) to afford **ICX1** (yield: 2.07%).

##### Method B: GSS reaction (modified method for MW)

A mixture of zinc chloride (13.25 g, 97.2 mmol) and phosphorus oxychloride (55 mL) was submitted to microwave irradiation at 400 W of potency during 10 min at 60 °C. Then, the 2,6-dihydroxybenzoic acid (5.00 g, 32.40 mmol) was added and the reaction mixture was subjected to microwave irradiation at 400 W of power for 10 min at 60 °C. Finally, phoroglucinol (4.10 g, 32.40 mmol) was added and the mixture was submitted to microwave irradiation at 400 W of power during 60 min at 60 °C. After cooling, the resulting mixture was quenched into crushed ice and extracted successively with CH<sub>2</sub>Cl<sub>2</sub> (9 x 200 mL) and saturated aqueous NaHCO<sub>3</sub> 5% w/v (3 x 250 mL). The organic layers were dried over anhydrous Na<sub>2</sub>SO<sub>4</sub> and evaporated under reduced pressure. The crude product was purified by flash column chromatography (SiO<sub>2</sub>, *n*-hexane : EtOAc (9.5:0.5 v/v)) to yield compound **ICX1** as yellow solid (yield: 2.38%).

**m.p.** 219-220 °C; **IR** (KBr,  $\nu$  (cm<sup>-1</sup>)): 3500-3400 (OH); 1663 (C=O); 1601, 1565, 1514, 1483 (aromatic C=C); 1293 (C-O); **<sup>1</sup>H NMR** (300 MHz, DMSO-d<sub>6</sub>),  $\delta$  (ppm): 11.89 (1 H, s, OH-1), 11.81 (1 H, s, OH-8), 7.68 (1 H, *brt*,  $J$  = 8.4 Hz, H-6), 7.00 (1 H, *dd*,  $J$  = 8.4, 0.9 Hz, H-5), 6.79 (1 H, *dd*,  $J$  = 8.4, 0.9 Hz, H-7), 6.38 (1 H, *d*,  $J$  = 2.1 Hz, H-4), 6.21 (1 H, *d*,  $J$

= 2.1 Hz, H-2);  $^{13}\text{C}$  NMR (75.47 MHz, DMSO- $d_6$ ),  $\delta$  (ppm): 183.26 (C-9), 167.06 (C-3), 162.16 (C-1), 160.27 (C-8), 157.51 (C-4a), 155.49 (C-10a), 137.18 (C-6), 110.60 (C-7), 107.10 (C-5), 106.88 (C-8a), 101.00 (C-9a), 98.70 (C-2), 94.48 (C-4).

### 3.2.2. Synthesis of 1,8-dihydroxy-3-methoxyxanthone (ICX2)

A mixture of 1,3,8-trihydroxyxanthone (**ICX1**) (0.30 g, 1.23 mmol), methyl iodide (0.803 mL, 12.30 mmol, 10 equiv.) and anhydrous  $\text{K}_2\text{CO}_3$  (0.21 g, 1.24 mmol, 1 equiv.) in anhydrous acetone (40 mL) was stirred at reflux (60 °C) for 3 h. The progress of the reaction was monitored by TLC. On completion, the solid was filtered, the solvent removed under reduced pressure and the crude product was purified by crystallization with acetone and by flash column chromatography ( $\text{SiO}_2$ , *n*-hexane) to yield compound **ICX2** as yellow needle solid. Yield: 74%; **m.p.** 170-172 °C; **IR** (KBr,  $\nu$  ( $\text{cm}^{-1}$ )): 3500-3400 (OH); 1662 (C=O); 1603, 1568, 1505, 1470 (aromatic C=C); 2959, 2925, 2852 (aliphatic C-H); 1294 (C-O);  $^1\text{H}$  NMR (300 MHz,  $\text{CDCl}_3$ ),  $\delta$  (ppm): 11.99 (1 H, s, OH-1), 11.92 (1 H, s, OH-8), 7.56 (1 H, *brt*,  $J$  = 8.4 Hz, H-6), 6.87 (1 H, *dd*,  $J$  = 8.4, 0.8 Hz, H-5), 6.78 (1 H, *dd*,  $J$  = 8.4, 0.8 Hz, H-7), 6.42 (1 H, *d*,  $J$  = 2.3 Hz, H-4), 6.35 (1 H, *d*,  $J$  = 2.3 Hz, H-2), 3.89 (3 H, s, 3-  $\text{OCH}_3$ );  $^{13}\text{C}$  NMR (75.47 MHz,  $\text{CDCl}_3$ ),  $\delta$  (ppm): 184.63 (C-9), 167.35 (C-3), 162.97 (C-1), 161.31 (C-8), 157.78 (C-4a), 156.14 (C-10a), 136.80 (C-6), 110.89 (C-7), 106.96 (C-5), 106.96 (C-8a), 102.70 (C-9a), 97.41 (C-2), 93.10 (C-4), 55.93 (3-  $\text{OCH}_3$ ).

### 3.2.3. Synthesis of 2-(dimethylamino)methyl-1,8-dihydroxy-3-methoxyxanthone (ICX2a)

Dimethylamine (0.420 mL, 0.8395 mmol, 4.35 equiv.) was cooled in the ice bath for about 5 min and were added dropwise 37% formaldehyde solution (0.104 mL, 1.28 mmol, 6.63 equiv.) and acetic acid (0.965 mL, 16.85 mmol). The reaction mixture was stirred at room temperature for 1 h and then, was added 1,8-dihydroxy-3-methoxyxanthone (**ICX2**) (0.050 g, 0.193 mmol). The mixture was stirred at room temperature for 6 days and then treated with water (5 mL) and continued stirring for about 12 h. The resulting solid was filtered and the filtrate was treated with NaOH (10% w/v) until the pH was 9~10. Finally, the

precipitate was also filtered, washed with water, dried and then purified by flash column chromatography (SiO<sub>2</sub>, petroleum ether:Chloroform:Ammonia (95:5:1 v/v/v)). Yield: 6.29%; **m.p.** 118-120 °C; **IR** (KBr,  $\nu$  (cm<sup>-1</sup>)): 3600-3400 (OH); 1653 (C=O); 1605, 1558, 1539, 1490 (aromatic C=C); 2923, 2853 (aliphatic C-H); 1296 (C-O); 1230 (C-N); **<sup>1</sup>H NMR** (300 MHz, CDCl<sub>3</sub>),  $\delta$  (ppm): 12.09 (1 H, s, OH-1), 12.09 (1 H, s, OH-8), 7.55 (1 H, *brt*,  $J$  = 8.3 Hz, H-6), 6.86 (1 H, *brd*,  $J$  = 8.3 Hz, H-5), 6.78 (1 H, *brd*,  $J$  = 8.3 Hz, H-7), 6.44 (1 H, s, H-4), 3.94 (3 H, s, 3- OCH<sub>3</sub>), 3.64 (2 H, s, CH<sub>2</sub>N), 2.37 (6 H, s, N(CH<sub>3</sub>)<sub>2</sub>); **<sup>13</sup>C NMR** (75.47 MHz, CDCl<sub>3</sub>),  $\delta$  (ppm): 184.33 (C-9), 165.79 (C-3), 161.39 (C-1), 161.39 (C-8), 157.69 (C-4a), 155.96 (C-10a), 136.58 (C-6), 110.90 (C-7), 107.85 (C-5), 106.79 (C-8a), 102.70 (C-9a), 103.5 (C-2), 90.05 (C-4), 56.34 (3- OCH<sub>3</sub>), 49.97(CH<sub>2</sub>N), 44.96 (N(CH<sub>3</sub>)<sub>2</sub>).

### 3.2.4. Synthesis of baicalein amino derivative (ICB1)

Baicalein (**B**) (0.2 g, 0.74 mmol) was dissolved in methanol (100 mL) and to this solution were added dropwise 37% (v/v) formaldehyde solution (0.018 mL, 0.98 mmol, 1.32 equiv.) and dimethylamine solution (1.00 mL, 2.00 mmol, 2.70 equiv.). The mixture was stirred at room temperature for 1 h 30 min. The precipitate was collected, filtered, and washed several times with methanol. Then, the precipitate was purified by flash column chromatography (SiO<sub>2</sub>, Chloroform:Methanol:Ammonia (90:10:2 v/v/v)). Yield: 10.50%; **m.p.** 286-288 °C; **IR** (KBr,  $\nu$  (cm<sup>-1</sup>)): 3500-3250 (OH); 1667 (C=O); 1608, 1572, 1536, 1468 (aromatic C=C); 2955, 2919 (aliphatic C-H); 1287 (C-O); 1247 (C-N); **<sup>1</sup>H NMR** (300 MHz, CDCl<sub>3</sub>),  $\delta$  (ppm): 12.52 (1 H, s, OH-5), 7.84- 7.82 (2 H, *m*, Ar-2',6'-H), 7.54-7.52 (3 H, *m*, Ar-3',4',5'-H), 6.63 (1 H, s, H-3), 4.01 (2 H, s, CH<sub>2</sub>N), 2.45 (6 H, s, N(CH<sub>3</sub>)<sub>2</sub>); **<sup>13</sup>C NMR** (75.47 MHz, CDCl<sub>3</sub>),  $\delta$  (ppm): 182.53 (C-4), 162.60 (C-2), 153.65 (C-7), 147.17 (C-8a), 145.43 (C-5), 132.05 (C-4'), 131.43 (C-1'), 129.10 (C-3',5'), 126.02 (C-2',6'), 119.78 (C-6), 105.18 (C-4a), 104.31 (C-3), 98.54 (C-8), 55.39 (CH<sub>2</sub>N), 44.47 (N(CH<sub>3</sub>)<sub>2</sub>).

### 3.3. Evaluation of the purity

The purity of each compound was determined by HPLC-DAD. LC analysis was performed by isocratic elution using a mixture of MeOH:H<sub>2</sub>O:MeCO<sub>2</sub>H (70:30:1 v/v/v) as

mobile phase and the flow rate was set at 1 mL/min. The injected volume was 10  $\mu$ L and the elution was monitored at 275 nm. The detector was set at a wavelength range of 220–500 nm with a spectral resolution of 1 nm. The purity parameters included a 95% active peak region and a scan threshold of 5 mAU.

## 4. Conclusions

The results obtained in different syntheses for xanthone and flavone derivatives allow us to draw some conclusions:

- We could synthesize totally the building block **ICX1** by two different one-spot methodologies: Eaton's reaction and modified GSS reaction assisted by MW. These two strategies were not very effective for the synthesis of **ICX1**, because, although they had short reaction times, **ICX1** was obtained with low yields;
- The synthesis of **ICX1** amino derivatives by Mannich reaction failed to obtain any Mannich base derivative;
- In the methylation reaction of **ICX1**, its methylated derivative **ICX2** was obtained in high yield (74%);
- The amino derivative of **ICX2** (**ICX2a**) was obtained by Mannich reaction with a low yield (6.29%);
- The Mannich reaction applied for baicalein (**B**) allowed to afford **ICB1** with a relatively low yield (10.50%).

# CHAPTER IV

## BIOLOGICAL ACTIVITY

## 1. Antioxidant activity

### 1.1. Introduction

Nowadays, there are a wide variety of methods for evaluation of antioxidant activity of natural and synthetic compounds. The most commonly used assays to determine antioxidant activity can be divided in several categories according to the aims, namely assays to determine the ability of compounds to scavenge free radicals (specific ROS/RNS or stable, non-biological radicals), the reducing capacity, metal chelating activity, interference with antioxidant enzyme activity and inhibition of oxidative enzymes. These methods have been exhaustively reviewed by several authors <sup>150-153</sup>.

Among all these methods, the DPPH assay is clearly the most often used to assess the antioxidant capacity of xanthenes and flavones <sup>101,106,116,118,154-163</sup>. This choice is mainly due to the stability of this non-biological radical, which cannot dimerize unlike what happens with other free radicals. Moreover, it is a quick, easy and economical method and allows the analysis of multiple samples if is performed in microplates <sup>164</sup>.

## 1.2. Results and discussion

The antioxidant activity of all synthesized compounds has been evaluated. Besides this, this biological activity was also studied for other structure related aminoxanthonic derivatives previously synthesized in our research group (**Figure 54**).

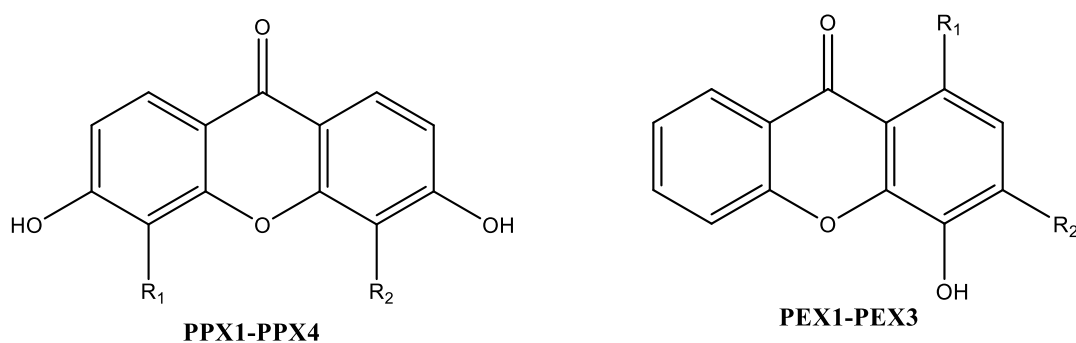


**Figure 54.** Basic structure of the aminoxanthonic derivatives previously synthesized in our research group.

### 1.2.1. DPPH radical scavenging activity

The DPPH assay is widely used to assess the ability of compounds to transfer labile H-atoms to this free radical. When this occurs, the color of DPPH radical changes from purple to yellow (non-radical form), being accompanied by a decrease in absorbance at 520 nm<sup>165</sup>. This assay was performed for all xanthonic and flavonic derivatives and the obtained results are summarized in **Table 16**.

**Table 16.** DPPH radical scavenging activity of tested compounds.

Compound	% of scavenging DPPH radical at 100 $\mu$ M	IC <sub>50</sub> ( $\mu$ M)
ICX1	n.a.	n.d.
ICX2	n.a.	n.d.
ICX2a	n.a.	n.d.
PPX1	5.92 $\pm$ 0.84**	n.d.
PPX2	2.32 $\pm$ 0.25*	n.d.
PPX3	5.74 $\pm$ 0.83*	n.d.
PPX4	n.a.	n.d.
PEX1	69.26 $\pm$ 2.11***	61.62 $\pm$ 0.72***
PEX3	47.09 $\pm$ 1.35***	108.99 $\pm$ 0.87***
B	96.03 $\pm$ 0.42***	35.09 $\pm$ 4.13***
ICB1	93.93 $\pm$ 0.20***	30.40 $\pm$ 1.28***

Results are given as mean  $\pm$  SEM of three independent experiments performed in triplicate; n.a.: not active; n.d.: not determined. Ascorbic Acid (positive control): IC<sub>50</sub>: 20.40  $\pm$  0.000213  $\mu$ M \*\*\*. \*p<0.05; \*\*p<0.01; \*\*\*p<0.001.

Regarding xanthone derivatives, the results indicate that **ICX1** and its methylated (**ICX2**) and Mannich base (**ICX2a**) derivatives did not possess scavenging activity against DPPH radical at 100  $\mu$ M. At this concentration, the other aminoxanthenes (except **PPX4**) showed activity against DPPH radical. Particularly, xanthenes **PPX1**, **PPX2** and **PPX3** demonstrated low activity, while **PEX1** and **PEX3** showed considerable scavenging activity at 100  $\mu$ M, revealing IC<sub>50</sub> values of 61.62  $\mu$ M and 108.99  $\mu$ M, respectively.

For the tested flavones, these results show that baicalein (**B**) and its Mannich base derivative (**ICB1**) exhibited high free radical scavenging activity on DPPH assay, with IC<sub>50</sub> values of 35.09  $\pm$  4.13  $\mu$ M and 30.40  $\pm$  1.28  $\mu$ M, respectively. This DPPH scavenging activity was very similar for both flavonic compounds, showing that the presence of a 8-(dimethylamino)methyl group on the flavone skeleton did not significantly alter its ability to scavenge free radicals.

### 1.2.2. Iron chelating activity

We also explored the iron-chelating ability of all xanthenes and flavones. In the method used, ferrozine forms complexes with  $\text{Fe}^{2+}$  and in the presence of chelating compounds, occurs a reduction in the formation of this complex, resulting in a decrease in the red color of this complex. Therefore, this chelating effect is due to the antioxidant capacity of tested compounds <sup>73</sup>.

The iron chelating activity of all tested compounds is summarized in **Table 17**.

**Table 17.** Iron chelating activity of tested compounds.

Compound	% of chelation at 100 $\mu\text{M}$	$\text{IC}_{50}$ ( $\mu\text{M}$ )
<b>ICX1</b>	12.19 $\pm$ 2.55*	n.d.
<b>ICX2</b>	n.a.	n.d.
<b>ICX2a</b>	88.40 $\pm$ 0.56***	65.94 $\pm$ 1.57***
<b>PPX1</b>	n.a.	n.d.
<b>PPX2</b>	n.a.	n.d.
<b>PPX3</b>	n.a.	n.d.
<b>PPX4</b>	n.a.	n.d.
<b>PEX1</b>	n.a.	n.d.
<b>PEX3</b>	n.a.	n.d.
<b>B</b>	18.24 $\pm$ 3.46*	n.d.
<b>ICB1</b>	49.90 $\pm$ 0.23***	100 $\pm$ 0.21***

Results are given as mean  $\pm$  SEM of three independent experiments performed in triplicate; n.a.: not active; n.d.: not determined. EDTA (positive control):  $\text{IC}_{50}$ : 30.66  $\pm$  0.17  $\mu\text{M}$  \*\*\*. \* $p$ <0.05; \*\*\* $p$ <0.001.

The overall results indicate that among the tested xanthenes, only **ICX1** and **ICX2a** had chelating activity at 100  $\mu\text{M}$ , being xanthone **ICX2a** the most active, with an  $\text{IC}_{50}$  value of 65.94  $\pm$  1.57  $\mu\text{M}$ .

Comparing the iron chelating effects of the structure related xanthenes **ICX1**, **ICX2** and **ICX2a**, it was found that not only the presence of an hydroxyl group instead of a methoxyl group at C-3 can favor the chelating activity, but also the presence of a 2-(dimethylamino)methyl group on the xanthonic scaffold has an important role for this activity.

For the tested flavones **B** and **ICB1**, both showed interesting chelating activity at 100  $\mu\text{M}$ , suggesting that the catechol moiety in the structure of these flavones was associated with their iron chelating capacity. In fact, it was reported that the presence of *ortho*-OH groups offers appropriate geometric and electronic environments to bind metal ions <sup>38,39</sup>.

In the case of baicalein (**B**) and attending to its structure, it was expected an higher activity than that obtained in this assay because in several papers baicalein (**B**) showed a strong metal chelating activity <sup>110,166-168</sup>. The same papers also reported that this strong chelating ability was linked to the presence of three adjacent hydroxyl groups and, consequently, the iron chelation will occur in the three different positions, such as, between C-4 oxo and C-5 hydroxyl group and between both hydroxyl groups at C-5 and C-6 or C-6 and C-7 <sup>110,112,121,166-169</sup>. Additionally, Woźniak *et al.* referred that in baicalein (**B**), chelation of iron can also take place between two molecules in C-6 and C-7 of the A ring, forming baicalein<sub>2</sub>-Fe<sup>2+</sup> complexes, causing this configuration a stronger iron chelation <sup>121</sup>.

Moreover, comparing the chelating activity of **B** (18.24 ± 3.46%) with **ICB1** (49.90 ± 0.23%), it is possible to infer that the introduction of a 8-(dimethylamino)methyl group on the baicalein scaffold (**B**), forming its Mannich base analogue **ICB1**, was associated with an improvement of the iron chelating activity.

### 1.2.3. Copper chelating activity

The copper chelating activity of xanthenes and flavones was assessed by UV-Vis spectroscopy, mainly through the detection of bathochromic shifts in the spectra of the tested compounds in the presence of Cu<sup>2+</sup> ions at pH 7.4. For this, the UV-Vis spectra of each tested compound in PBS at pH 7.4 alone (red spectra, **Figure 55**; **Figure 56** and **Figure 57**) and in the presence of a solution of CuSO<sub>4</sub> 50 µM (blue spectra, **Figure 55**; **Figure 56** and **Figure 57**) or 25 µM (green spectra, **Figure 55**; **Figure 56** and **Figure 57**) were recorded. In addition, the UV-Vis spectrum of each compound in the presence of CuSO<sub>4</sub> 25 µM after addition of EDTA 125 µM (pink spectra, **Figure 55**; **Figure 56** and **Figure 57**) was also registered.

The results obtained for copper chelating activity of xanthone **ICX1** and its derivatives **ICX2** and **ICX2a** are showed in **Figure 55**; **Figure 56** and **Figure 57**.

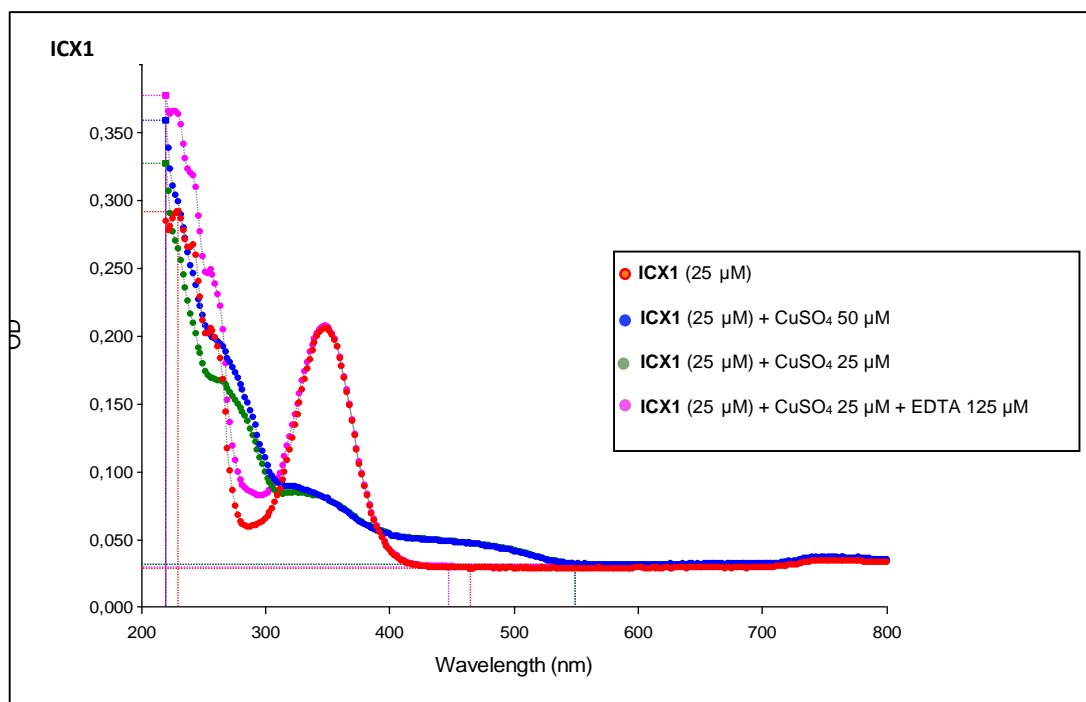


**Figure 55.** Copper interaction with **ICX1** and its effect in UV-Vis spectrum of this compound. Red - spectrum, **ICX1** (25  $\mu\text{M}$ ); Blue - spectrum, **ICX1** (25  $\mu\text{M}$ ) plus  $\text{Cu}^{2+}$  ions (50  $\mu\text{M}$ ); Green - spectrum, **ICX1** (25  $\mu\text{M}$ ) plus  $\text{Cu}^{2+}$  ions (25  $\mu\text{M}$ ); Pink - spectrum, **ICX1** (25  $\mu\text{M}$ ) plus  $\text{Cu}^{2+}$  ions (25  $\mu\text{M}$ ) after addition of EDTA (125  $\mu\text{M}$ ).

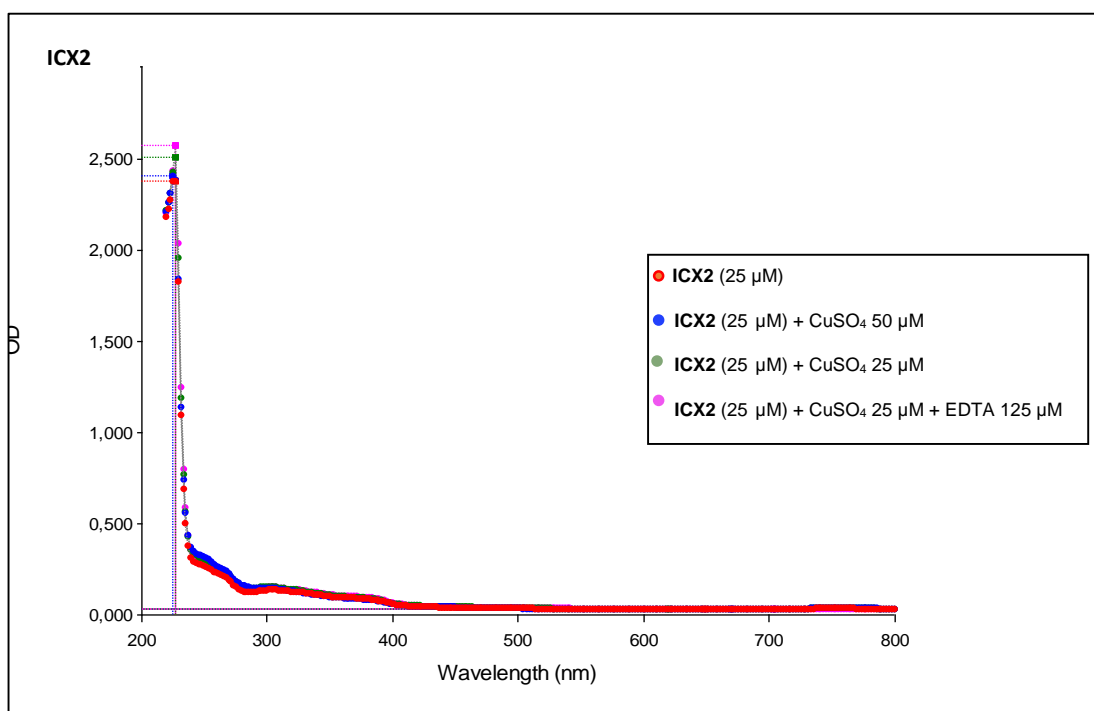


**Figure 56.** Copper interaction with **ICX2** and its effect in UV-Vis spectrum of this compound. Red - spectrum, **ICX2** (25  $\mu\text{M}$ ); Blue - spectrum, **ICX2** (25  $\mu\text{M}$ ) plus  $\text{Cu}^{2+}$  ions (50  $\mu\text{M}$ ); Green - spectrum, **ICX2** (25  $\mu\text{M}$ ) plus  $\text{Cu}^{2+}$  ions (25  $\mu\text{M}$ ); Pink - spectrum, **ICX2** (25  $\mu\text{M}$ ) plus  $\text{Cu}^{2+}$  ions (25  $\mu\text{M}$ ) after addition of EDTA (125  $\mu\text{M}$ ).

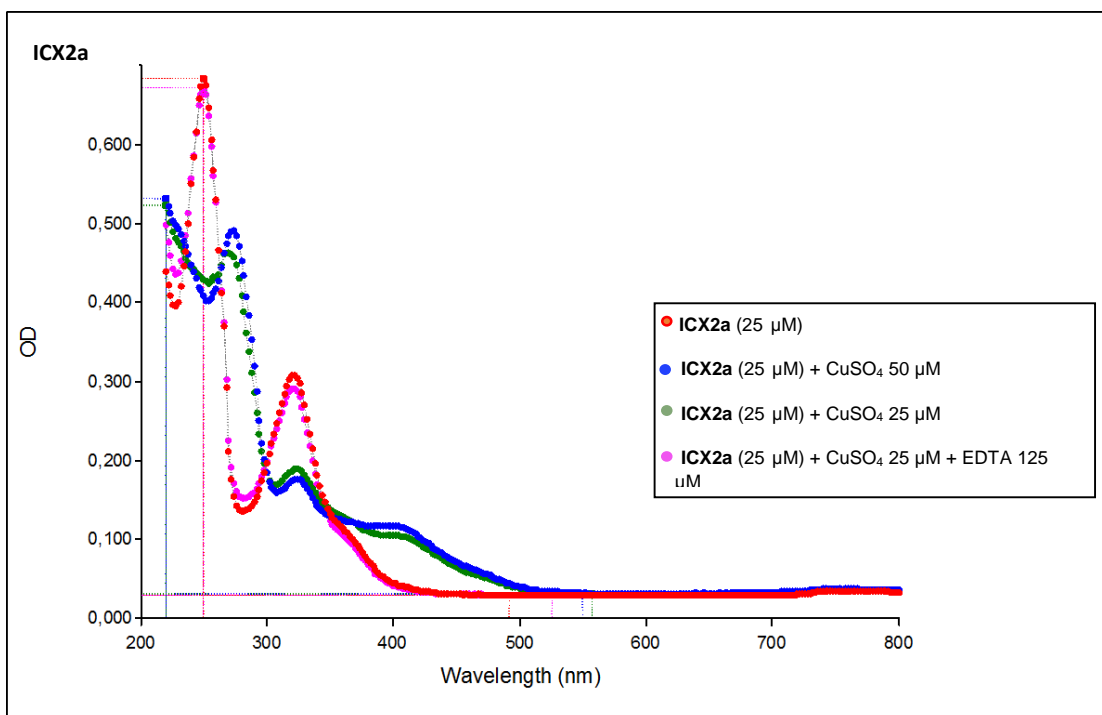


**Figure 57.** Copper interaction with **ICX2a** and its effect in UV-Vis spectrum of this compound. Red-spectrum, **ICX2a** (25  $\mu\text{M}$ ); Blue - spectrum, **ICX2a** (25  $\mu\text{M}$ ) plus  $\text{Cu}^{2+}$  ions (50  $\mu\text{M}$ ); Green - spectrum, **ICX2a** (25  $\mu\text{M}$ ) plus  $\text{Cu}^{2+}$  ions (25  $\mu\text{M}$ ); Pink - spectrum, **ICX2a** (25  $\mu\text{M}$ ) plus  $\text{Cu}^{2+}$  ions (25  $\mu\text{M}$ ) after addition of EDTA (125  $\mu\text{M}$ ).

The differences observed in the spectrum of **ICX1** after the addition of  $\text{Cu}^{2+}$  (blue and green spectra, **Figure 55**) in comparison with the spectrum in the absence of this metal ion (red spectrum, **Figure 55**) and the regeneration of the original spectrum (pink spectrum, **Figure 55**) after the addition of EDTA suggest that **ICX1** has some  $\text{Cu}^{2+}$  chelating effect.

Nevertheless, no chelating activity was observed for the **ICX1** methylated derivative (**ICX2**) since all spectra are overlapped (**Figure 56**).

For **ICX2** Mannich base derivative (**ICX2a**) some chelating activity was observed. In fact, interactions of **ICX2a** with  $\text{Cu}^{2+}$  ions at 25  $\mu\text{M}$  (green spectrum, **Figure 57**) and 50  $\mu\text{M}$  (blue spectrum, **Figure 57**) produced bathochromic shifts in band at 250 nm of 18 nm (**Table 18**) and 24 nm (**Table 18**), respectively, associated with a small decrease in absorbance. Although no changes in the position of the band at 324 nm were detected, it was observed an increase in absorbance for wavelengths near 400 nm (absorbance increased from 0.05 to 0.118) in the spectrum of **ICX2a** plus  $\text{Cu}^{2+}$  (blue and green spectra, **Figure 57**).

**Table 18.** UV spectral shifts of **ICX2a**.

<b>Xanthone</b>	<b><math>\lambda_{\text{max}}</math> (nm)</b>			
	<b>Spectra in PBS pH 7.4</b>	<b>Spectra in PBS pH 7.4 with CuSO<sub>4</sub> 50 <math>\mu\text{M}</math></b>	<b>Spectra in PBS pH 7.4 with CuSO<sub>4</sub> 25 <math>\mu\text{M}</math></b>	<b>Spectra in PBS pH 7.4 with CuSO<sub>4</sub> 25 <math>\mu\text{M}</math> and EDTA 125 <math>\mu\text{M}</math></b>
<b>ICX2a</b>	250	274	268	250

In conclusion, comparing the results obtained for **ICX2** and **ICX2a**, is possible to infer that the aminomethylation at C-2 of the xanthone nucleus potentiates its chelating activity.

Considering the spectra obtained for aminoxanthonenes **PPX1**, **PPX2**, **PPX3**, **PPX4**, **PEX1** and **PEX3** presented in **Figure 58**, no chelating activity was detected since the spectrum of each compound in the presence of copper was overlapped with the spectrum of the compound alone.

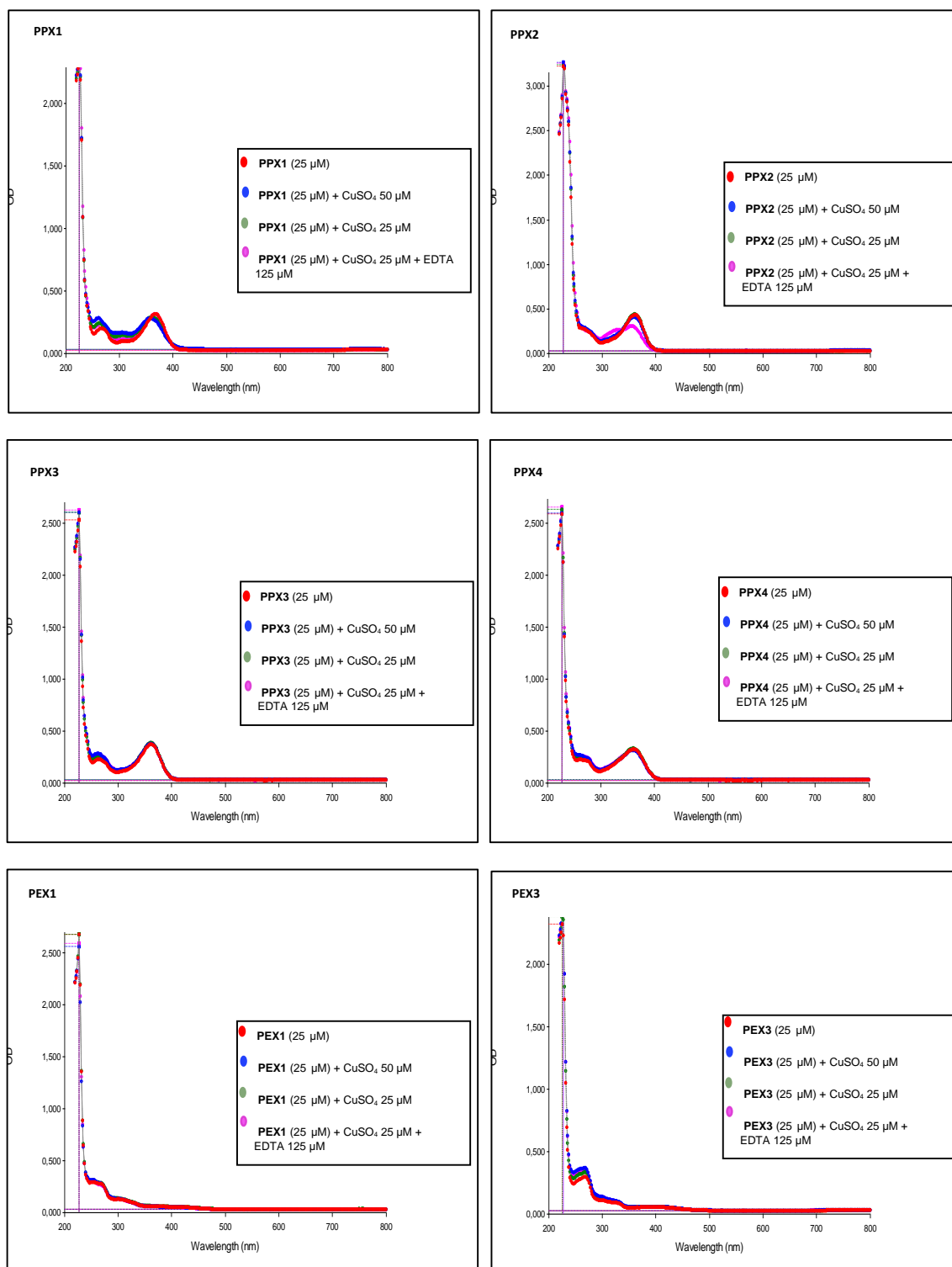


**Figure 58.** Copper interaction with **PPX1**, **PPX2**, **PPX3**, **PPX4**, **PEX1** and **PEX3** and its effect in UV-Vis spectrum of each compound. Red - spectrum, **PPX1**, **PPX2**, **PPX3**, **PPX4**, **PEX1** and **PEX3** (25  $\mu\text{M}$ ); Blue - spectrum, **PPX1**, **PPX2**, **PPX3**, **PPX4**, **PEX1** and **PEX3** (25  $\mu\text{M}$ ) plus  $\text{Cu}^{2+}$  ions (50  $\mu\text{M}$ ); Green - spectrum, **PPX1**, **PPX2**, **PPX3**, **PPX4**, **PEX1** and **PEX3** (25  $\mu\text{M}$ ) plus  $\text{Cu}^{2+}$  ions (25  $\mu\text{M}$ ); Pink - spectrum, **PPX1**, **PPX2**, **PPX3**, **PPX4**, **PEX1** and **PEX3** (25  $\mu\text{M}$ ) plus  $\text{Cu}^{2+}$  ions (25  $\mu\text{M}$ ) after addition of EDTA (125  $\mu\text{M}$ ).

The results obtained for copper chelating activity of the tested flavones **B** and **ICB1** are illustrated in **Figure 59**.

The interactions of baicalein (**B**) with  $\text{Cu}^{2+}$  produced hypsochromic shifts (10 nm) in band at 266 nm (blue and green spectra, **Figure 59**) and slight bathochromic shifts in band at 359 nm of 6 nm (with  $\text{CuSO}_4$  50  $\mu\text{M}$ , blue spectrum, **Figure 59**) and 3 nm (with  $\text{CuSO}_4$  25  $\mu\text{M}$ , green spectrum, **Figure 59**). Moreover, the addition of EDTA (pink spectrum, **Figure 59**) regenerated the original spectrum (**Table 19**).

The interaction of copper with baicalein Mannich base derivative (**ICB1**) also induced changes in its spectrum. Particularly, this interaction caused bathochromic shifts in band at 268 nm of 18 nm for both copper concentrations (50  $\mu\text{M}$  and 25  $\mu\text{M}$ , blue and green spectra, **Figure 59**). In addition, a slight hypsochromic shift (6 nm) accompanied by a decrease in absorbance for compound plus  $\text{Cu}^{2+}$  at 50  $\mu\text{M}$  and 25  $\mu\text{M}$  was observed for the band at 362 nm (blue and green spectra, **Figure 59**). On addition of EDTA, the original spectrum was recovered (pink spectrum, **Figure 59**). Thus, according to these results, it can be concluded that **ICB1** as well as the precursor (**B**) possess copper chelating activity.

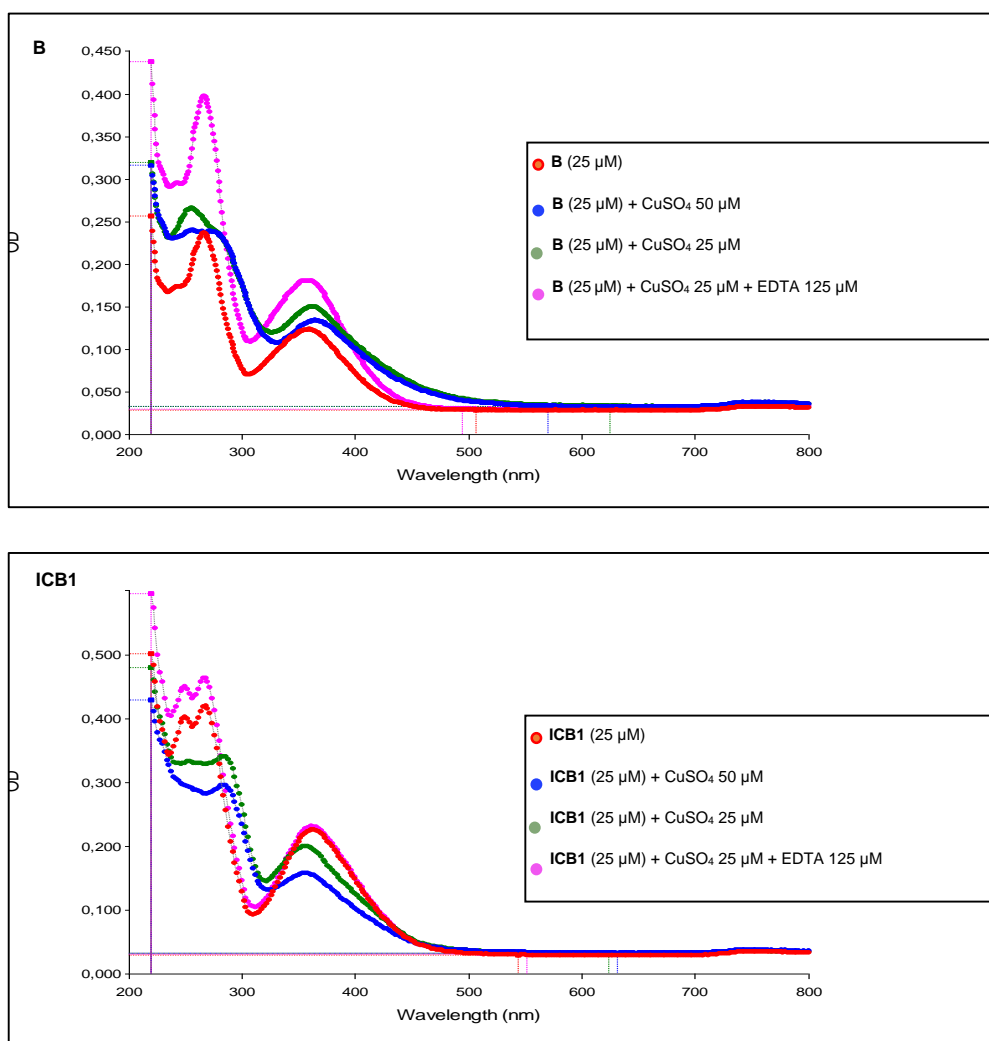


**Figure 59.** Copper interaction with **B** and **ICB1** and its effect in UV-Vis spectrum of each compound. Red - spectrum, **B** and **ICB1** (25  $\mu\text{M}$ ); Blue - spectrum, **B** and **ICB1** (25  $\mu\text{M}$ ) plus  $\text{Cu}^{2+}$  ions (50  $\mu\text{M}$ ); Green - spectrum, **B** and **ICB1** (25  $\mu\text{M}$ ) plus  $\text{Cu}^{2+}$  ions (25  $\mu\text{M}$ ); Pink - spectrum, **B** and **ICB1** (25  $\mu\text{M}$ ) plus  $\text{Cu}^{2+}$  ions (25  $\mu\text{M}$ ) after addition of EDTA (125  $\mu\text{M}$ ).

**Table 19.** UV spectral shifts of **B** and **ICB1**.

Flavone	$\lambda_{\text{max}}$ (nm)			
	Spectra in PBS pH 7.4	Spectra in PBS pH 7.4 with $\text{CuSO}_4$ 50 $\mu\text{M}$	Spectra in PBS pH 7.4 with $\text{CuSO}_4$ 25 $\mu\text{M}$	Spectra in PBS pH 7.4 with $\text{CuSO}_4$ 25 $\mu\text{M}$ and EDTA 125 $\mu\text{M}$
<b>B</b>	266	256	256	266
	359	365	362	359
<b>ICB1</b>	268	284	284	268
	362	356	356	362



These false-positive results are due to the fact that some compounds (aldehydes and amines) may interact in the second step of the reaction preventing the formation of the yellow compound <sup>173</sup>.

In 2001, this research group has also adapted for the microscale the methodology developed by Ellman *et al.*, by simply monitoring the production of colored compound in 96-well plates using a microplate reader. This assay revealed to be more sensitive than the TLC method; allowed greater automation and a faster analysis of a larger number of samples <sup>173</sup>.

Marston *et al.*, in 2002, developed another method based on TLC. This assay utilizes a different reaction, where the substrate  $\alpha$ -naphthyl acetate is hydrolyzed by acetylcholinesterase, forming  $\alpha$ -naphthol. This reacts with the colorimetric reagent Fast Blue Salt B to produce a diazonium salt (violet) (**Figure 61**). Thus, the AChE inhibitors are directly detected by the presence of white stains over the violet background in the chromatographic plate. It should be noted that this test does not require the false-positive tests <sup>174</sup>.

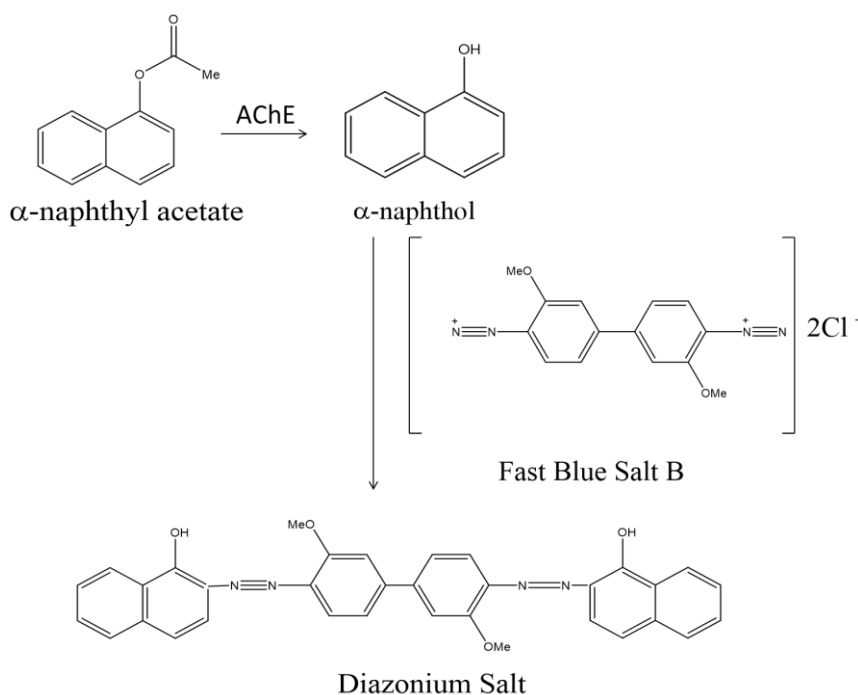


**Figure 61.** Reaction from detection of AChE activity by the Marston's method (adapted <sup>174</sup>).

In addition to this methodology based on TLC, other assays for the screening of AChE inhibitors have been developed using HPLC. Andrisano *et al.*, in 2001, have created a method for determining the anticholinesterase activity by HPLC, using an AChE

derivatized column, connected with a DAD detection system. This methodology also makes use of the substrate acetylthiocholine and it is based on the conventional measurement (by ultra-violet) of the production of yellow compound in the presence of potential anticholinesterase agent. Thus, due to the automation of the HPLC system, this method allows the continuous analysis of several compounds <sup>175</sup>.

Over the years, other methods were also developed for the assessment of anticholinesterase activity, such as fluorometric methods with fluorogenic substrates; radiometric assays; methods based on electrochemical activity or pH change <sup>170,176,177</sup>.

In 2003, a fluorometric flow method has been developed by Rhee *et al.* to determine the anticholinesterase activity in plant extracts. These researchers created this assay in order to improve the sensitivity of the HPLC coupled colorimetric flow assay that had already been developed. This fluorometric method is based on the use of the direct fluorogenic substrate 7-acetoxy-1-methylquinolinium iodide (AMQI), a fluorescent compound with  $\lambda_{\text{excitation}} = 320 \text{ nm}$  and  $\lambda_{\text{emission}} = 410 \text{ nm}$ . In this case, the substrate AMQI is hydrolyzed by AChE forming the 7-hydroxy-1-methylquinolinium iodide (HMQI), an highly fluorescent compound with  $\lambda_{\text{excitation}} = 406 \text{ nm}$  and,  $\lambda_{\text{emission}} = 505 \text{ nm}$  (**Figure 62**). Then, the production of the HMQI is detected using a fluorometer. The use of a direct fluorogenic substrate reduces the risk of false - positive results <sup>177</sup>.

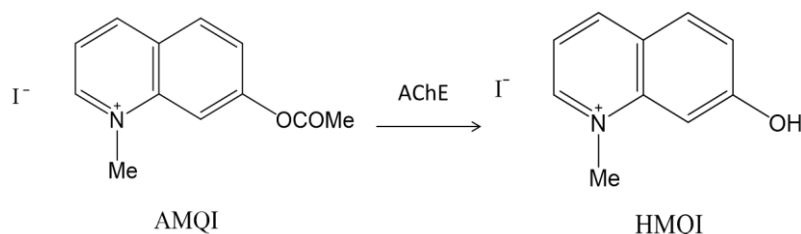


**Figure 62.** Conversion of 7-acetoxy-1-methylquinolinium iodide to 7-hydroxy-1-methylquinolinium iodide by AChE (adapted <sup>177</sup>).

Despite all of these methods that have been developed, the evaluation of the anticholinesterase activity of xanthone and flavone derivatives is performed mainly using the two methods described by Ellman in 1961 and Rhee in 2001 <sup>41,42,56,62,107,178</sup>. These two methods are widely used to test the anticholinesterase activity of xanthenes and flavones, because they are easy to perform and allow getting information very quickly. In addition, these assays do not require very expensive equipment and allow analyzing various natural crude extracts at the same time <sup>170</sup>.

Particularly, Ellman's assay is more used than Marston's method because the substrate acetylcholine and the Ellman's reagent are more stable and soluble in the buffer than  $\alpha$ -naphthyl acetate. Thus, the first assay avoids the use of large amounts of DMSO as solvent. This aspect is very important, because it was observed in screening tests that DMSO also showed ability to inhibit the AChE, affecting the kinetics of inhibition of the tested compounds. Also, the method developed by Ellman requires a lower amount of enzyme and the formation of product of enzymatic reaction can be monitored continuously <sup>170</sup>.

## 2.2. Results and discussion

The AChE inhibitory activity of all synthesized compounds as well as of other structure related aminoxanthonic derivatives previously synthesized in our research group has been evaluated (see section 1.2.). For screening of AChE inhibitory activity of all xanthone and flavones, we applied the photometric assay described by Ellman *et al.* with some modifications<sup>171</sup>. In this assay, the thiol group of the thiocholine reacts with Ellman's reagent to produce a yellow anion of 5-thio-2-nitrobenzoic acid. In the presence of an AChE inhibitor, the rate of production of thiocholine decreases and consequently, decreases the production of this cation that can be detected by reading the absorbance at 412 nm.

The results obtained for the AChE inhibitory activity of all tested compounds are summarized in **Table 20**.

**Table 20.** AChE inhibitory activity of tested compounds.

Compound	% of inhibition at 100 $\mu$ M	IC <sub>50</sub> ( $\mu$ M)
<b>ICX1</b>	n.a.	n.d.
<b>ICX2</b>	34.04 $\pm$ 3.12*	n.d.
<b>ICX2a</b>	49.08 $\pm$ 2.78**	100.00 $\pm$ 2.76**
<b>PPX1</b>	29.28 $\pm$ 5.79**	n.d.
<b>PPX2</b>	17.34 $\pm$ 2.45*	n.d.
<b>PPX3</b>	21.50 $\pm$ 4.023*	n.d.
<b>PPX4</b>	29.74 $\pm$ 3.70**	n.d.
<b>PEX1</b>	n.a.	n.d.
<b>PEX3</b>	n.a.	n.d.
<b>B</b>	n.a.	n.d.
<b>ICB1</b>	69.34 $\pm$ 0.72**	81.99 $\pm$ 1.16**

Results are given as mean  $\pm$  SEM of three independent experiments performed in triplicate; n.a.: not active; n.d.: not determined. Galantamine (positive control): IC<sub>50</sub>: 6.59  $\pm$  0.15  $\mu$ M \*\*\*. \*p<0.05; \*\*p<0.01; \*\*\*p<0.001.

The overall results indicate that most of the xanthenes evaluated exhibited AChE inhibitory activity, except xanthenes **ICX1**, **PEX1** and **PEX3**.

Additionally, our results show that the methylation of **ICX1**, led to the formation of a methyl derivative **ICX2** with inhibitory activity at 100  $\mu$ M (% of AChE inhibition = 34.04  $\pm$  3.12). Therefore, this suggests that the introduction of a methyl group at C-3 of the **ICX1** skeleton enhances its AChE inhibitory activity.

Comparing the results obtained for **ICX1**, **ICX2** and **ICX2a**, it was found that the Mannich base analogue **ICX2a** was the most active xanthone with an IC<sub>50</sub> value of 100.00

$\pm 2.76 \mu\text{M}$ . Thus, the presence of a 2-(dimethylamino)methyl group on the xanthone nucleus appears to be an important role for AChE inhibition.

Regarding the tested flavones, in opposition to baicalein (**B**) which did not possess AChE inhibitory activity, its Mannich base derivative **ICB1** reveals to be a moderate AChE inhibitor, showing an  $\text{IC}_{50}$  value of  $81.99 \pm 1.16 \mu\text{M}$ . Considering this, it can be concluded that the presence of a 8-(dimethylamino)methyl group on the flavone skeleton is responsible for its AChE inhibitory activity.

### 3. Xanthones and flavones as dual agents: antioxidants and AChE inhibitors

AD is the most prevalent form of dementia and it is known that the malfunctions of different, but interconnected, biochemical complex pathways are related to this pathogenesis. Inhibition of AChE is one of the most accepted therapy strategies for AD, like already described in this thesis. Consequently, several AChE inhibitors have been approved for commercial use. Nevertheless, these AChE inhibitors show lack selectivity for AChE and AD-patients suffer from side-effects. Therefore, there is a considerable need for strategies for development of new AChE inhibitors <sup>4</sup>. Due to the multifactorial nature of AD, this disease requires new therapeutic strategies. Among the multipotent approaches, the association between cholinesterase inhibition and antioxidant activity has been considered as an attractive methodology <sup>38,39</sup>.

Considering that concept, the main aim of this work consists in obtaining new AChE inhibitors with antioxidant activity based on the xanthonic and flavonic scaffolds.

Taking into account the results obtained for antioxidant activity (DPPH radical scavenging activity and iron and copper chelating activities) and the AChE inhibitory property for all xanthones and flavones tested in this work (sections 1.2. and 2.2.), it can be seen that only Mannich base analogues of xanthone (**ICX2a**) and flavone (**ICB1**) showed both activities.

Attending to these results (**Table 21**), it can be verified that **ICX2a** and **ICB1** had moderate AChE inhibitory activities, being **ICB1** the most active compound. However, their antioxidant properties are slightly different. While **ICX2a** exerted its antioxidant activity by chelating metal ions, **ICB1** was an antioxidant agent through scavenging free radicals, as well as by chelation metal ions.

**Table 21.** DPPH radical scavenging, iron chelating and AChE inhibitory activities of **ICX2a** and **ICB1**.

Compound	DPPH, IC <sub>50</sub> (μM)	Iron chelation, IC <sub>50</sub> (μM)	Copper chelation	AChE inhibition, IC <sub>50</sub> (μM)
<b>ICX2a</b>	n.a.	65.94 ± 1.57***	bathochromic shifts on the spectrum	100.00 ± 2.76**
<b>ICB1</b>	30.40 ± 1.28***	100.00 ± 0.23***	bathochromic shifts on the spectrum	81.99 ± 1.16**

Results are given in mean ± SEM of three independent experiments performed in triplicate; n.a.: not active; \*\*p<0.01; \*\*\*p<0.001.

Therefore, from this study, the Mannich base derivatives **ICB1** and **ICX2a** emerged as dual agents with antioxidant and AChE inhibitory activities. Thus, it can be concluded that these compounds constitute promising multipotent agents for treating AD and possibly, they can be hit compounds for the design and synthesis of other xanthonic and flavonic compounds with these desired biological/pharmacological activities.

## 4. Experimental

### 4.1. DPPH radical scavenging activity

Scavenging activities of the all xanthone and flavone derivatives for stable 1,1-diphenyl-2-picrylhydrazyl (DPPH) free radical were evaluated according to a method previously described<sup>179,180</sup> with some modifications. A solution of the radical DPPH in methanol was prepared daily and protected from light. Reaction mixtures containing 100-1.56  $\mu$ M of the tested compounds solutions in methanol (100  $\mu$ L) and 0.03 mg/mL DPPH methanolic solution (100  $\mu$ L) in a 96 well microtiter plates were shaken and incubated for 30 min in darkness at room temperature (until stable absorbance values were obtained). Controls containing 100  $\mu$ L of methanol instead of compounds and 100  $\mu$ L of DPPH methanolic solution (0.03 mg/mL) and blanks containing 200  $\mu$ L of methanol were also made. In this assay, sample's blanks containing 100  $\mu$ L of methanol instead of DPPH methanolic solution were also performed.

The absorbances were measured at 520 nm in a microplate reader (BioTeck Instruments, Vermont, US). The percentage of inhibition activity was calculated as:

$$\text{DPPH radical scavenging effect (\%)} = [1 - (A_1 - A_{bs} / A_0 - A_b)] \times 100$$

where  $A_0$  was the absorbance of control,  $A_{bs}$  was the absorbance of sample's blanks,  $A_b$  was the absorbance of blank and  $A_1$  was the absorbance in the presence of the positive control or tested compounds at different concentrations. Ascorbic acid was used as positive control as well as for validating of the method. All the tests were performed in triplicate. The scavenging activities of the tested compounds towards DPPH radical were expressed as  $IC_{50}$ , which was determined to be the effective concentration at which DPPH radical was scavenged by 50%. The  $IC_{50}$  value was obtained by interpolation from linear regression analysis.

## 4.2. Iron chelating activity

The chelation of iron ions by xanthone and flavone derivatives was assessed by the methodology described by Dinis *et al.* with modifications <sup>181</sup>. This assay was performed in a 96 well plate and the absorbance was measured at 562 nm. Briefly, 10  $\mu\text{L}$  of  $\text{FeCl}_2$  (50  $\mu\text{M}$ ) were added to a 50  $\mu\text{L}$  of solution of compounds in different concentrations (100-75  $\mu\text{M}$ ) and 120  $\mu\text{L}$  of methanol. The mixture was allowed to stand 5 minutes and the reaction was initiated by the addition of 20  $\mu\text{L}$  of 3-(2-pyridyl)-5,6-bis(4-phenylsulphonic acid)-1,2,4-triazine (ferrozine, 100  $\mu\text{M}$ ) and the mixture was shaken at room temperature for 10 min. Then, the absorbance of the solution was measured in a microplate reader (BioTeck Instruments, Vermont, US). Controls containing 50  $\mu\text{L}$  of solvent instead of compounds and blanks containing 50  $\mu\text{L}$  of solvent instead of compounds and 20  $\mu\text{L}$  milliQ<sup>TM</sup> purified water instead of ferrozine were made. In this assay, sample's blanks containing 20  $\mu\text{L}$  milliQ<sup>TM</sup> purified water instead of ferrozine were also performed.

All tests and analyses were carry out in triplicate and EDTA was used as positive control as well as for validating the method. The percentage of inhibition of  $\text{Fe}^{2+}$ –ferrozine complex formation was given below:

$$\% \text{Inhibition} = [((C-C_0)-(S-S_0))/(C-C_0)] \times 100$$

where C was the absorbance of the control,  $C_0$  was the absorbance of the blank, S was the absorbance in the presence of the solutions of compounds and  $S_0$  was the absorbance of sample's blank. The chelating activities of the purified compounds towards iron ions were expressed as  $\text{IC}_{50}$ , which was determined to be the effective concentration at which iron ions were chelated by 50%. The  $\text{IC}_{50}$  value was obtained by interpolation from linear regression analysis.

## 4.3. Copper chelating activity

The chelation of copper ions by xanthone and flavone derivatives was estimated in consistent with Brown *et al.* <sup>182</sup> and adapted to a 96 well plate. Stock solutions of each compound (1 mM) were prepared in methanol or DMSO, and then, 50  $\mu\text{M}$  of these solutions were prepared with PBS solution (10 mM) pH 7.4 and 50  $\mu\text{L}$  of each was taken to 96 well

UV plate (well A-D). Then, 100  $\mu\text{L}$  of ultra pure water (well A), or 50  $\mu\text{L}$  of ultra pure water and 50  $\mu\text{L}$   $\text{CuSO}_4$  (200  $\mu\text{M}$ ) (well B), or 50  $\mu\text{L}$  of ultra pure water and 50  $\mu\text{L}$  of  $\text{CuSO}_4$  (100  $\mu\text{M}$ ) (well C), or 50  $\mu\text{L}$  of EDTA (500  $\mu\text{M}$ ) and 50  $\mu\text{L}$   $\text{CuSO}_4$  (200  $\mu\text{M}$ ) (well D) was added. The absorption spectra were recorded between 200 and 800 nm in a micro plate reader (BioTeck Instruments, Vermont, US), and the scans in the presence of 1:1 (green spectrum) and 2:1 (blue spectrum) of copper-to-compound ratios were compared with the scan with compound alone (red spectrum). All tests and analyses were carried out in triplicate.

#### 4.4. Acetylcholinesterase inhibitory activity

Acetylcholinesterase inhibitory activity was measured using the Ellman's microplate assay with modification <sup>171</sup>. Briefly, for AChE inhibitory assay, 20  $\mu\text{L}$  of 0.22 U/mL AChE from *Electrophorus electricus* was added to the wells containing 20  $\mu\text{L}$  of tested compounds (100  $\mu\text{M}$  in methanol or DMSO), 100  $\mu\text{L}$  of 3 mM 5,5'-dithiobis(2-nitrobenzoic acid) (DTNB) and 20  $\mu\text{L}$  of 15 mM acetylthiocholine iodide. Absorbance of the colored end product was measured at 412 nm for 10 minutes. Controls containing 20  $\mu\text{L}$  of methanol instead of compounds and blanks containing 20  $\mu\text{L}$  of buffer (0.1% (w/v) bovine serum albumin in 50 mM Tris-HCl) instead of enzyme were made. In this assay, sample's blanks containing 20  $\mu\text{L}$  of buffer (0.1% (w/v) bovine serum albumin in 50 mM Tris-HCl) instead of AChE were also performed. Percentage of enzymatic inhibition was calculated as:

$$\text{Percentage of inhibition} = 100 - [(S - S_0)/(C - C_0)] \times 100$$

where C was the absorbance of the control,  $C_0$  was the absorbance of blank, S was the absorbance in the presence of the sample compounds and  $S_0$  was the absorbance of sample's blank. Every experiments were done in triplicate and galantamine was used as positive control as well as for validating the method. The inhibitory activities of the purified compounds towards AChE were expressed as  $\text{IC}_{50}$ , which was determined to be the effective concentration at which AChE was inhibited by 50%. The  $\text{IC}_{50}$  value was obtained by interpolation from linear regression analysis.

#### **4.5. Statistical analyses**

Data were reported as means  $\pm$  standard error of the mean (SEM) of at least three independent experiments. Statistical analysis of the results was performed with GraphPad Prism (GraphPad Software, San Diego, CA). Unpaired t-test were carried out to test for any significant differences between the means. Differences at the 5% confidence level were considered significant.

## 5. Conclusions

Considering the results obtained in the biological evaluation of the antioxidant and AChE inhibitory activities of all xanthone and flavone derivatives some conclusions can be made:

- On DPPH assay, baicalein (**B**) and its Mannich base analogue **ICB1** were the most active compounds, with  $IC_{50}$  values of 35.09  $\mu$ M and 30.40  $\mu$ M, respectively;
- Xanthones **PEX1** and **PEX3** were the most active xanthonic derivatives against DPPH free radical, with  $IC_{50}$  values of 61.62  $\mu$ M and 108.99  $\mu$ M, respectively;
- In the iron chelation assay, Mannich base derivatives **ICX2a** and **ICB1** had interesting chelating effect, showing  $IC_{50}$  values of 65.94  $\mu$ M and 100.00  $\mu$ M, respectively;
- Xanthones **ICX1** and **ICX2a**, as well as baicalein (**B**) and its Mannich derivative **ICB1** were the only compounds that showed copper chelating activity;
- Xanthones **ICX2**, **PPX1**, **PPX2**, **PPX3** and **PPX4** showed some activity against AChE at 100  $\mu$ M;
- In AChE assay, Mannich base derivatives **ICX2a** and **ICB1** had moderate activity, being **ICB1** the most active compound ( $IC_{50}$  value of 81.99  $\mu$ M);

# CHAPTER V

## DOCKING STUDIES

## 1. Results and discussion

In the current work, a flavone amino derivative **ICB1** has been discovered with moderate activity against AChE. Since its inhibitory mechanism against AChE is still unclear, the binding mechanism was studied by molecular docking. In addition to **ICB1**, docking studies were also performed for a series of compounds already described in the literature as AChE inhibitors<sup>183</sup>, being these used as positive controls. For these molecules docking scores values ranging from -5.7 to -12.1 kcal.mol<sup>-1</sup> were obtained (**Table 22**). The **ICB1**:AChE complex originated a free binding energy within that range (-10 kcal.mol<sup>-1</sup>), suggesting the formation of a stable complex between **ICB1** and AChE.

**Table 22.** Docking scores of known AChE inhibitors and **ICB1**.

Compound	Docking scores (kcal.mol <sup>-1</sup> )
Trichlorfon	-5.7
Echothiophate	-5.9
Isoflurophate	-5.9
Pyridostigmine	-6.3
Neostigmine	-7.5
Parathion	-7.6
Rivastigmine	-7.9
Tacrine	-8.8
Ladostigil	-9.1
Physostigmine	-9.1
HuperzineA	-9.7
Ungeremine	-10
Galantamine	-10.2
Donepezil	-12.1
<b>ICB1</b>	<b>-10</b>

In order to further understand the binding mode of the **ICB1** to AChE, a careful inspection of the most stable docking pose of that small molecule was performed.

AChE is a serine hydrolase and the crystallographic structures reveal the presence of a narrow, long, and hydrophobic cavity (**Figure 63A**). The active site of AChE comprises

2 subsites - the esteratic and anionic subsites <sup>183</sup>. The esteratic subsite, where AChE is hydrolyzed to acetate and choline, contains the catalytic triad of three amino acids: Ser203, His447, and Glu334, the lining of which contains mostly aromatic residues that form a narrow entrance to the catalytic Ser203 <sup>184</sup>. The activation of Ser203 allows the acylation between hydroxyl group of that residue and AChE oxygen. In the anionic site, the indole side chain of the conserved residue Trp86 makes a cation- $\pi$  interaction with the quaternary amino group of AChE. A peripheral site is composed of several aromatic residues, lining an hydrophobic region that traps AChE and transfers it to the deep catalytic site <sup>185</sup>.

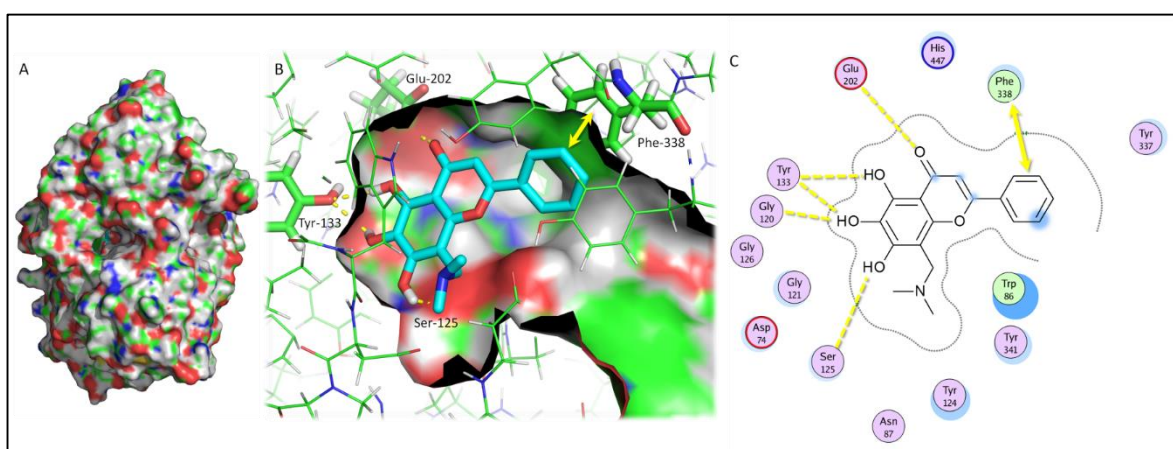


**Figure 63.** (A) AChE (surface) and docked **ICB1** (blue sticks). (B) AChE active site (surface) bound to **ICB1** (blue sticks). Residues involved in hydrogen interactions (yellow broken line) and  $\pi$  stacking interactions (yellow double arrow) are displayed using a stick model. AChE carbon, oxygen, nitrogen, and hydrogen are represented in green, red, blue, and grey, respectively. (C) 2D depiction of the **ICB1** docked into the binding site of AChE highlighting the protein residues that form the main interactions with the different structural units of the inhibitor. Hydrogen-bonding interactions are represented with yellow broken lines.  $\pi$  stacking interactions are represented with a yellow double arrow. Receptor residues that are close to the **ICB1**, but whose interactions with the ligand are weak or diffuse, such as collective hydrophobic or electrostatic interactions, are also represented (all the ones that have no indication for hydrogen-bonding or  $\pi$  stacking). Hydrophobic residues are colored with a green interior, polar residues are colored in light purple, basic residues are annotated by a blue ring, and acidic residues with a red ring. Solvent accessible surface area of the **ICB1** is plotted directly onto the atoms in the form of a blue smudge.

The interactions between inhibitors such as donepezil, galantamine, huperzine A, and the enzyme, as observed from their crystallographic structures (**Figure 64**), are characterized by hydrogen bonds; and  $\pi$ - $\pi$  stacking and cation- $\pi$  interactions involving aromatic residues of AChE <sup>186</sup>. Most ligands are located at the bottom of the binding groove

that form a hydrophobic pocket base, although larger ligands as donepezil extend to the periphery of the pocket.

The narrower gorge in AChE results in a conformation where the phenyl ring of the **ICB1** packs against the aromatic hydrophobic portions of the side chain of Phe-338. Packing in this region is quite tight, and only the smallest substituents might be accommodated. In contrast, the chromenone ring system of the flavone molecule faces a larger, negatively charged, and hydrophilic cavity, that includes hydroxyl and carbonyl groups of Gly120, Ser125, Tyr133, and Glu202. Upon analysis of the interaction of the **ICB1** in AChE binding site domains, it is observed that the residues Gly120, Ser125, Tyr133, and Glu202 participate in H-interactions. These residues are present in the buried region of the groove.  $\pi$  stacking interactions are established between the phenyl ring of the **ICB1** and Phe338. Although the **ICB1** has a protonable amine group, and cation- $\pi$  interactions between protonated nitrogens and AChE aromatic residues is described as being important for the activity of the highly potent inhibitors, such as donepezil (**Figure 64A** and **Figure 64B**), this interaction is not predicted to occur between **ICB1** and AChE binding site (**Figure 63B** and **Figure 63C**).

Therefore, molecular modifications on the flavone scaffold placing the amine group on different positions on A ring will be further explored in order to facilitate a cation- $\pi$  interaction. Moreover, molecular modifications that would allow the establishment of hydrogen interactions with the catalytic residue Ser203 (described for galantamine; **Figure 64C** and **Figure 64D**); and elongation of the molecule that would favor the establishment of additional  $\pi$ - $\pi$  or cation- $\pi$  interactions with residues such as Trp86, Trp286, or Tyr337 (described for donepezil and huperzine A; **Figure 64A**, **Figure 64B**, **Figure 64E** and **Figure 64F**), are foreseen as being important for the AChE inhibitory ability of flavones.

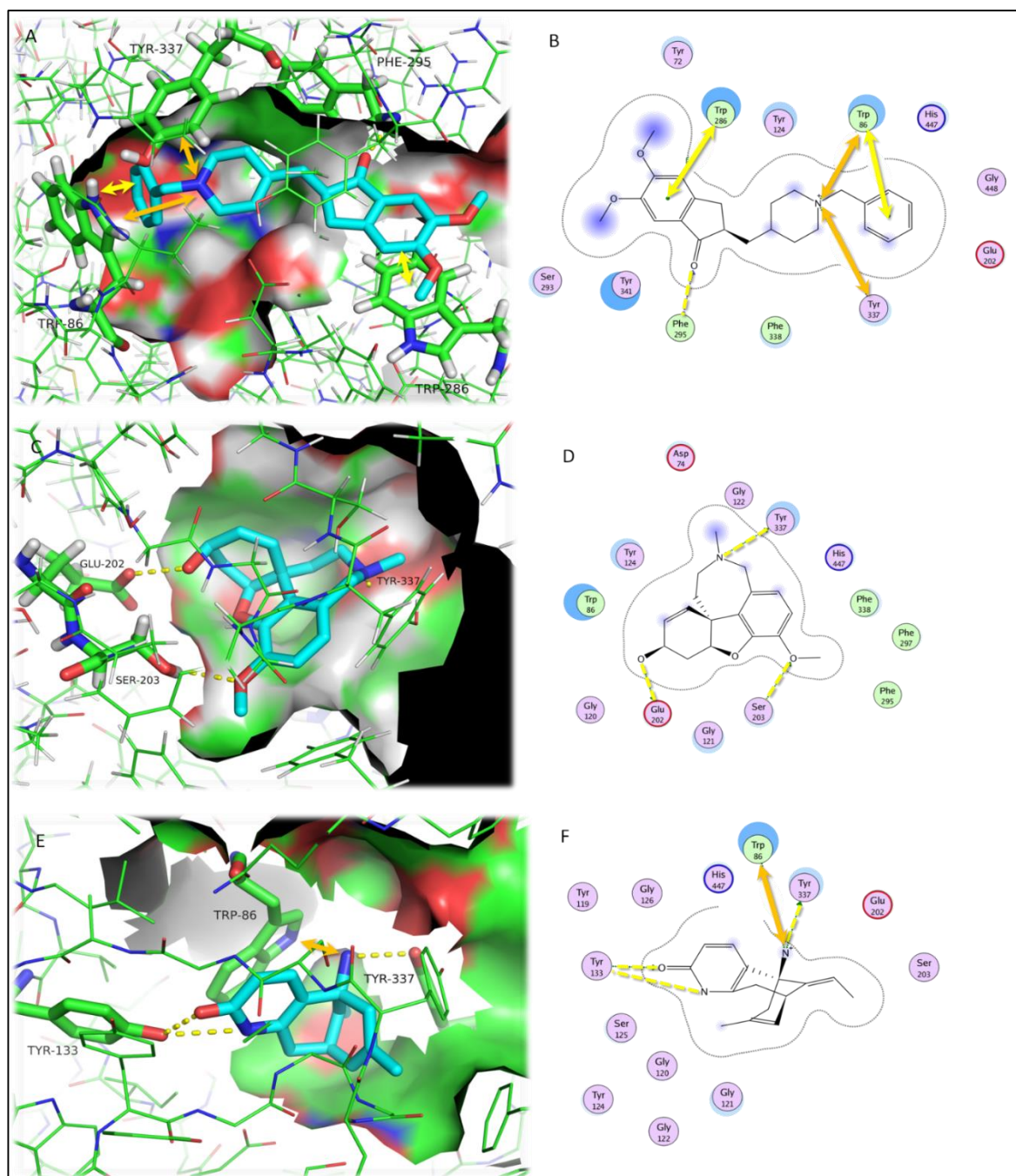


**Figure 64.** AChE active site (surface) bound to crystallographic donepezil (pdb ID: 4EY7) (**A**), galantamine (pdb ID: 4EY6) (**C**), and huperzine A (pdb ID: 4EY5) (**E**) (blue sticks). Residues involved in hydrogen interactions (yellow broken line),  $\pi$  stacking interactions (yellow double arrow), and  $\pi$ -cation interactions (orange double arrow) are displayed using a stick model. AChE carbon, oxygen, nitrogen, and hydrogen are represented in green, red, blue, and grey, respectively. 2D depiction of crystallographic donepezil (**B**), galantamine (**D**), and huperzine A (**F**) in the binding site of AChE, highlighting the protein residues that form the main interactions with the different structural units of the inhibitor. Hydrogen-bonding,  $\pi$  stacking, and  $\pi$ -cation interactions are represented with yellow broken lines, yellow double arrow, and orange double arrow, respectively.

## 2. Experimental

Crystal structure of AChE (PDB code: 4EY7) <sup>186</sup>, downloaded from the protein databank (PDB) (2) <sup>187</sup>, was used for the study. Structure files of 14 known AChE inhibitors and **ICB1** were created and minimized using the chemical structure drawing tool Hyperchem 7.5 (Hypercube, FL, USA) <sup>188</sup>. Structure-based docking was carried out using AutoDock Vina (Molecular Graphics Lab, CA, USA) <sup>189</sup>. The active site was defined as the region of AChE that comes within 12 Å from the crystallographic ligand. Default settings for small molecule-protein docking were used throughout the simulations. Top 9 poses were collected for each molecule and the lowest docking score value was associated with the more favorable binding conformation. PyMol1.3 (Schrödinger, NY, USA) <sup>190</sup> and MOE (Chemical Computing Group, Montreal, Canada) <sup>191</sup> was used for visual inspection of results and graphical representations.

### 3. Conclusions

Considering the results obtained in the docking studies of **ICB1** with AChE, some conclusions can be draw:

- Docking studies indicated that **ICB1** binds stably to enzyme with a free binding energy of  $-10 \text{ kcal.mol}^{-1}$ ;
- Docking analyzes also showed that hydroxyl and carbonyl groups of **ICB1** establish hydrogen interactions with the Gly120, Ser125, Tyr133, and Glu202 residues of AChE which are situated in the buried region of the groove. Additionally, the phenyl ring of **ICB1** establishes  $\pi$  stacking interactions with Phe338 residue of AChE. Cation- $\pi$  interactions between protonated nitrogens of **ICB1** and AChE aromatic residues were not observed.

# CHAPTER VI

## FINAL CONCLUSIONS AND FUTURE WORK

Considering the proposed objectives indicated previously, the following main conclusions from this work are as follow:

- Hydroxylated xanthone **ICX1** was obtained by two synthetic strategies: Eaton's reaction and GSS;
- The synthetic approach used for obtaining methylated derivative of **ICX1** was successfully applied, affording **ICX2** in high yield and with moderate reaction time;
- Amino derivatives of **ICX2** and **B** were obtained (**ICX2a** and **ICB1**, respectively) by applying the Mannich reaction. However, this synthetic approach was not suitable to the synthesis of the amino derivative of **ICX1**, because in this reaction several by-products were generated;
- Xanthone **ICX1** showed some antioxidant activity by chelation iron and copper ions, but did not possess AChE inhibitory activity;
- Xanthones **PEX1** and **PEX3** only had moderate antioxidant activity by scavenging DPPH free radical;
- Xanthone **ICX2a** showed antioxidant activity by chelation iron and copper ions.
- Flavones **B** and **ICB1** exerted their antioxidant activity through DPPH scavenging free radical and by chelation metal ions;
- **ICX2a** was the most active xanthone against AChE;
- Among all tested compounds, Mannich base derivative of baicalein **ICB1** was the most active compound with AChE inhibitory activity;
- **ICX2a** and **ICB1** were the only compounds that showed dual activity (antioxidant and AChE inhibitory activities);
- Docking studies of the most active compound **ICB1** with AChE showed that this Mannich base derivative binds stably to enzyme;
- The principal interactions established between **ICB1** and AChE are: hydrogen interactions between the hydroxyl and carbonyl groups of **ICB1** and Gly120, Ser125, Tyr133, and Glu202 residues of AChE that are present in the buried region of the groove and  $\pi$  stacking interactions between the phenyl ring of **ICB1** and Phe338 residue of AChE.

This work allowed the identification of xanthone and flavone Mannich base derivatives with dual activity that may will serve as model for the design and synthesis of new xanthonic and flavonic derivatives with potential AChE inhibitory and antioxidant dual activity.

In the future, it becomes important to optimize experimental conditions for the total synthesis of hydroxylated xanthenes, in order to achieve better yields in these reactions. Moreover, it is also necessary to improve the protocols and the reaction conditions of the Mannich reaction to overcome its limitations, making it more selective and applicable to any substrate, including to hydroxylated xanthenes.

According to the docking studies performed for the most active compound **ICB1** with AChE, in the future, in order to optimize the dual activity of flavonic derivatives, some molecular modifications on the flavone scaffold may be carried out. With the purpose of exploring the importance of the presence and position of amino groups for the AChE inhibitory activity of flavones, other aminoflavones can be synthesized through the introduction of other amino groups on A ring at different positions.

Considering the synthesis of aminoxanthenes and taking into account that **ICX2a** showed interesting antioxidant and AChE inhibitory effects, other way for future work will possibly consist in the synthesis of other aminoxanthenes by introduction of different amino groups on the xanthone scaffold, in order to afford xanthonic derivatives with better dual activity.

# CHAPTER VII

## REFERENCES

1. Stelzmann, R. A.; Norman Schnitzlein, H.; Reed Murtagh, F. An English translation of Alzheimer's 1907 paper, "Über eine eigenartige Erkrankung der Hirnrinde". *Clin Anat.* **1995**, 8 (6), 429-431.
2. K, F.; C, M.; K, B. Alzheimer's disease: molecular concepts and therapeutic targets. *Naturwissenschaften.* **2001**, 88 (6), 261-267.
3. LaFerla, F. M.; Oddo, S. Alzheimer's disease: Abeta, tau and synaptic dysfunction. *Trends. Mol. Med.* **2005**, 11 (4), 170-6.
4. Cavalli, A.; Bolognesi, M. L.; Minarini, A.; Rosini, M.; Tumiatti, V.; Recanatini, M.; Melchiorre, C. Multi-target-directed ligands to combat neurodegenerative diseases. *J. Med. Chem.* **2008**, 51 (3), 347-372.
5. Kumar, S.; Khan, S. A.; Bhakuni, L.; Singh, P.; Singh, A.; Sharma, P.; Kumar, A. Global Burden Of Alzheimer's Disease and Promising Potential Of Herbal Medicines. *Indian J. Drugs.* **2013**, 1 (2), 55-62.
6. Armstrong, R. A. The molecular biology of senile plaques and neurofibrillary tangles in Alzheimer's disease. *Folia Neuropathol.* **2009**, 47 (4), 289-299.
7. Mandelkow, E.-M.; Mandelkow, E. Tau in Alzheimer's disease. *Trends. Cell. Biol.* **1998**, 8 (11), 425-427.
8. Götz, J.; Ittner, L. M. Animal models of Alzheimer's disease and frontotemporal dementia. *Nat. Rev. Neurosci.* **2008**, 9 (7), 532-544.
9. Silman, I.; Sussman, J. L. Acetylcholinesterase: 'classical' and 'non-classical' functions and pharmacology. *Curr. Opin. Pharmacol.* **2005**, 5 (3), 293-302.
10. Hanisch, U. K.; Kettenmann, H. Microglia: active sensor and versatile effector cells in the normal and pathologic brain. *Nat. Neurosci.* **2007**, 10 (11), 1387-94.
11. Gella, A.; Durany, N. Oxidative stress in Alzheimer disease. *Cell. Adh. Migr.* **2009**, 3 (1), 88-93.
12. Chauhan, V.; Chauhan, A. Oxidative stress in Alzheimer's disease. *Pathophysiology.* **2006**, 13 (3), 195-208.
13. Inestrosa, N. C.; Alvarez, A.; Perez, C. A.; Moreno, R. D.; Vicente, M.; Linker, C.; Casanueva, O. I.; Soto, C.; Garrido, J. Acetylcholinesterase accelerates assembly of amyloid- $\beta$ -peptides into Alzheimer's fibrils: possible role of the peripheral site of the enzyme. *Neuron.* **1996**, 16 (4), 881-891.
14. Cai, Z. Monoamine oxidase inhibitors: Promising therapeutic agents for Alzheimer's disease *Mol. Med. Rep.* **2014**, 9 (5), 1533-1541.
15. Carradori, S.; D'Ascenzio, M.; Chimenti, P.; Secci, D.; Bolasco, A. Selective MAO-B inhibitors: a lesson from natural products. *Mol. Divers.* **2014**, 18 (1), 219-243.

16. Schelterns, P.; Feldman, H. Treatment of Alzheimer's disease; current status and new perspectives. *Lancet Neurol.* **2003**, 2 (9), 539-547.
17. Morphy, R.; Rankovic, Z. Designed multiple ligands. An emerging drug discovery paradigm. *J. Med. Chem.* **2005**, 48 (21), 6523-6543.
18. Bolognesi, M. L.; Matera, R.; Minarini, A.; Rosini, M.; Melchiorre, C. Alzheimer's disease: new approaches to drug discovery. *Curr. Opin. Chem. Biol.* **2009**, 13 (3), 303-308.
19. Peres, V.; Nagem, T. J.; de Oliveira, F. F. Tetraoxygenated naturally occurring xanthones. *Phytochemistry.* **2000**, 55 (7), 683-710.
20. Negi, J. S.; Bisht, V. K.; Singh, P.; Rawat, M. S. M.; Joshi, G. P. Naturally Occurring Xanthones: Chemistry and Biology. *J. Appl. Chem.* **2013**, 1-9.
21. Pinto, M.; Sousa, M.; Nascimento, M. Xanthone derivatives: new insights in biological activities. *Curr. Med. Chem.* **2005**, 12 (21), 2517-2538.
22. Diderot; Nougoué; Silvere, N.; Etienne, T. Xanthones as therapeutic agents: chemistry and pharmacology. *Adv. Phytomedicine.* **2006**, 2, 273-298.
23. Pinto, M. M. M.; Castanheiro, R. A. P. Natural Prenylated Xanthones: Chemistry and Biological Activities. In *Natural Products: Chemistry, Biochemistry and Pharmacology*, Brachmachari, G., Ed.; Narosa Publishing House PVT.LTD.: West Bengal, India, 2009; pp 521-619.
24. El-Seedi, H. R.; El-Barbary, M.; El-Ghorab, D.; Bohlin, L.; Borg-Karlson, A.-K.; Goransson, U.; Verpoorte, R. Recent insights into the biosynthesis and biological activities of natural xanthones. *Curr. med. chem.* **2010**, 17 (9), 854-901.
25. Bennett, G. J.; Lee, H.-H. Xanthones from guttiferæ. *Phytochemistry.* **1989**, 28 (4), 967-998.
26. Carpenter, I.; Locksley, H.; Scheinmann, F. Xanthones in higher plants: biogenetic proposals and a chemotaxonomic survey. *Phytochemistry.* **1969**, 8 (10), 2013-2025.
27. Sultanbawa, M. Xanthonoids of tropical plants. *Tetrahedron.* **1980**, 36 (11), 1465-1506.
28. Peres, V.; Nagem, T. J. Trioxygenated naturally occurring xanthones. *Phytochemistry.* **1997**, 44 (2), 191-214.
29. Martens, S.; Mithöfer, A. Flavones and flavone synthases. *Phytochemistry.* **2005**, 66 (20), 2399-2407.
30. Singh, M.; Kaur, M.; Silakari, O. Flavones: An important scaffold for medicinal chemistry. *Eur. J. Med. Chem.* **2014**, 84, 206-239.
31. Verma, A. K.; Pratap, R. The biological potential of flavones. *Nat. Prod. Rep.* **2010**, 27 (11), 1571-1593.

32. Verma, A. K.; Pratap, R. Chemistry of biologically important flavones. *Tetrahedron*. **2012**, 68 (41), 8523-8538.
33. Khoobi, M.; Alipour, M.; Zarei, S.; Jafarpour, F.; Shafiee, A. A facile route to flavone and neoflavone backbones via a regioselective palladium catalyzed oxidative Heck reaction. *Chem. Commun.* **2012**, 48 (24), 2985-2987.
34. Qin, J.; Lan, W.; Liu, Z.; Huang, J.; Tang, H.; Wang, H. Synthesis and biological evaluation of 1, 3-dihydroxyxanthone mannich base derivatives as anticholinesterase agents. *Chem. Cent. J.* **2013**, 7 (1), 78.
35. Bhullar, K. S.; Rupasinghe, H. Polyphenols: multipotent therapeutic agents in neurodegenerative diseases. *Oxid. Med. Cell. Longev.* **2013**, 1-18.
36. Panda, S.; Chand, M.; Sakhuja, R.; Jain, S. Xanthoness as Potential Antioxidants. *Curr. Med. Chem.* **2013**, 20 (36), 4481-4507.
37. Zhang, H.-Y.; Yang, D.-P.; Tang, G.-Y. Multipotent antioxidants: from screening to design. *Drug. Discov. Today*. **2006**, 11 (15), 749-754.
38. Ji, H.-F.; Zhang, H.-Y. Theoretical evaluation of flavonoids as multipotent agents to combat Alzheimer's disease. *Theochem.* . **2006**, 767 (1), 3-9.
39. Zhang, H.-Y. One-compound-multiple-targets strategy to combat Alzheimer's disease. *FEBS letters*. **2005**, 579 (24), 5260-5264.
40. Lee, M.-H.; Lin, R.-D.; Shen, L.-Y.; Yang, L.-L.; Yen, K.-Y.; Hou, W.-C. Monoamine oxidase B and free radical scavenging activities of natural flavonoids in *Melastoma candidum* D. Don. *J. Agr. Food Chem.* **2001**, 49 (11), 5551-5555.
41. Brühlmann, C.; Marston, A.; Hostettmann, K.; Carrupt, P. A.; Testa, B. Screening of Non-Alkaloidal Natural Compounds as Acetylcholinesterase Inhibitors. *Chem. Biodivers.* **2004**, 1 (6), 819-829.
42. Urbain, A.; Marston, A.; Grilo, L. S.; Bravo, J.; Purev, O.; Purevsuren, B.; Batsuren, D.; Reist, M.; Carrupt, P.-A.; Hostettmann, K. Xanthoness from *Gentianella amarella* ssp. *acuta* with acetylcholinesterase and monoamine oxidase inhibitory activities. *J. Nat. Prod.* **2008**, 71 (5), 895-897.
43. Chimenti, F.; Fioravanti, R.; Bolasco, A.; Chimenti, P.; Secci, D.; Rossi, F.; Yáñez, M.; Orallo, F.; Ortuso, F.; Alcaro, S. A new series of flavones, thioflavones, and flavanones as selective monoamine oxidase-B inhibitors. *Bioorgan. Med. Chem.* **2010**, 18 (3), 1273-1279.
44. Uriarte-Pueyo, I.; I Calvo, M. Flavonoids as acetylcholinesterase inhibitors. *Curr. Med. Chem.* **2011**, 18 (34), 5289-5302.

45. Uvarani, C.; Chandraprakash, K.; Sankaran, M.; Ata, A.; Mohan, P. S. Antioxidant and structure–activity relationships of five tetraoxygenated xanthones from *Swertia minor* (Griseb.) Knobl. *Nat. Prod. Res.* **2012**, *26* (13), 1265-1270.
46. Grazul, M.; Budzisz, E. Biological activity of metal ions complexes of chromones, coumarins and flavones. *Coordin. Chem. Rev.* **2009**, *253* (21), 2588-2598.
47. Hanasaki, Y.; Ogawa, S.; Fukui, S. The correlation between active oxygens scavenging and antioxidative effects of flavonoids. *Free Radical Bio. Med.* **1994**, *16* (6), 845-850.
48. Magnani, L.; Gaydou, E. M.; Hubaud, J. C. Spectrophotometric measurement of antioxidant properties of flavones and flavonols against superoxide anion. *Anal. Chim. Acta.* **2000**, *411* (1), 209-216.
49. Santos, C. M.; Freitas, M.; Ribeiro, D.; Gomes, A.; Silva, A.; Cavaleiro, J. A.; Fernandes, E. 2, 3-Diarylxanthenes as strong scavengers of reactive oxygen and nitrogen species: A structure–activity relationship study. *Bioorgan. Med. Chem.* **2010**, *18* (18), 6776-6784.
50. Rizzo, S.; Cavalli, A.; Ceccarini, L.; Bartolini, M.; Belluti, F.; Bisi, A.; Andrisano, V.; Recanatini, M.; Rampa, A. Structure–Activity Relationships and Binding Mode in the Human Acetylcholinesterase Active Site of Pseudo-Irreversible Inhibitors Related to Xanthostigmine. *Chem. Med. Chem.* **2009**, *4* (4), 670-679.
51. Wang, Y.; Xia, Z.; Xu, J.-R.; Wang, Y.-X.; Hou, L.-N.; Qiu, Y.; Chen, H.-Z.  $\alpha$ -Mangostin, a polyphenolic xanthone derivative from mangosteen, attenuates  $\beta$ -amyloid oligomers-induced neurotoxicity by inhibiting amyloid aggregation. *Neuropharmacology.* **2012**, *62* (2), 871-881.
52. Choi, R. C.; Zhu, J. T.; Yung, A. W.; Lee, P. S.; Xu, S. L.; Guo, A. J.; Zhu, K. Y.; Dong, T. T.; Tsim, K. W. Synergistic action of flavonoids, baicalein, and daidzein in estrogenic and neuroprotective effects: a development of potential health products and therapeutic drugs against Alzheimer's disease. *Evid.-Based Compl. Alt.* **2013**, *2013*.
53. Jiménez-Aliaga, K.; Bermejo-Bescós, P.; Benedí, J.; Martín-Aragón, S. Quercetin and rutin exhibit antiamyloidogenic and fibril-disaggregating effects in vitro and potent antioxidant activity in APPswe cells. *Life Sci.* **2011**, *89* (25), 939-945.
54. Degen, S. J.; Mueller, K. L.; Shen, H. C.; Mulder, J. A.; Golding, G. M.; Wei, L.-I.; Zifcsak, C. A.; Neeno-Eckwall, A.; Hsung, R. P. Synthesis of dihydroxanthone derivatives and evaluation of their inhibitory activity against acetylcholinesterase: unique structural analogs of tacrine based on the BCD-ring of arisugacin. *Bioorg. Med. Chem. Lett.* **1999**, *9* (7), 973-978.

55. Pinho, B. R.; Ferreres, F.; Valentão, P.; Andrade, P. B. Nature as a source of metabolites with cholinesterase-inhibitory activity: an approach to Alzheimer's disease treatment. *J. Pharm. Pharmacol.* **2013**, *65* (12), 1681-1700.
56. Piazzzi, L.; Belluti, F.; Bisi, A.; Gobbi, S.; Rizzo, S.; Bartolini, M.; Andrisano, V.; Recanatini, M.; Rampa, A. Cholinesterase inhibitors: SAR and enzyme inhibitory activity of 3-[ $\omega$ -(benzylmethylamino) alkoxy] xanthen-9-ones. *Bioorg. Med. Chem. Lett.* **2007**, *15* (1), 575-585.
57. Rampa, A.; Piazzzi, L.; Belluti, F.; Gobbi, S.; Bisi, A.; Bartolini, M.; Andrisano, V.; Cavrini, V.; Cavalli, A.; Recanatini, M. Acetylcholinesterase Inhibitors: SAR and Kinetic Studies on  $\omega$ -[N-Methyl-N-(3-alkylcarbamoyloxyphenyl) methyl] aminoalkoxyaryl Derivatives. *J. Med. Chem.* **2001**, *44* (23), 3810-3820.
58. Rampa, A.; Bisi, A.; Valenti, P.; Recanatini, M.; Cavalli, A.; Andrisano, V.; Cavrini, V.; Fin, L.; Buriani, A.; Giusti, P. Acetylcholinesterase inhibitors: synthesis and structure-activity relationships of  $\omega$ -[N-Methyl-N-(3-alkylcarbamoyloxyphenyl)-methyl] aminoalkoxyheteroaryl derivatives. *J. Med. Chem.* **1998**, *41* (21), 3976-3986.
59. Belluti, F.; Rampa, A.; Piazzzi, L.; Bisi, A.; Gobbi, S.; Bartolini, M.; Andrisano, V.; Cavalli, A.; Recanatini, M.; Valenti, P. Cholinesterase inhibitors: Xanthostigmine derivatives blocking the acetylcholinesterase-induced  $\beta$ -amyloid aggregation. *J. Med. Chem.* **2005**, *48* (13), 4444-4456.
60. Gupta, S.; Mohan, C. G. 3D-pharmacophore model based virtual screening to identify dual-binding site and selective acetylcholinesterase inhibitors. *Med. Chem. Res.* **2011**, *20* (9), 1422-1430.
61. Khan, M. T. H.; Orhan, I.; Şenol, F.; Kartal, M.; Şener, B.; Dvorská, M.; Šmejkal, K.; Šlapetová, T. Cholinesterase inhibitory activities of some flavonoid derivatives and chosen xanthone and their molecular docking studies. *Chem.-Biol. Interact.* **2009**, *181* (3), 383-389.
62. Sawasdee, P.; Sabphon, C.; Sitthiwongwanit, D.; Kokpol, U. Anticholinesterase activity of 7-methoxyflavones isolated from *Kaempferia parviflora*. *Phytother. Res.* **2009**, *23* (12), 1792-1794.
63. Sheng, R.; Lin, X.; Zhang, J.; Chol, K. S.; Huang, W.; Yang, B.; He, Q.; Hu, Y. Design, synthesis and evaluation of flavonoid derivatives as potent AChE inhibitors. *Bioorg. Med. Che.* **2009**, *17* (18), 6692-6698.
64. Loizzo, M. R.; Tundis, R.; Menichin, F.; Bonesi, M.; Statt, G. A.; Deguin, B.; Tillequin, F.; Menichini, F.; Houghton, P. J. Acetyl-cholinesterase inhibition by extracts and isolated Flavones from *Linaria reflexa* Desf.(Scrophulariaceae). *Nat. Prod. Commun.* **2007**, *2* (7), 759-763.

65. Duan, K.; Liu, H.; Fan, H.; Zhang, J.; Wang, Q. Synthesis and anticholinesterase inhibitory activity of Mannich base derivatives of flavonoids. *J. Chem. Res.* **2014**, 38 (7), 443-446.
66. Ames, B. N.; Shigenaga, M. K.; Hagen, T. M. Oxidants, antioxidants, and the degenerative diseases of aging. *P. Natl. A. Sci.* **1993**, 90 (17), 7915-7922.
67. Nakatani, K.; Nakahata, N.; Arakawa, T.; Yasuda, H.; Ohizumi, Y. Inhibition of cyclooxygenase and prostaglandin E2 synthesis by  $\gamma$ -mangostin, a xanthone derivative in mangosteen, in C6 rat glioma cells. *Biochem. Pharmacol.* **2002**, 63 (1), 73-79.
68. Zou, J.; Jin, D.; Chen, W.; Wang, J.; Liu, Q.; Zhu, X.; Zhao, W. Selective Cyclooxygenase-2 Inhibitors from *Calophyllum m. embranaceum*. *J. Nat. Prod.* **2005**, 68 (10), 1514-1518.
69. Hu, L.; Hu, H.; Wu, W.; Chai, X.; Luo, J.; Wu, Q. Discovery of novel xanthone derivatives as xanthine oxidase inhibitors. *Bioorg. Med. Chem. Lett.* **2011**, 21 (13), 4013-4015.
70. Pardo-Andreu, G. L.; Delgado, R.; Núñez-Sellés, A. J.; Vercesi, A. E. *Mangifera indica* L. extract (Vimang®) inhibits 2-deoxyribose damage induced by Fe (III) plus ascorbate. *Phytother. Res.* **2006**, 20 (2), 120-124.
71. Devi, P.; Vijayaraghavan, K. Cardioprotective effect of  $\alpha$ -mangostin, a xanthone derivative from mangosteen on tissue defense system against isoproterenol-induced myocardial infarction in rats. *J. Biochem. Mol. Toxic.* **2007**, 21 (6), 336-339.
72. Pedraza-Chaverri, J.; Cárdenas-Rodríguez, N.; Orozco-Ibarra, M.; Pérez-Rojas, J. M. Medicinal properties of mangosteen ( *Garcinia mangostana*). *Food. Chem. Toxicol.* **2008**, 46 (10), 3227-3239.
73. Raghavendra, H.; Kumar, S. P.; Kekuda, T. P.; Ramalingappa; Ejeta, E.; Mulatu, K.; Khanum, F.; Anilakumar, K. Extraction and Evaluation of  $\alpha$ -Mangostin for its Antioxidant and Acetylcholinesterase Inhibitory Activity. *Journal of Biologically Active Products from Nature.* **2011**, 1 (5-6), 314-324.
74. Gutierrez-Orozco, F.; Failla, M. L. Biological activities and bioavailability of mangosteen xanthenes: A critical review of the current evidence. *Nutrients.* **2013**, 5 (8), 3163-3183.
75. Ryu, H. W.; Oh, S. R.; Curtis-Long, M. J.; Lee, J. H.; Song, H. H.; Park, K. H. Rapid identification of cholinesterase inhibitors from the seedcases of mangosteen using an enzyme affinity assay. *J. Agric. Food. Chem.* **2014**, 62 (6), 1338-43.
76. Jung, H.-A.; Su, B.-N.; Keller, W. J.; Mehta, R. G.; Kinghorn, A. D. Antioxidant xanthenes from the pericarp of *Garcinia mangostana* (Mangosteen). *J. Agr. Food Chem.* **2006**, 54 (6), 2077-2082.

77. Pauletti, P. M.; Castro-Gamboa, I.; Siqueira Silva, D. H.; Young, M. C. M.; Tomazela, D. M.; Eberlin, M. N.; da Silva Bolzani, V. New antioxidant C-glucosylxanthenes from the stems of *Arrabidaea samydoides*. *J. Nat. Prod.* **2003**, *66* (10), 1384-1387.
78. Minami, H.; Takahashi, E.; Fukuyama, Y.; Kodama, M.; Yoshizawa, T.; Nakagawa, K. Novel xanthenes with superoxide scavenging activity from *Garcinia subelliptica*. *Chem. Pharm. Bull.* **1995**, *43* (2), 347-349.
79. Minami, H.; Takahashi, E.; Kodama, M.; Fukuyama, Y. Three xanthenes from *Garcinia subelliptica*. *Phytochemistry*. **1996**, *41* (2), 629-633.
80. Santos, C. M.; Silva, A. M.; Filipe, P.; Santus, R.; Patterson, L. K.; Maziere, J.-C.; Cavaleiro, J. A.; Morliere, P. Structure–activity relationships in hydroxy-2, 3-diaryl-xanthone antioxidants. Fast kinetics spectroscopy as a tool to evaluate the potential for antioxidant activity in biological systems. *Org. Biomol. Chem.* **2011**, *9* (10), 3965-3974.
81. Catarino, M. D.; M Alves-Silva, J.; R Pereira, O.; M Cardoso, S. Antioxidant capacities of flavones and benefits in oxidative-stress related diseases. *Curr. Top. Med. Chem.* **2015**, *15* (2), 105-119.
82. Procházková, D.; Boušová, I.; Wilhelmová, N. Antioxidant and prooxidant properties of flavonoids. *Fitoterapia*. **2011**, *82* (4), 513-523.
83. Hyun, J.; Woo, Y.; Hwang, D.-s.; Jo, G.; Eom, S.; Lee, Y.; Park, J. C.; Lim, Y. Relationships between structures of hydroxyflavones and their antioxidative effects. *Bioorg. Med. Chem. Lett.* **2010**, *20* (18), 5510-5513.
84. Treesuwan, W.; Suramitr, S.; Hannongbua, S. Elucidation of hydroxyl groups-antioxidant relationship in mono-and dihydroxyflavones based on OH bond dissociation enthalpies. *J. Mol. Model.* **2015**, *21* (6), 1-10.
85. Kim, H. K.; Cheon, B. S.; Kim, Y. H.; Kim, S. Y.; Kim, H. P. Effects of naturally occurring flavonoids on nitric oxide production in the macrophage cell line RAW 264.7 and their structure–activity relationships. *Biochem. Pharmacol.* **1999**, *58* (5), 759-765.
86. Liang, Y.-C.; Huang, Y.-T.; Tsai, S.-H.; Lin-Shiau, S.-Y.; Chen, C.-F.; Lin, J.-K. Suppression of inducible cyclooxygenase and inducible nitric oxide synthase by apigenin and related flavonoids in mouse macrophages. *Carcinogenesis*. **1999**, *20* (10), 1945-1952.
87. Raso, G. M.; Meli, R.; Di Carlo, G.; Pacilio, M.; Di Carlo, R. Inhibition of inducible nitric oxide synthase and cyclooxygenase-2 expression by flavonoids in macrophage J774A. 1. *Life sciences*. **2001**, *68* (8), 921-931.
88. Rastelli, G.; Costantino, L.; Albasini, A. A model of the interaction of substrates and inhibitors with xanthine oxidase. *J. Am. Chem. Soc.* **1997**, *119* (13), 3007-3016.
89. Cos, P.; Ying, L.; Calomme, M.; Hu, J. P.; Cimanga, K.; Van Poel, B.; Pieters, L.; Vlietinck, A. J.; Berghe, D. V. Structure-activity relationship and classification of flavonoids

- as inhibitors of xanthine oxidase and superoxide scavengers. *J. Nat. Prod.* **1998**, 61 (1), 71-76.
90. Greig, N. H.; Lahiri, D. K.; Sambamurti, K. Butyrylcholinesterase: an important new target in Alzheimer's disease therapy. *Int. Psychogeriatr.* **2002**, 14 (S1), 77-91.
  91. Anand, P.; Singh, B. Flavonoids as lead compounds modulating the enzyme targets in Alzheimer's disease. *Med. Chem. Res.* **2013**, 22 (7), 3061-3075.
  92. Lee, B. W.; Lee, J. H.; Lee, S.-T.; Lee, H. S.; Lee, W. S.; Jeong, T.-S.; Park, K. H. Antioxidant and cytotoxic activities of xanthonones from *Cudrania tricuspidata*. *Bioorg. Med. Chem. Lett.* **2005**, 15 (24), 5548-5552.
  93. Teh, S. S.; Ee, G. C.; Mah, S. H.; Lim, Y. M.; Ahmad, Z. Cytotoxicity and structure-activity relationships of xanthone derivatives from *Mesua beccariana*, *Mesua ferrea* and *Mesua congestiflora* towards nine human cancer cell lines. *Molecules.* **2013**, 18 (2), 1985-94.
  94. Biradar, S. M.; Joshi, H.; Chhedha, T. K. Neuropharmacological effect of mangiferin on brain cholinesterase and brain biogenic amines in the management of Alzheimer's disease. *Eur. J. Pharmacol.* **2012**, 683 (1), 140-147.
  95. Sato, T.; Kawamoto, A.; Tamura, A.; Tatsumi, Y.; Fujii, T. Mechanism of antioxidant action of pueraria glycoside (PG)-1 (an isoflavonoid) and mangiferin (a xanthonoid). *Chem. Pharm. Bull.* **1992**, 40 (3), 721-724.
  96. Sánchez, G. M.; Re, L.; Giuliani, A.; Nunez-Selles, A.; Davison, G. P.; Leon-Fernandez, O. Protective effects of *Mangifera indica* L. extract, mangiferin and selected antioxidants against TPA-induced biomolecules oxidation and peritoneal macrophage activation in mice. *Pharmacol. Res.* **2000**, 42 (6), 565-573.
  97. Ali, M.; Firdous, S.; Moin, S. T. Analgesic and antioxidant activity of mangiferin and its derivatives: the structure activity relationship. *Biol. Pharm. Bull.* **2005**, 28 (4), 596-600.
  98. Bandaruk, Y.; Mukai, R.; Terao, J. Cellular uptake of quercetin and luteolin and their effects on monoamine oxidase-A in human neuroblastoma SH-SY5Y cells. *Toxicol. Rep.* **2014**, 1, 639-649.
  99. Choi, J. S.; Chung, H. Y.; Kang, S. S.; Jung, M. J.; Kim, J. W.; No, J. K.; Jung, H. A. The structure-activity relationship of flavonoids as scavengers of peroxynitrite. *Phytother. Res.* **2002**, 16 (3), 232-235.
  100. Kumar, M.; Kumar, S.; Kaur, S. Role of ROS and COX-2/iNOS inhibition in cancer chemoprevention: a review. *Phytochem. Rev.* **2012**, 11 (2-3), 309-337.
  101. Wang, S.-Q.; Han, X.-Z.; Li, X.; Ren, D.-M.; Wang, X.-N.; Lou, H.-X. Flavonoids from *Dracocephalum tanguticum* and their cardioprotective effects against doxorubicin-induced toxicity in H9c2 cells. *Bioorg. Med. Chem. Lett.* **2010**, 20 (22), 6411-6415.

102. Husain, S. R.; Cillard, J.; Cillard, P. Hydroxyl radical scavenging activity of flavonoids. *Phytochemistry*. **1987**, 26 (9), 2489-2491.
103. Huguet, A. I.; Máñez, S.; Alcaraz, M. J. Superoxide scavenging properties of flavonoids in a non-enzymic system. *Zeitschrift für Naturforschung C*. **1990**, 45 (1-2), 19-24.
104. Ohshima, H.; Yoshie, Y.; Auriol, S.; Gilibert, I. Antioxidant and pro-oxidant actions of flavonoids: effects on DNA damage induced by nitric oxide, peroxynitrite and nitroxyl anion. *Free Radical Biol. Med.* **1998**, 25 (9), 1057-1065.
105. Sugihara, N.; Arakawa, T.; Ohnishi, M.; Furuno, K. Anti-and pro-oxidative effects of flavonoids on metal-induced lipid hydroperoxide-dependent lipid peroxidation in cultured hepatocytes loaded with  $\alpha$ -linolenic acid. *Free Radical Biol. Med.* **1999**, 27 (11), 1313-1323.
106. Hirano, R.; Sasamoto, W.; Matsumoto, A.; Itakura, H.; Igarashi, O.; Kondo, K. Antioxidant ability of various flavonoids against DPPH radicals and LDL oxidation. *J. Nutr. Sci. Vitaminol.* **2001**, 47 (5), 357-362.
107. Guo, A. J.; Xie, H. Q.; Choi, R. C.; Zheng, K. Y.; Bi, C. W.; Xu, S. L.; Dong, T. T.; Tsim, K. W. Galangin, a flavonol derived from *Rhizoma Alpiniae Officinarum*, inhibits acetylcholinesterase activity in vitro. *Chem.-biol. Interact.* **2010**, 187 (1), 246-248.
108. Zhang, S. Q.; Obregon, D.; Ehrhart, J.; Deng, J.; Tian, J.; Hou, H.; Giunta, B.; Sawmiller, D.; Tan, J. Baicalein reduces  $\beta$ -amyloid and promotes nonamyloidogenic amyloid precursor protein processing in an Alzheimer's disease transgenic mouse model. *J. Neurosci. Res.* **2013**, 91 (9), 1239-1246.
109. Huang, Y.; Tsang, S.-Y.; Yao, X.; Chen, Z.-Y. Biological properties of baicalein in cardiovascular system. *Curr. Drug. Targets-Cardiov. Hem. Dis.* **2005**, 5 (2), 177-184.
110. Perez, C. A.; Wei, Y.; Guo, M. Iron-binding and anti-Fenton properties of baicalein and baicalin. *J. Inorg. Biochem.* **2009**, 103 (3), 326-332.
111. Adhikari, S.; Tilak, J. C.; Devasagayam, T. Free radical reactions of a naturally occurring flavone baicalein and possible mechanisms towards its membrane protective properties. *Indian J. Biochem. Bio.* **2011**, 48.
112. Selvaraj, S.; Krishnaswamy, S.; Devashya, V.; Sethuraman, S.; Krishnan, U. M. Flavonoid-metal ion complexes: a novel class of therapeutic agents. *Med. Res. Rev.* **2014**, 34 (4), 677-702.
113. Guo, L.-L.; Guan, Z.-Z.; Huang, Y.; Wang, Y.-L.; Shi, J.-S. The neurotoxicity of  $\beta$ -amyloid peptide toward rat brain is associated with enhanced oxidative stress, inflammation and apoptosis, all of which can be attenuated by scutellarin. *Exp. Toxicol. Pathol.* **2013**, 65 (5), 579-584.

114. Liu, H.; Yang, X.; Zhou, L.; Xu, H. Study on effects of scutellarin on scavenging reactive oxygen. *J. Chinese Med. Mat.* **2002**, *25* (7), 491-493.
115. Liu, H.; Yang, X.; Tang, R.; Liu, J.; Xu, H. Effect of scutellarin on nitric oxide production in early stages of neuron damage induced by hydrogen peroxide. *Pharmacol. Res.* **2005**, *51* (3), 205-210.
116. Li, N.-G.; Shen, M.-Z.; Wang, Z.-J.; Tang, Y.-P.; Shi, Z.-H.; Fu, Y.-F.; Shi, Q.-P.; Tang, H.; Duan, J.-A. Design, synthesis and biological evaluation of glucose-containing scutellarein derivatives as neuroprotective agents based on metabolic mechanism of scutellarin in vivo. *Bioorg. Med. Chem. Lett.* **2013**, *23* (1), 102-106.
117. Sohn, H.-Y.; Son, K.; Kwon, C.-S.; Kwon, G.-S.; Kang, S. Antimicrobial and cytotoxic activity of 18 prenylated flavonoids isolated from medicinal plants: *Morus alba* L., *Morus mongolica* Schneider, *Broussonetia papyrifera* (L.) Vent, *Sophora flavescens* Ait and *Echinosophora koreensis* Nakai. *Phytomedicine.* **2004**, *11* (7), 666-672.
118. Mazimba, O.; Majinda, R. R.; Motlhanka, D. Antioxidant and antibacterial constituents from *Morus nigra*. *Acad. J.* **2011**, *5* (6), 751-754.
119. Abbas, G. M.; Abdel Bar, F. M.; Baraka, H. N.; Gohar, A. A.; Lahloub, M.-F. A new antioxidant stilbene and other constituents from the stem bark of *Morus nigra* L. *Nat. Prod. Res.* **2014**, *28* (13), 952-959.
120. Fukai, T.; Satoh, K.; Nomura, T.; Sakagami, H. Antinephritis and radical scavenging activity of prenylflavonoids. *Fitoterapia.* **2003**, *74* (7), 720-724.
121. Woźniak, D.; Dryś, A.; Matkowski, A. Antiradical and antioxidant activity of flavones from *Scutellariae baicalensis* radix. *Nat. Prod. Res.* **2014**, 1-4.
122. Shieh, D.-e.; Liu, L.-T.; Lin, C.-C. Antioxidant and free radical scavenging effects of baicalein, baicalin and wogonin. *Anti-cancer Res.* **1999**, *20* (5A), 2861-2865.
123. Awad, R.; Arnason, J.; Trudeau, V.; Bergeron, C.; Budzinski, J.; Foster, B.; Merali, Z. Phytochemical and biological analysis of skullcap (*Scutellaria lateriflora* L.): a medicinal plant with anxiolytic properties. *Phytomedicine.* **2003**, *10* (8), 640-649.
124. Kang, K. A.; Zhang, R.; Piao, M. J.; Chae, S.; Kim, H. S.; Park, J. H.; Jung, K. S.; Hyun, J. W. Baicalein inhibits oxidative stress-induced cellular damage via antioxidant effects. *Toxicol. Ind. Health.* **2011**, 1-10.
125. Jantan, I.; Saputri, F. C. Benzophenones and xanthenes from *Garcinia cantleyana* var. *cantleyana* and their inhibitory activities on human low-density lipoprotein oxidation and platelet aggregation. *Phytochemistry.* **2012**, *80*, 58-63.
126. Sousa, E.; Pinto, M. Synthesis of Xanthenes: An Overview. *Curr. Med. Chem.* **2005**, *12* (21).

127. Nessler, B. Synthesen von Oxyxanthonen. *Berichte der deutschen chemischen Gesellschaft*. **1891**, 24 (1), 1894-1897.
128. Azevedo, C.; Manuel Magalhaes Afonso, C.; Maria Magalhaes Pinto, M. Routes to xanthones: an update on the synthetic approaches. *Curr. Org. Chem.* **2012**, 16 (23), 2818-2867.
129. Grover, P.; Shah, G.; Shah, R. Xanthones. Part IV. A new synthesis of hydroxyxanthones and hydroxybenzophenones. *J. Chem. Soc.* **1955**, 3982-3985.
130. Zhao, J.; Larock, R. C. One-pot synthesis of xanthones and thioxanthones by the tandem coupling-cyclization of arynes and salicylates. *Org. Lett.* **2005**, 7 (19), 4273-4275.
131. Dubrovskiy, A. V.; Larock, R. C. Intermolecular C–O addition of carboxylic acids to arynes. *Org. Lett.* **2010**, 12 (14), 3117-3119.
132. Wang, S.; Xie, K.; Tan, Z.; An, X.; Zhou, X.; Guo, C.-C.; Peng, Z. One-step preparation of xanthones via Pd-catalyzed annulation of 1, 2-dibromoarenes and salicylaldehydes. *Chem. Commun.* **2009**, (42), 6469-6471.
133. Hu, J.; Adogla, E. A.; Ju, Y.; Fan, D.; Wang, Q. Copper-catalyzed ortho-acylation of phenols with aryl aldehydes and its application in one-step preparation of xanthones. *Chem. Commun.* **2012**, 48 (91), 11256-11258.
134. Menendez, C. A.; Nador, F.; Radivoy, G.; Gerbino, D. C. One-Step Synthesis of Xanthones Catalyzed by a Highly Efficient Copper-Based Magnetically Recoverable Nanocatalyst. *Org. Lett.* **2014**, 16 (11), 2846-2849.
135. Genovese, S.; Fiorito, S.; Specchiulli, M. C.; Taddeo, V. A.; Epifano, F. Microwave-assisted synthesis of xanthones promoted by ytterbium triflate. *Tetrahedron Lett.* **2015**, 56 (6), 847-850.
136. Quillinan, A. J.; Scheinmann, F. Studies in the xanthone series. Part XII. A general synthesis of polyoxygenated xanthones from benzophenone precursors. *J. Chem. Soc.* **1973**, 1329-1337.
137. El-Desoky, S.; Abozeid, M.; Kandeel, E.; Abdel-Rahmana, A. Domino Reactions of 3-Vinylchromone Leading to Different Heterocyclic Compounds. *J. Heterocyclic Chem.* **2014**, 51, 1270-1276.
138. Castanheiro, R. A.; Pinto, M. M.; Silva, A. M.; Cravo, S. M.; Gales, L.; Damas, A. M.; Nazareth, N.; Nascimento, M. S.; Eaton, G. Dihydroxyxanthones prenylated derivatives: synthesis, structure elucidation, and growth inhibitory activity on human tumor cell lines with improvement of selectivity for MCF-7. *Bioorg. Med. Chem.* **2007**, 15 (18), 6080-6088.
139. Sharifi, A.; Mirzaei, M.; Naimi-Jamal, M. R. Solvent-free aminoalkylation of phenols and indoles assisted by microwave irradiation. *Chem. Monthly.* **2001**, 132 (7), 875-880.

140. Roman, G. Mannich bases in medicinal chemistry and drug design. *Eur. J. Med. Chem.* **2015**, *89*, 743-816.
141. Tramontini, M.; Angiolini, L. Synthesis of Mannich-bases. In *Mannich bases-chemistry and uses*, Tramontini, M.; Angiolini, L., Eds.; CRC Press: Florida, USA, 1994; pp 1-70.
142. Enders, D.; Grondal, C.; Vrettou, M.; Raabe, G. Asymmetric synthesis of selectively protected amino sugars and derivatives by a direct organocatalytic Mannich reaction. *Angewandte Chemie International Edition.* **2005**, *44* (26), 4079-4083.
143. Lin, C. N.; Chung, M. i.; Liou, S. J.; Lee, T. H.; Wang, J. P. Synthesis and anti-inflammatory effects of xanthone derivatives. *J. Pharm. Pharmacol.* **1996**, *48* (5), 532-538.
144. Scheme, B. G. R. Baker-Venkataraman Rearrangement. **2010**.
145. Donnelly, J. A.; Emerson, G. M. Amine-effected cyclization of chalcone dihalides to aurones. *Tetrahedron.* **1990**, *46* (20), 7227-7236.
146. Seijas, J. A.; Vázquez-Tato, M. P.; Carballido-Reboredo, R. Solvent-free synthesis of functionalized flavones under microwave irradiation. *J. Org. Chem.* **2005**, *70* (7), 2855-2858.
147. Liang, B.; Dai, M.; Chen, J.; Yang, Z. Copper-free Sonogashira coupling reaction with PdCl<sub>2</sub> in water under aerobic conditions. *J. Org. Chem.* **2005**, *70* (1), 391-393.
148. Kumar, P.; Bodas, M. S. A Novel Synthesis of 4 *H*-Chromen-4-ones via Intramolecular Wittig Reaction. *Org. Lett.* **2000**, *2* (24), 3821-3823.
149. Zhang, S.; Ma, J.; Bao, Y.; Yang, P.; Zou, L.; Li, K.; Sun, X. Nitrogen-containing flavonoid analogues as CDK1/cyclin B inhibitors: synthesis, SAR analysis, and biological activity. *Bioorg. Med. Chem.* **2008**, *16* (15), 7127-7132.
150. Magalhães, L. M.; Segundo, M. A.; Reis, S.; Lima, J. L. Methodological aspects about in vitro evaluation of antioxidant properties. *Anal. Chim. Acta.* **2008**, *613* (1), 1-19.
151. Pisoschi, A. M. Methods for total antioxidant activity determination: a review. *Biochem. Anal. Biochem.* **2011**, *1* (106).
152. Alam, M. N.; Bristi, N. J.; Rafiquzzaman, M. Review on in vivo and in vitro methods evaluation of antioxidant activity. *Saudi Pharm. J.* **2013**, *21* (2), 143-152.
153. López-Alarcón, C.; Denicola, A. Evaluating the antioxidant capacity of natural products: a review on chemical and cellular-based assays. *Anal. Chim. Acta.* **2013**, *763*, 1-10.
154. Chiang, Y.-M.; Kuo, Y.-H.; Oota, S.; Fukuyama, Y. Xanthoness and benzophenones from the stems of *Garcinia multiflora*. *J. Nat. Prod.* **2003**, *66* (8), 1070-1073.

155. Merza, J.; Aumond, M.-C.; Rondeau, D.; Dumontet, V.; Le Ray, A.-M.; Séraphin, D.; Richomme, P. Prenylated xanthenes and tocotrienols from *Garcinia virgata*. *Phytochemistry*. **2004**, *65* (21), 2915-2920.
156. Phuwapraisirisan, P.; Udomchotphruet, S.; Surapinit, S.; Tip-Pyang, S. Antioxidant xanthenes from *Cratoxylum cochinchinense*. *Nat. Prod. Res.* **2006**, *20* (14), 1332-1337.
157. Dharmaratne, H.; Napagoda, M.; Tennakoon, S. Xanthenes from roots of *Calophyllum thwaitesii* and their bioactivity. *Nat. Prod. Res.* **2009**, *23* (6), 539-545.
158. Chen, Y.; Fan, H.; Yang, G.-z.; Jiang, Y.; Zhong, F.-f.; He, H.-w. Prenylated xanthenes from the bark of *Garcinia xanthochymus* and their 1, 1-diphenyl-2-picrylhydrazyl (DPPH) radical scavenging activities. *Molecules*. **2010**, *15* (10), 7438-7449.
159. Trisuvan, K.; Rukachaisirikul, V.; Kaewpet, M.; Phongpaichit, S.; Hutadilok-Towatana, N.; Preedanon, S.; Sakayaroj, J. Sesquiterpene and xanthone derivatives from the sea fan-derived fungus *Aspergillus sydowii* PSU-F154. *J. Nat. Prod.* **2011**, *74* (7), 1663-1667.
160. Hamada, H.; Hiramatsu, M.; Edamatsu, R.; Mori, A. Free radical scavenging action of baicalein. *Arch. Biochem. Biophys.* **1993**, *306* (1), 261-266.
161. Okawa, M.; Kinjo, J.; Nohara, T.; ONO, M. DPPH (1, 1-diphenyl-2-picrylhydrazyl) radical scavenging activity of flavonoids obtained from some medicinal plants. *Bio. Pharma. Bull.* **2001**, *24* (10), 1202-1205.
162. Cotellet, N.; Bernier, J.-L.; Catteau, J.-P.; Pommery, J.; Wallet, J.-C.; Gaydou, E. M. Antioxidant properties of hydroxy-flavones. *Free Radical Bio. Med.* **1996**, *20* (1), 35-43.
163. Zhou, G.; Lv, G. Comparative studies on scavenging DPPH free radicals activity of flavone C-glycosides from different parts of *Dendrobium officinale*. *China J. Chinese Materia Medica*. **2012**, *37* (11), 1536-1540.
164. Karadag, A.; Ozcelik, B.; Saner, S. Review of methods to determine antioxidant capacities. *Food Anal. Method.* **2009**, *2* (1), 41-60.
165. Nag, G.; Das, S.; Das, S.; Mandal, S.; De, B. Antioxidant, anti-acetylcholinesterase and antiglycosidase properties of three species of *Swertia*, their xanthenes and amarogentin: a comparative study. *Phcog. J.* **2015**, *7*, 117-123.
166. Říha, M.; Karlíčková, J.; Filipský, T.; Macáková, K.; Rocha, L.; Bovicelli, P.; Silvestri, I. P.; Saso, L.; Jahodář, L.; Hrdina, R. In vitro evaluation of copper-chelating properties of flavonoids. *RSC Adv.* **2014**, *4* (62), 32628-32638.
167. Mladěnka, P.; Macáková, K.; Filipský, T.; Zatloukalová, L.; Jahodář, L.; Bovicelli, P.; Silvestri, I. P.; Hrdina, R.; Saso, L. In vitro analysis of iron chelating activity of flavonoids. *J. Inorg. Biochem.* **2011**, *105* (5), 693-701.

168. Wang, X.; Li, X.; Li, H. Reassessment of Antioxidant Activity of Baicalein in vitro. *Asian J. Pharm. Biol. Res.* **2011**, 1 (2), 186-194.
169. Cheng, I. F.; Breen, K. On the ability of four flavonoids, baicilein, luteolin, naringenin, and quercetin, to suppress the Fenton reaction of the iron-ATP complex. *Biometals.* **2000**, 13 (1), 77-83.
170. Di Giovanni, S.; Borloz, A.; Urbain, A.; Marston, A.; Hostettmann, K.; Carrupt, P.-A.; Reist, M. In vitro screening assays to identify natural or synthetic acetylcholinesterase inhibitors: Thin layer chromatography versus microplate methods. *Eur. J. Pharm. Sci.* **2008**, 33 (2), 109-119.
171. Ellman, G. L.; Courtney, K. D.; Andres, V.; Featherstone, R. M. A new and rapid colorimetric determination of acetylcholinesterase activity. *Biochem. Pharm.* **1961**, 7 (2), 88-95.
172. Kiely, J. S.; Moos, W. H.; Pavia, M. R.; Schwarz, R. D.; Woodard, G. L. A silica gel plate-based qualitative assay for acetylcholinesterase activity: A mass method to screen for potential inhibitors. *Anal. Biochem.* **1991**, 196 (2), 439-442.
173. Rhee, I. K.; van de Meent, M.; Ingkaninan, K.; Verpoorte, R. Screening for acetylcholinesterase inhibitors from Amaryllidaceae using silica gel thin-layer chromatography in combination with bioactivity staining. *J. Chromatogr. A.* **2001**, 915 (1), 217-223.
174. Marston, A.; Kissling, J.; Hostettmann, K. A rapid TLC bioautographic method for the detection of acetylcholinesterase and butyrylcholinesterase inhibitors in plants. *Phytochem. Analysis.* **2002**, 13 (1), 51-54.
175. Andrisano, V.; Bartolini, M.; Gotti, R.; Cavrini, V.; Felix, G. Determination of inhibitors' potency (IC<sub>50</sub>) by a direct high-performance liquid chromatographic method on an immobilised acetylcholinesterase column. *J. Chromatogr. B.* **2001**, 753 (2), 375-383.
176. Devonshire, A. L.; Moores, G. D. A carboxylesterase with broad substrate specificity causes organophosphorus, carbamate and pyrethroid resistance in peach-potato aphids (*Myzus persicae*). *Pestic. Biochem. Phys.* **1982**, 18 (2), 235-246.
177. Rhee, I. K.; Appels, N.; Luijendijk, T.; Irth, H.; Verpoorte, R. Determining acetylcholinesterase inhibitory activity in plant extracts using a fluorimetric flow assay. *Phytochem. Analysis.* **2003**, 14 (3), 145-149.
178. Ibrahim, S. N.; Ahmad, F. Synthesis and Biological Evaluation of Flavonoids as Antiacetyl-cholinesterase Agent. *Jurnal Teknologi.* **2014**, 69 (1).
179. Fukumoto, L.; Mazza, G. Assessing antioxidant and prooxidant activities of phenolic compounds. *J. Agr. Food Chem.* **2000**, 48 (8), 3597-3604.

180. Brand-Williams, W.; Cuvelier, M.; Berset, C. Use of a free radical method to evaluate antioxidant activity. *LWT-Food Science and Technology*. **1995**, 28 (1), 25-30.
181. Dinis, T. C.; Madeira, V. M.; Almeida, L. M. Action of phenolic derivatives (acetaminophen, salicylate, and 5-aminosalicylate) as inhibitors of membrane lipid peroxidation and as peroxyl radical scavengers. *Arch. Biochem. Biophys.* **1994**, 315 (1), 161-169.
182. Brown, J.; Khodr, H.; Hider, R.; Rice-Evans, C. Structural dependence of flavonoid interactions with Cu<sup>2+</sup> ions: implications for their antioxidant properties. *Biochem. J.* **1998**, 330, 1173-1178.
183. Čolović, M. B.; Krstić, D. Z.; Lazarević-Pašti, T. D.; Bondžić, A. M.; Vasić, V. M. Acetylcholinesterase inhibitors: Pharmacology and toxicology. *Curr. Neuropharmacol.* **2013**, 11 (3), 315.
184. Lu, S.-H.; Wu, J. W.; Liu, H.-L.; Zhao, J.-H.; Liu, K.-T.; Chuang, C.-K.; Lin, H.-Y.; Tsai, W.-B.; Ho, Y. The discovery of potential acetylcholinesterase inhibitors: a combination of pharmacophore modeling, virtual screening, and molecular docking studies. *J. Biomed. Sci.* **2011**, 18 (8), b22.
185. Dvir, H.; Silman, I.; Harel, M.; Rosenberry, T. L.; Sussman, J. L. Acetylcholinesterase: from 3D structure to function. *Chem.-Biol. Interact.* **2010**, 187 (1), 10-22.
186. Cheung, J.; Rudolph, M. J.; Burshteyn, F.; Cassidy, M. S.; Gary, E. N.; Love, J.; Franklin, M. C.; Height, J. J. Structures of human acetylcholinesterase in complex with pharmacologically important ligands. *J. Med. Chem.* **2012**, 55 (22), 10282-10286.
187. Sussman, J. L.; Lin, D.; Jiang, J.; Manning, N. O.; Prilusky, J.; Ritter, O.; Abola, E. Protein Data Bank (PDB): database of three-dimensional structural information of biological macromolecules. *Acta Crystallogr. D.* **1998**, 54 (6), 1078-1084.
188. Froimowitz, M. HyperChem: a software package for computational chemistry and molecular modeling. *Biotechniques*. **1993**, 14 (6), 1010-1013.
189. Trott, O.; Olson, A. J. AutoDock Vina: improving the speed and accuracy of docking with a new scoring function, efficient optimization, and multithreading. *J. Comput. Chem.* **2010**, 31 (2), 455-461.
190. Seeliger, D.; de Groot, B. L. Ligand docking and binding site analysis with PyMOL and Autodock/Vina. *J. Comput. Aid. Mol. Des.* **2010**, 24 (5), 417-422.
191. Vilar, S.; Cozza, G.; Moro, S. Medicinal chemistry and the molecular operating environment (MOE): application of QSAR and molecular docking to drug discovery. *Curr. Top. Med. Chem.* **2008**, 8 (18), 1555-1572.